In presenting the dissertation as a partial fulfillment of the requirements for an advanced degree from the Georgia Institute of Technology, I agree that the Library of the Institute shall make it available for inspection and circulation in accordance with its regulations governing materials of this type. I agree that permission to copy from, or to publish from, this dissertation may be granted by the professor under whose direction it was written, or, in his absence, by the Dean of the Graduate Division when such copying or publication is solely for scholarly purposes and does not involve potential financial gain. It is understood that any copying from, or publication of, this dissertation which involves potential financial gain will not be allowed without written permission.

7/25/68

THE EFFECT OF RADIATION AND FLUID PROPERTIES ON TRANSIENT FILM BOILING ON A HORIZONTAL CYLINDRICAL SURFACE

A THESIS

Presented to

The Faculty of the Graduate Division

by

David Paul Wehmeyer

In Partial Fulfillment

of the Requirements for the Degree

Doctor of Philosophy

in the School of Mechanical Engineering

Georgia Institute of Technology

June, 1970

THE EFFECT OF RADIATION AND FLUID
PROPERTIES ON TRANSIENT FILM BOILING
ON A HORIZONTAL CYLINDRICAL SURFACE

Approved:

Chairman

Date approved by Chairman: 4-27-70

ACKNOWLEDGMENTS

The author wishes to express the deepest gratitude to Dr. T. W. Jackson, chairman of the Reading Committee, for his enthusiasm, friendship, and helpfulness throughout this research. Completion of this investigation could not have been accomplished without his suggestions and advice.

Appreciation is also expressed to the thesis examination committee members, Drs. M. R. Carstens, G. T. Colwell, J. H. Rust, and W. Wulff for their active interest and advice. Dr. Colwell and Dr. Rust also served on the author's Reading Committee.

Special thanks are due to Dr. H. H. Yen and Dr. E. L. Richards for their ideas and help concerning the experimental portion of the research. Thanks are also due to Dr. S. H. Bomar, Jr. and Mr. W. W. Carr for proof reading this thesis.

The author also expresses sincere appreciation to Dr. S. P. Kezios and Dr. P. Durbetaki for their efforts and encouragement during the years that they were his academic advisors.

Indebtedness is expressed to Mr. Louis Cavalli and Mr. Joe Doyal for their constant willingness to aid in solving problems with experimental apparatus.

The author would like to express gratitude to the National Science Foundation for Grant GK 1416 which supported this investigation.

A genuine feeling of indebtedness is expressed towards the author's parents, who instilled in him the desire to obtain as much education as

possible.

The author sincerely appreciates the encouragement, patience, and understanding of his wife, Barbara, and the sacrifices that both she and their boy made during his years of post-graduate study. He would also like to thank Barbara, his wife, for typing the rough draft of this thesis.

TABLE OF CONTENTS

TABLE OF CONTENTS (Continued)

TABLE OF CONTENTS (Concluded)

LIST OF TABLES

LIST OF TABLES (Continued)

LIST OF FIGURES

LIST OF FIGURES (Continued)

LIST OF FIGURES (Concluded)

NOMENCLATURE

Symbol		Units
C_1	Constant in solution of energy equation	dimensionless
C_2	Constant in solution of energy equation	dimensionless
C_p	Specific heat of vapor	Btu/lb_m
C	Constant defined by Equation (2.29)	dimensionless
D	Vapor film diameter	in
h_{fg}	Heat of vaporization	Btu/lb
$h_{\ell m}$	Convective heat transfer coefficient	$Btu/sec\ in^2\ °F$
J	Energy conversion factor	$in\ lb_f/Btu$
$K(\theta)$	Function defined by Equations (D.2) and (2.28)	°F
k	Thermal conductivity	Btu/sec in °F
L	Wire length	in
m	Constant defined by Equation (2.29)	dimensionless
n	Constant defined by Equation (2.29)	dimensionless
Nu	Nusselt number	dimensionless
P	Pressure	lb_f/in^2
Pr	Prandtl number	dimensionless
R	Vapor-liquid interfacial radius	in
Re	Reynolds number	dimensionless
r	Radius	in
T	Temperature	°F
u_i	Velocity in i th direction	in/sec
V	Volume	in^3

NOMENCLATURE (Continued)

Symbol		Units
v	Velocity	in/sec
x	Argument for exponential integral	dimensionless
Z	Variable of integration	dimensionless

GREEK LETTER SYMBOLS

α	Thermal diffusivity	in^2/sec
ϵ	Emissivity	dimensionless
ν	Kinematic viscosity	in^2/sec
σ	Surface tension	dynes/cm
ρ	Density	lb/in^3
θ	Time	sec
Φ	Dummy function in solution of energy equation	$^\circ F$
η	Dummy function in solution of energy equation	dimensionless
τ_{ij}	Stress tensor	$lb_m/in\ sec^2$

Subscripts

ℓ	Refers to liquid phase
m	Refers to evaluation at mean temperature of liquid phase, $(T_\infty + T_{SAT})/2$
SAT	Refers to saturation conditions
v	Refers to vapor phase
w	Refers to wire condition
∞	Refers to pool conditions

SUMMARY

An analytical and experimental investigation was made to determine the film growth during the initial regimes of transient film boiling from a horizontal wire for Freon 113 and carbon tetrachloride. Typical experimental results from two previous theses for water were also analytically considered. All experimental tests were run at atmospheric pressure.

A horizontal, electrically heated platinum wire 0.010 inches in diameter was used in the experimental investigation. This wire was subjected to an approximate step change in temperature by a rapid discharge of energy from an electrical capacitor. The resulting wire temperature history was essentially constant for the time period considered in this investigation.

The analytical model considered convection heat transfer to the liquid pool from the cylindrical vapor-liquid interface. The coefficient of convective heat transfer from the vapor-liquid interface to the liquid phase was taken to be of the same form as that of the stagnation point at a cylinder in forced transverse flow. The interface temperature was the saturation temperature of the liquid and the transverse flow velocity is taken to be the growth velocity of the vapor film. Constant wire temperature was assumed and heat transfer through the vapor phase was due to radiation and conduction. The solution to the energy equation in the vapor phase gave the temperature distribution in the vapor as a function of the first-order exponential integral, $E_1\left(-\frac{r^2}{4\alpha_v\theta}\right)$. All radiation

from the wire was found to pass through the vapor and to be absorbed in depth within the liquid phase. An energy balance at the vapor-liquid interface was obtained by applying the solution for the vapor phase, convection to the liquid, and the energy required to vaporize the liquid at the interface. The transcendental equation obtained by this energy balance provided an initial value problem the solution of which yielded the vapor-liquid interface radius as a function of time. This equation was solved for all representative runs of this investigation by means of Runge-Kutta integration on a Burroughs 5500 digital computer.

A total of eighteen transient boiling experiments were conducted with pool temperatures ranging from saturation conditions to fifteen degrees of subcooling.

The investigation was carried out using Freon 113 and carbon tetrachloride as the experimental fluids. A test run was also made using distilled water to compare with results given by previous investigators. The transient film growth was recorded by means of high speed motion pictures.

The motion picture data were reduced to yield vapor growth rates. Volume mean radii were computed from these data and are presented as a function of time for eleven representative runs. The analytical model was solved for each of these runs and compared to the experimental results.

Heat transfer rates through the vapor by conduction and into the liquid by convection are presented as a function of time for selected test runs for each fluid analyzed.

CHAPTER I

INTRODUCTION

At the present time there is interest at the Georgia Institute of Technology in the possibility of creating small volume periodic fluid flows by means of transient film boiling. This flow could conceivably be obtained by an electrical energy discharge into a small-diameter wire that is located within a small, partially confined space with a liquid in contact with the wire surface. With each discharge of energy a small volume of vapor would be formed and this in turn could displace a slightly smaller volume of liquid from the partially confining space. An example of this phenomenon may be found in Reference 1. In order to gain more insight into the phenomenon encountered during this transient period the present investigation was carried out.

Related Literature

A discussion of the related literature, prior to the work of Pitts (2), may be found in Chapter I of Reference 2.

Pitts (2) obtained experimental values of vapor growth rates for transient film boiling and compared these with a theoretical solution. His experiment and theory were limited to saturated water, and radiation effects were neglected.

Yen (3) studied the film formation for the subcooled liquid case. His experiments indicated a definite reduction in final film thickness with increased subcooling of the liquid pool. Again, water was the

liquid under investigation, and radiation effects were ignored.

Richards (1) was concerned with the axial flow of the vapor film that resulted from transient film boiling in a horizontal annulus filled with saturated liquid. He obtained experimental data for vapor growth rates under the stated conditions and compared these with his theoretical computer solution. Water was the liquid under investigation, and radiation effects were ignored.

Thus, prior to the present research there appears to be no published results of experimental studies for liquids other than water nor theoretical studies of the effects of radiation on the transient film boiling.

An excellent historical background discussion may be found in Chapter I of Reference 2.

Purpose of this Research

This research is an investigation of the initial period of transient film boiling of carbon tetrachloride and Freon 113 on a submerged horizontal cylindrical surface. The primary objectives were to obtain experimental data for the vapor film formation around the cylindrical surface and to develop an analytical model which will serve to predict the initial vapor growth rate and the heat transfer.

CHAPTER II

ANALYSIS

The Analytical Model

Consider a horizontal cylindrical wire submerged in a liquid pool and initially in thermal equilibrium with the liquid as shown in Figure 1. The wire is then subjected to a sudden step change in temperature which is sufficiently large to result in film boiling. Some initial radius, R_o, is reached by the vapor film in a time that is short compared to the total transient time. This uniform vapor film is analyzed as it continues to grow with time. The initial temperature of the vapor is assumed to be equal to that of the saturation temperature of the liquid at the system pressure, which is one atmosphere for this investigation. The film is considered to be cylindrical, with no axial variation in thickness. The wire temperature is considered to be constant with negligible axial or radial variation. As shown in Appendix C these approximations seem to be reasonable.

Heat transfer through the vapor is by conduction, convection, and radiation. It is shown in Appendix A that the vapor film is optically thin and thus absorbs and emits radiation negligibly due to its low extinction coefficient.

In Appendix C the convective heat transfer effect within the vapor phase is shown to be negligible when compared to the conductive heat transfer.

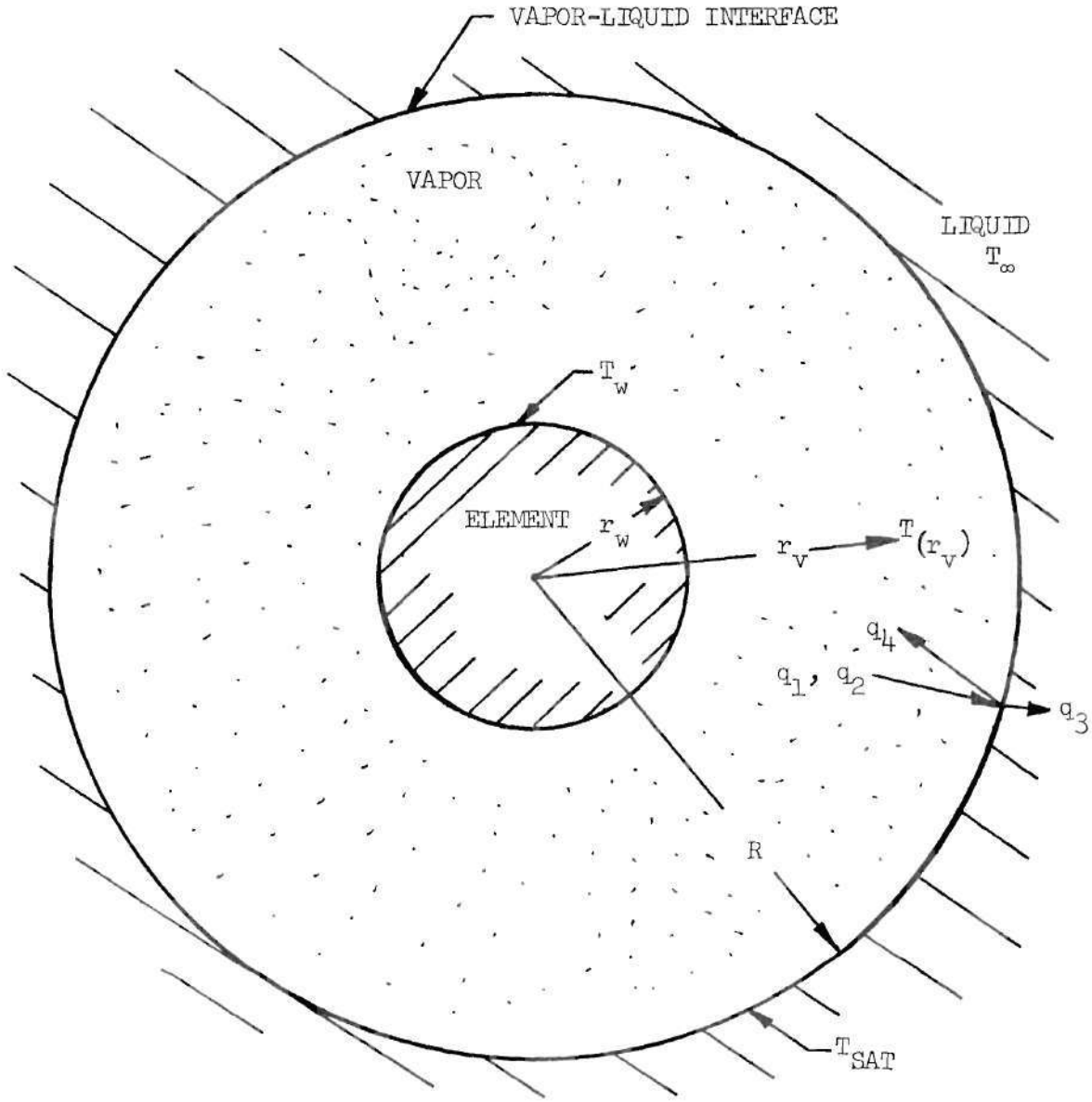

q_1 - transferred by conduction

q_2 - transferred by radiation

q_3 - transferred by convection

q_4 - heat of vaporization

Figure 1. Physical Model of Transient Film Boiling from a Cylindrical Surface.

Heat transfer to the liquid from the vapor-liquid interface is approximated by the formula for the heat transfer coefficient at the stagnation point of a solid cylinder in forced transverse flow. This approximation is somewhat arbitrary but was used because the flow field relative to and around the vapor cylinder resembles locally the stagnation conditions at a cylinder. It is recognized, however, that it is a transient process and the Reynolds number does depend on time.

The pressure variation within the vapor and the buoyancy force on the vapor are shown to be negligible in Appendix B. The temperature of the liquid at the vapor-liquid interface varies negligibly from that of the saturation temperature of the liquid as is also shown in Appendix B.

The temperature distribution within the vapor phase will now be determined for the case of negligible convective effects. Next the convective model for heat transfer from the vapor-liquid interface into the liquid phase will be presented. Use of these two effects along with an energy balance at the vapor-liquid interface will provide an initial value problem that describes the vapor film growth rate.

Temperature Distribution Within the Vapor Phase

As given by Equation (B.8) of Appendix B the energy equation within the vapor phase is

$$\frac{\partial T}{\partial \theta} - \alpha_v \left(\frac{\partial^2 T}{\partial r^2} + \frac{1}{r} \frac{\partial T}{\partial r}\right) = 0. \qquad (2.1)$$

The initial condition is

$$T(r,0) = T_{SAT} \qquad r_w < r \leq R \tag{2.2}$$

and the boundary conditions are

$$T(r_w,\theta) = T_w \qquad \theta > 0 \tag{2.3}$$

and

$$T(R,\theta) = T_{SAT} \, . \qquad \theta > 0 \tag{2.4}$$

Under the similarity transformation

$$\eta = \frac{r}{2\sqrt{\alpha_v \theta}} \tag{2.5}$$

the temperature becomes a function of η alone

$$T = T\ (\eta) \tag{2.6}$$

and Equation (2.1) reduces to

$$\frac{d^2T}{d\eta^2} + (2\ \eta + \frac{1}{\eta})\ \frac{dT}{d\eta} = 0. \tag{2.7}$$

Equation (2.7) is subject to the boundary conditions

$$T\ (\eta_w) = T\ \left(\frac{r_w}{2\sqrt{\alpha_v \theta}}\right) = T_w \tag{2.8}$$

and

$$T\ (\eta_R) = T\ \left(\frac{R}{2\sqrt{\alpha_v \theta}}\right) = T_{SAT}. \tag{2.9}$$

After introducing

$$\Phi = \frac{dT}{d\eta}\ , \tag{2.10}$$

Equation (2.7) becomes this first-order differential equation

$$\frac{d\Phi}{d\eta} + \left(2\ \eta + \frac{1}{\eta}\right)\ \Phi = 0 \tag{2.11}$$

whose integral is

$$\Phi = C_1\ \frac{e^{-\eta^2}}{\eta}\ . \tag{2.12}$$

This yields the temperature gradient

$$\frac{dT}{d\eta} = C_1\ \frac{e^{-\eta^2}}{\eta}\ . \tag{2.13}$$

Multiplication and division of Equation (2.13) by η gives

$$dT = C_2 \frac{e^{-\eta^2}}{\eta^2} \, d\eta^2 \tag{2.14}$$

where $C_2 = C_1/2$.

Integration of Equation (2.14) using the boundary condition of Equation (2.8), yields

$$\int_{T_w}^{T} dT = C_2 \int_{\eta_w^2}^{\eta^2} \frac{e^{-Z}}{Z} \, dZ \tag{2.15}$$

or

$$T - T_w = C_2 \left[\int_{\eta_w^2}^{\infty} \frac{e^{-Z}}{Z} \, dZ - \int_{\eta^2}^{\infty} \frac{e^{-Z}}{Z} \right] dZ \quad . \tag{2.16}$$

Noting that the first-order exponential integral, $E_1(x)$, is defined as

$$E_1(x) = \int_{x}^{\infty} \frac{e^{-Z}}{Z} \, dZ \tag{2.17}$$

Equation (2.16) becomes

$$T - T_w = C_2 \left[E_1 \left(\eta_w^{\,2}\right) - E_1 \left(\eta^2\right) \right]. \tag{2.18}$$

Now use the other boundary condition, Equation (2.9), with Equation (2.18) to obtain

$$T_{SAT} - T_w = C_2 \left[E_1 \left(\eta_w^{\,2}\right) - E_1 \left(\eta_R^{\,2}\right) \right] \tag{2.19}$$

so that

$$C_2 = \frac{\left(T_{SAT} - T_w\right)}{E_1 \left(\eta_w^{\,2}\right) - E_1 \left(\eta_R^{\,2}\right)} \; . \tag{2.20}$$

Substitution of Equation (2.20) into Equation (2.18) yields

$$T = T_w + \frac{\left(T_{SAT} - T_w\right) \left[E_1 \left(\frac{r^2}{4\alpha_v \theta}\right) - E_1 \left(\frac{r_w^{\,2}}{4\alpha_v \theta}\right) \right]}{E_1 \left(\frac{R^2}{4\alpha_v \theta}\right) - E_1 \left(\frac{r_w^{\,2}}{4\alpha_v \theta}\right)} \tag{2.21}$$

which is the temperature distribution in the vapor phase.

To show that Equation (2.21) is a solution to Equations (2.1) through (2.4) consider first Equations (2.1) and (2.2). Recognize that as $\theta \to 0$, x approaches infinity. For large values of x, E_1 (x) approaches $\frac{e^{-x}}{x}$. Thus for $\theta \to 0$

$$\lim_{\theta\to 0} T = \lim_{\theta\to 0}\left\{ T_w + (T_{SAT} - T_w)\frac{\left[\dfrac{e^{-\frac{r^2}{4\alpha_v\theta}}}{\frac{r^2}{4\alpha_v\theta}} - \dfrac{e^{-\frac{r_w^2}{4\alpha_v\theta}}}{\frac{r_w^2}{4\alpha_v\theta}}\right]}{\left[\dfrac{e^{-\frac{R^2}{4\alpha_v\theta}}}{\frac{R^2}{4\alpha_v\theta}} - \dfrac{e^{-\frac{r_w^2}{4\alpha_v\theta}}}{\frac{r_w^2}{4\alpha_v\theta}}\right]}\right\} \tag{2.22}$$

$$= \lim_{\theta\to 0}\left\{ T_w + (T_{SAT} - T_w)\frac{\left[\dfrac{e^{-\frac{(r^2 - r_w^2)}{4\alpha_v\theta}}}{r^2} - \dfrac{1}{r_w^2}\right]}{\left[\dfrac{e^{-\frac{(R^2 - r_w^2)}{4\alpha_v\theta}}}{R^2} - \dfrac{1}{r_w^2}\right]}\right\} \tag{2.23}$$

$$\lim_{\theta\to 0} T = T_w + (T_{SAT} - T_w)\left\{\frac{-\frac{1}{r_w^2}}{-\frac{1}{r_w^2}}\right\} = T_{SAT} \tag{2.24}$$

for all $r_w < r \leq R$.

From Equation (2.23) it is seen that for $r = r_w$

$$\lim_{\theta\to 0} T = T_w + (T_{SAT} - T_w) \times 0 = T_w. \tag{2.25}$$

Equation (2.3) is satisfied because at $r = r_w$, $\theta > 0$

$$T = T_w + (T_{SAT} - T_w) \times 0 = T_w. \tag{2.26}$$

Equation (2.4) is also satisfied because for $r = R$, $\theta \geq 0$

$$T = T_w + (T_{SAT} - T_w) \times 1 = T_{SAT}. \tag{2.27}$$

Thus it has been shown that Equation (2.21) is a solution for the temperature distribution in the cylinder, based on the proposed model.

Partial differentiation of Equation (2.21) with respect to r yields

$$\frac{\partial T}{\partial r} = \frac{(T_{SAT} - T_w)}{E_1\left(\frac{R^2}{4\alpha_v\theta}\right) - E_1\left(\frac{r_w^2}{4\alpha_v\theta}\right)} \left(\frac{-2e^{-\frac{r^2}{4\alpha_v\theta}}}{r} \right) . \tag{2.28}$$

This result is used in Equation (2.35) to represent the conductive heat flux arriving at the vapor-liquid interface.

Convection Energy Transfer Within the Liquid Phase

The convective heat transfer coefficient from the vapor cylinder to the liquid phase is taken as that of the stagnation point of a cylinder in forced transverse flow and is computed from the Nusselt number

$$Nu = c\ Re^n\ Pr^m \tag{2.29}$$

where n, m, and c may tentatively be taken from Jacob (4) to be

$$n = 0.5 \tag{2.30}$$

$$m = 0.31 \tag{2.31}$$

and

$$c = 1.20 \tag{2.32}$$

and where Re and Pr represent, respectively, the Reynolds and Prandtl numbers.

The above value of c will be varied in the numerical solution for the vapor film growth rate to see if better agreement between theory and experiment may be obtained. The velocity of the interface is given by

$$v = \frac{dR}{d\theta} \ . \tag{2.33}$$

Substitution of Equations (2.30), (2.31), (2.32), and (2.33) into Equation (2.29) gives

$$\frac{h_{\ell m}\, 2R}{k_{\ell m}} = 1.20 \left(\frac{\frac{dR}{d\theta}\, 2R}{\nu_{\ell m}} \right)^{0.5} Pr_{\ell m}^{\ 0.31} \tag{2.34}$$

which is an expression for the convective heat transfer coefficient, $h_{\ell m}$,

in terms of fluid properties, vapor film radius, and vapor film velocity.

Energy Balance at the Vapor-Liquid Interface

As given by Equation (D.12) of Appendix D, the energy balance is

$$\rho_v \, h_{fg} \, \dot{R} = - k_v \left. \frac{\partial T}{\partial r} \right|_{r=R} - h_{\ell m} \, (T_{SAT} - T_\infty). \tag{2.35}$$

Substitution of Equations (2.28) and (2.34) into Equation (2.35) gives

$$\rho_v \, h_{fg} \, \dot{R} = \frac{k_v \, (T_{SAT} - T_w)}{E_1\left(\frac{R^2}{4\alpha_v \theta}\right) - E_1\left(\frac{r_w^2}{4\alpha_v \theta}\right)} \; \frac{2 \, e^{-\frac{R^2}{4\alpha_v \theta}}}{R} - \frac{0.60 \, k_{\ell m}}{R} \, x$$

$$\frac{\sqrt{2R} \; \sqrt{dR/d\theta}}{\sqrt{\nu_{\ell m}}} \; Pr_{\ell m}^{\;0.31} \; (T_{SAT} - T_\infty). \tag{2.36}$$

Multiplication of Equation (2.36) by R yields

$$\rho_v \, h_{fg} \, R \, \dot{R} = \frac{2 \, k_v \, (T_{SAT} - T_w) \, e^{-\frac{R^2}{4\alpha_v \theta}}}{E_1\left(\frac{R^2}{4\alpha_v \theta}\right) - E_1\left(\frac{r_w^2}{4\alpha_v \theta}\right)}$$

$$- \frac{0.60 \, k_{\ell m} \, Pr_{\ell m}^{\;0.31} \, (T_{SAT} - T_\infty) \sqrt{2R} \sqrt{\dot{R}}}{\sqrt{\nu_{\ell m}}} \; . \tag{2.37}$$

Equation (2.37), subject to the initial condition

$$R = R_o \quad \text{at } \theta = 0,$$

constitutes an initial value problem the solution of which should yield the vapor-liquid interface radius as a function of time.

CHAPTER III

NUMERICAL SOLUTION

A Burroughs B-5500 digital computer was used to solve Equation (2.37) by means of Runge-Kutta integration. The program was written in FORTRAN and is listed in Appendix H.

The computer program is composed of five parts: A main part designated MAIN TFBHT, an integration subroutine designated RKS, a control subroutine designated CNTRL, a derivative subroutine designated DERIV, and a function routine designated E1(X).

MAIN TFBHT

This part serves to accept physical property values and equation constants for the derivative subroutine; absolute and relative allowable errors for the integration subroutine; and run number, initial time (TSTART), initial vapor film radius (RAD), and the cutoff time (TEND) for MAIN TFBHT. All input data units are in terms of °F, in, sec, lb_m, and Btu or else are dimensionless. The information received from the data cards is then printed out for a later reference. Initialization is then carried out for J1, J2, T, DEL, IFVD, IBKP, NTRY, IERR, and N, where,

J1 = "counter" integer used in control subroutine,

J2 = "counter" integer used in control subroutine,

T = initial value of time (zero for this analysis),

DEL = initial increment of time to be used by integration

subroutine,

IFVD = 0 for variable interval integration,

= 1 for fixed interval integration,

IBKP = 0 allows integration subroutine to cut interval once and then repeat integration (with IFVD = 0),

= 1 allows integration subroutine to cut interval as required,

NTRY = 1 causes return from control to integration subroutine for further integration,

= 2 causes return from integration subroutine to MAIN TFBHT,

= 3 causes return to integration subroutine with new value of interval (DEL),

= 4 causes restart of integration process,

IERR = 0 for normal integration,

= -1 when the interval value (DEL) becomes equal to zero and thus causes a return to MAIN TFBHT from the integration subroutine,

= 1 when the absolute error, A(1), plus the product of the relative error, R(1), times the absolute value of the variable being integrated, Y(1), equals zero. This causes a return to MAIN TFBHT from the integration subroutine,

and

N = the number of differential equations being integrated.

Calculation of the total interval of integration (TEND-TSTART) is then made and divided into twenty equal intervals. These intervals are labeled TWRITE. The interval TWRITE is then divided into twenty equal

intervals. These intervals are labeled ZWRITE. The interval ZWRITE is used in the control subroutine to cause the bubble growth output to be printed twenty times in equal time intervals in the first period of rapid growth or decay during the first five per cent of the total time period of integration. The interval TWRITE is then used to cause the bubble growth output to be printed after each succeeding five per cent of the total time period of integration. A multiplication factor, QMUL, is calculated which facilitates conversion from $(in^2 sec)^{-1}$ to $(ft^2\ hr)^{-1}$ in the derivative subroutine.

After printing of the necessary title for the tabulated bubble growth history the integration subroutine is called. The integration subroutine completes the integration process and then returns to MAIN TFBHT. Since the bubble interface velocity had been stored, in DR(40), at the end of each subinterval of calculation the acceleration can be calculated for the bubble interface. The acceleration is necessary to estimate the vapor pressure in the vapor film (see Appendix B). Values of time, interface velocity, and interface acceleration are printed at TSTART and at the end of each subinterval of integration until TEND is reached.

It should be noted that since the analysis of Chapter II started with a vapor film of finite size at T = 0, the integration process has been started at T = 0 for time equal to TSTART and Y(1) = RAD. Thus all values of T must be added to TSTART to obtain actual values of time which may be compared to experimentally determined values of time. This shifting of the zero of time is contained within the computer program so that all printed values of time correspond directly to experimental values.

SUBROUTINE RKS

The integration subroutine, designated by SUBROUTINE RKS, is a fourth-order Runge-Kutta integration and communicates with SUBROUTINE DERIV and SUBROUTINE CNTRL. It integrates over the interval of interest with variable step size which is selected, after Simpson integration, to produce limited absolute and relative errors.

SUBROUTINE CNTRL

The control subroutine, designated by SUBROUTINE CNTRL, controls output of the numerically calculated variables and termination of the integration procedure. It is entered after every integration step from the integration subroutine as well as after the initial conditions are given. This subroutine causes the print-out of the initial values of time, vapor film radius, vapor film velocity, conduction heat flux through the vapor into the interface, and convective heat flux into the liquid from the interface. These variables are subsequently printed at the end of each integration subinterval of time for the complete integration process. The subintervals have the value of ZWRITE for the first twenty integration steps and the value TWRITE for the next nineteen integration steps. The last of the nineteen steps is calculated to end just at time equal to TEND. After the integration has been carried out over the complete time interval, NTRY is set equal to 2 and thus a return to MAIN TFBHT is made.

SUBROUTINE DERIV

The derivative subroutine, designated by SUBROUTINE DERIV,

contains the expression for the differential equation in the form dY/dT = f (Y, T, VARIABLES). In this subroutine DY(1) = dY/dT. There is direct communication between DERIV and RKS in that DERIV is supplied current values of Y(1) and T and then computes DY(1) for return to RKS.

ROUTINE E1(X)

The function routine, designated by FUNCTION E1(X), is used by the derivative subroutine for calculation of the first-order exponential integral.

INPUT DATA

The following data are read from three input cards.

RHOV = mean vapor film density

EXPPRN = exponent for Prandtl number in Nusselt number relationship

CONDV = mean vapor film thermal conductivity

DIFFV = mean vapor film thermal diffusivity

RWALL = wire radius

CONDLM = mean liquid thermal conductivity

TVISLM = mean liquid kinematic viscosity

THFG = heat of vaporization of liquid

TEND = time at end of transient period

TSAT = saturation temperature of liquid at given external pressure

TWALL = wire temperature

PRDTLM = mean Prandtl number of liquid

TLIQ = liquid pool temperature

COEFOV = coefficient of Nusselt number relationship for heat transfer to liquid

NWR = number of equal time steps in integration interval

A = absolute error allowed in single integration step

R = relative error allowed in single integration step

RAD = initial radius of vapor film obtained experimentally

TSTART = initial time at which first vapor film data were obtained experimentally

RUNNO = run number being integrated

The above data are read from data cards that are arranged in the following order.

DATA CARD NO. 1, FORMAT (7E10.4)

RHOV	EXPPRN	CONDV	DIFFV	RWALL	CONDLM	TVISLM
10	20	30	40	50	60	70

DATA CARD NO. 2, FORMAT (7F10.4, I10)

THFG	TEND	TSAT	TWALL	PRDTLM	TLIQ	COEFOV	NWR
10	20	30	40	50	60	70	80

DATA CARD NO. 3, FORMAT (4E10.4, I5)

A	R	RAD	TSTART	RUNNO
10	20	30	40	50

The numbers below the variable names indicate the column in which the last digit of the variable shall appear on the data card. All variable units are in terms of °F, in, sec, lb_m, and Btu or else are dimensionless.

A block diagram of the input values necessary for the solution of

Equation (2.37) is shown in Figure 2.

All of the physical properties of the vapor were evaluated at the mean temperature of the vapor. The physical properties necessary to evaluate the heat transferred from the vapor-liquid interface to the liquid pool were evaluated at the mean between saturation and pool temperatures. Physical property data for Freon 113 were obtained from References (5) through (10) and for carbon tetrachloride from References (10) and (11). Physical property data for water were taken from Kreith (12) and from Keenan and Keyes (13).

A listing of the computer output may be found in Table 1.

As a result of the analytical model used, there is a short initial time interval during which the vapor film thickness decreases because of the convective heat losses into the liquid at the vapor-liquid interface in the absence of a conductive heat supply from the vapor film whose temperature has not yet responded to the large wire temperature. As may be seen from Table 1 this phenomenon lasts for approximately five per cent of the transient film boiling period. The decrease in vapor film size is seen to be less than one per cent and is thus negligible during this time interval. This effect may be noted in Figures 13 through 27 where the initial vapor film radius stays essentially constant for a short initial period of time.

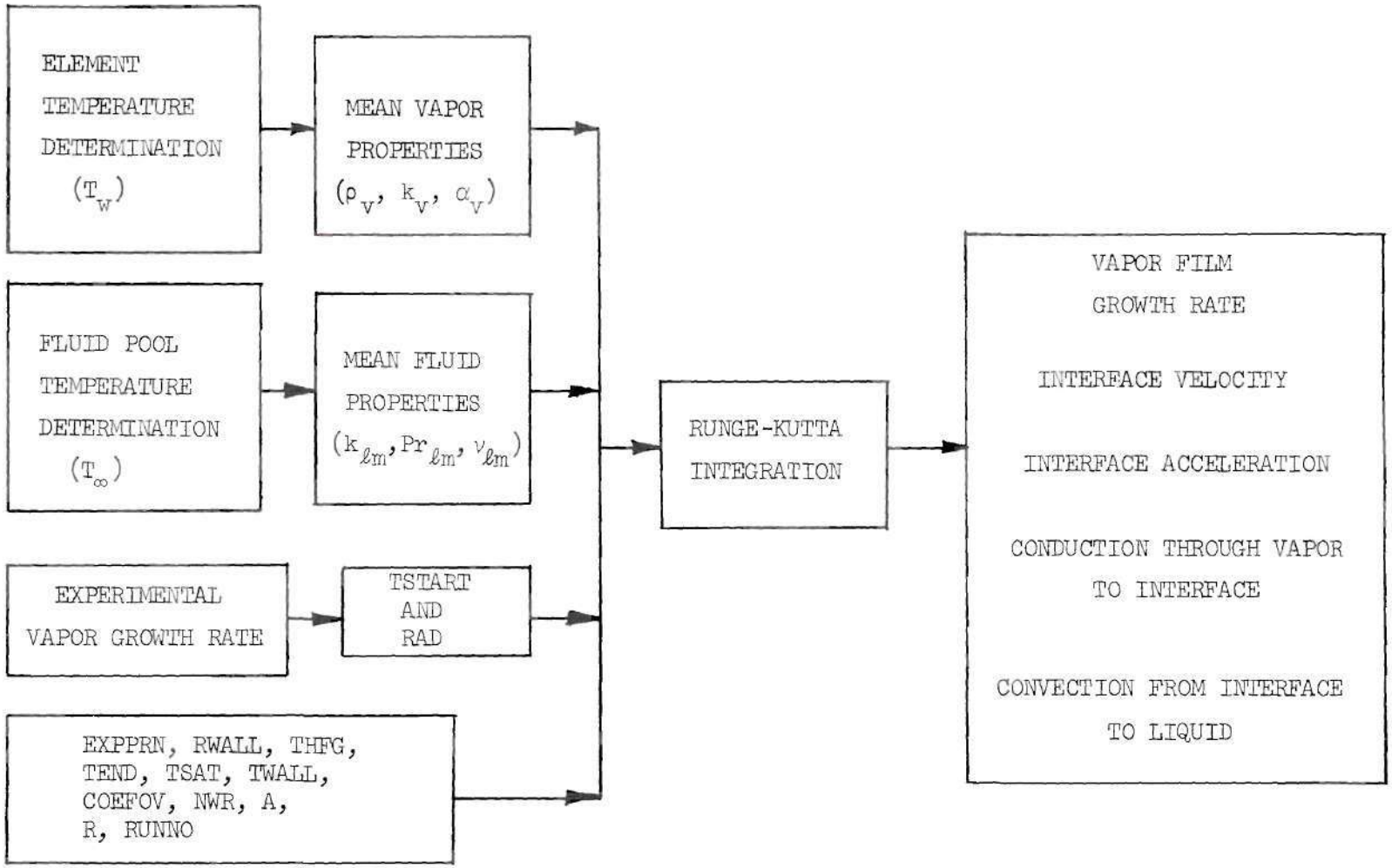

Figure 2. Block Diagram of Input Valves Necessary for Solution of Equation (2.37).

COMPUTER INPUT VALUES

RHOV=	.7880E-04	EXPPRN=	.3100E 00
CONDV=	.3110E-06	DIFFV=	.2450E-01
RWALL=	.5000E-02	CONDLM=	.1214E-05
TVISLM=	.5000E-03	THFG=	83.7000
TSAT=	170.0000	TWALL=	1972.0000
PRDTLM=	4.7300	TLIQ=	157.5000
COEFOV=	2.2000	TEND=	0.0100
TSTART=	.1228E-02	A(1)=	.1000E-03
R(1)=	.1000E-03	Y(1)=	.1048E-01
NWR=	20		

RUN NUMBER= 2

BUBBLE GROWTH HISTORY

TIME (SEC)	BUBBLE RADIUS (IN)	INTFACE VELOCITY (IN/SEC)	CONDUCTION HEAT FLUX AT INTERFACE (BTU/HR SQ-FT)	CONVECTION HEAT FLUX AT INTERFACE (BTU/HR SQ-FT)
.1228E-02	.1048E-01	-.6407E 01	0.	-.2191E 05
.1250E-02	.1041E-01	0.	.1004E-10	0.
.1272E-02	.1041E-01	.2654E-13	.1415E-02	-.1415E-02
.1294E-02	.1041E-01	.5430E-08	.6399E 00	-.6399E 00
.1316E-02	.1041E-01	.2162E-05	.1277E 02	-.1277E 02
.1338E-02	.1041E-01	.7277E-04	.7433E 02	-.7408E 02
.1360E-02	.1041E-01	.7182E-03	.2352E 03	-.2327E 03
.1382E-02	.1041E-01	.3524E-02	.5275E 03	-.5155E 03
.1403E-02	.1041E-01	.1119E-01	.9568E 03	-.9186E 03
.1425E-02	.1041E-01	.2665E-01	.1509E 04	-.1418E 04
.1447E-02	.1041E-01	.5203E-01	.2159E 04	-.1981E 04
.1469E-02	.1041E-01	.8819E-01	.2880E 04	-.2578E 04
.1491E-02	.1041E-01	.1347E 00	.3647E 04	-.3187E 04
.1513E-02	.1042E-01	.1904E 00	.4439E 04	-.3788E 04
.1535E-02	.1042E-01	.2535E 00	.5237E 04	-.4370E 04
.1557E-02	.1043E-01	.3222E 00	.6027E 04	-.4925E 04
.1579E-02	.1044E-01	.3947E 00	.6798E 04	-.5448E 04
.1601E-02	.1045E-01	.4693E 00	.7543E 04	-.5938E 04
.1622E-02	.1046E-01	.5418E 00	.8229E 04	-.6377E 04
.1645E-02	.1047E-01	.6196E 00	.8934E 04	-.6815E 04
.1667E-02	.1049E-01	.6932E 00	.9574E 04	-.7204E 04
.2105E-02	.1102E-01	.1544E 01	.1577E 05	-.1049E 05
.2544E-02	.1173E-01	.1656E 01	.1618E 05	-.1052E 05
.2982E-02	.1245E-01	.1582E 01	.1540E 05	-.9989E 04
.3421E-02	.1312E-01	.1477E 01	.1445E 05	-.9400E 04
.3860E-02	.1374E-01	.1375E 01	.1356E 05	-.8861E 04
.4298E-02	.1432E-01	.1284E 01	.1278E 05	-.8388E 04
.4737E-02	.1487E-01	.1205E 01	.1210E 05	-.7976E 04
.5175E-02	.1538E-01	.1136E 01	.1150E 05	-.7615E 04
.5614E-02	.1587E-01	.1076E 01	.1098E 05	-.7297E 04
.6053E-02	.1633E-01	.1024E 01	.1052E 05	-.7015E 04
.6491E-02	.1677E-01	.9770E 00	.1010E 05	-.6763E 04
.6930E-02	.1719E-01	.9353E 00	.9734E 04	-.6536E 04
.7368E-02	.1759E-01	.8980E 00	.9401E 04	-.6331E 04
.7807E-02	.1797E-01	.8643E 00	.9099E 04	-.6144E 04
.8246E-02	.1835E-01	.8336E 00	.8823E 04	-.5972E 04
.8684E-02	.1871E-01	.8057E 00	.8569E 04	-.5815E 04
.9123E-02	.1905E-01	.7801E 00	.8336E 04	-.5669E 04
.9561E-02	.1939E-01	.7565E 00	.8121E 04	-.5534E 04
.1000E-01	.1972E-01	.7347E 00	.7920E 04	-.5408E 04

Table 1. Computer Output Listing.

BUBBLE VELOCITY AND ACCELERATION

TIME (SEC)	INTFACE VELOCITY (IN/SEC)	INTFACE ACCELERATION (IN/SEC-SQ)
.1228E-02	-.6407E 01	.4382E 06
.1250E-02	0.	.1461E 06
.1272E-02	.2654E-13	.1238E-03
.1294E-02	.5430E-08	.4928E-01
.1316E-02	.2162E-05	.1659E 01
.1338E-02	.7277E-04	.1633E 02
.1360E-02	.7182E-03	.7868E 02
.1382E-02	.3524E-02	.2387E 03
.1403E-02	.1119E-01	.5272E 03
.1425E-02	.2665E-01	.9312E 03
.1447E-02	.5203E-01	.1403E 04
.1469E-02	.8819E-01	.1885E 04
.1491E-02	.1347E 00	.2331E 04
.1513E-02	.1904E 00	.2709E 04
.1535E-02	.2535E 00	.3006E 04
.1557E-02	.3222E 00	.3219E 04
.1579E-02	.3947E 00	.3353E 04
.1601E-02	.4693E 00	.3352E 04
.1623E-02	.5418E 00	.3426E 04
.1645E-02	.6196E 00	.3452E 04
.1667E-02	.6932E 00	.3258E 04
.2105E-02	.1544E 01	.1097E 04
.2544E-02	.1656E 01	.4376E 02
.2982E-02	.1582E 01	-.2041E 03
.3421E-02	.1477E 01	-.2366E 03
.3860E-02	.1375E 01	-.2195E 03
.4298E-02	.1284E 01	-.1933E 03
.4737E-02	.1205E 01	-.1683E 03
.5175E-02	.1136E 01	-.1466E 03
.5614E-02	.1076E 01	-.1285E 03
.6053E-02	.1024E 01	-.1133E 03
.6491E-02	.9770E 00	-.1007E 03
.6930E-02	.9353E 00	-.9003E 02
.7368E-02	.8980E 00	-.8103E 02
.7807E-02	.8643E 00	-.7336E 02
.8246E-02	.8336E 00	-.6676E 02
.8684E-02	.8057E 00	-.6106E 02
.9123E-02	.7801E 00	-.5608E 02
.9561E-02	.7565E 00	-.5173E 02
.1000E-01	.7347E 00	-.4765E 02

Table 1. Computer Output Listing (Continued).

CHAPTER IV

EXPERIMENTAL EQUIPMENT

General Requirements for the Experimental Apparatus

In order to accomplish the goals of this research a system was needed that satisfied three main requirements: (a) provision for extremely rapid energy transfer to the heating element to minimize the time spent in the nucleate boiling regime, (b) the capability of monitoring the temperature history of the heating element, and (c) a means to determine the growth rate of the vapor film.

A discussion of the transient film boiling system electrical design, heating element temperature measurement system, Wheatstone bridge design, temperature calibration equipment, and photographic equipment may be found in Chapter II of Reference 2.

Test Container Description

The test tank was constructed from a bored-out piece of aluminum 2 inches thick by 9 inches square as shown in Figure 3. One-half inch thick glass plates, seven inches in diameter, were mounted on both sides of the aluminum to form the container for the test fluid. The actual fluid containing cavity measured six inches in diameter and two inches in width. An immersion resistance type heater was mounted in the container to control the liquid pool temperature. The liquid pool temperature was monitored by means of a copper constantan thermocouple extending into the fluid. A pressure gauge was provided to enable

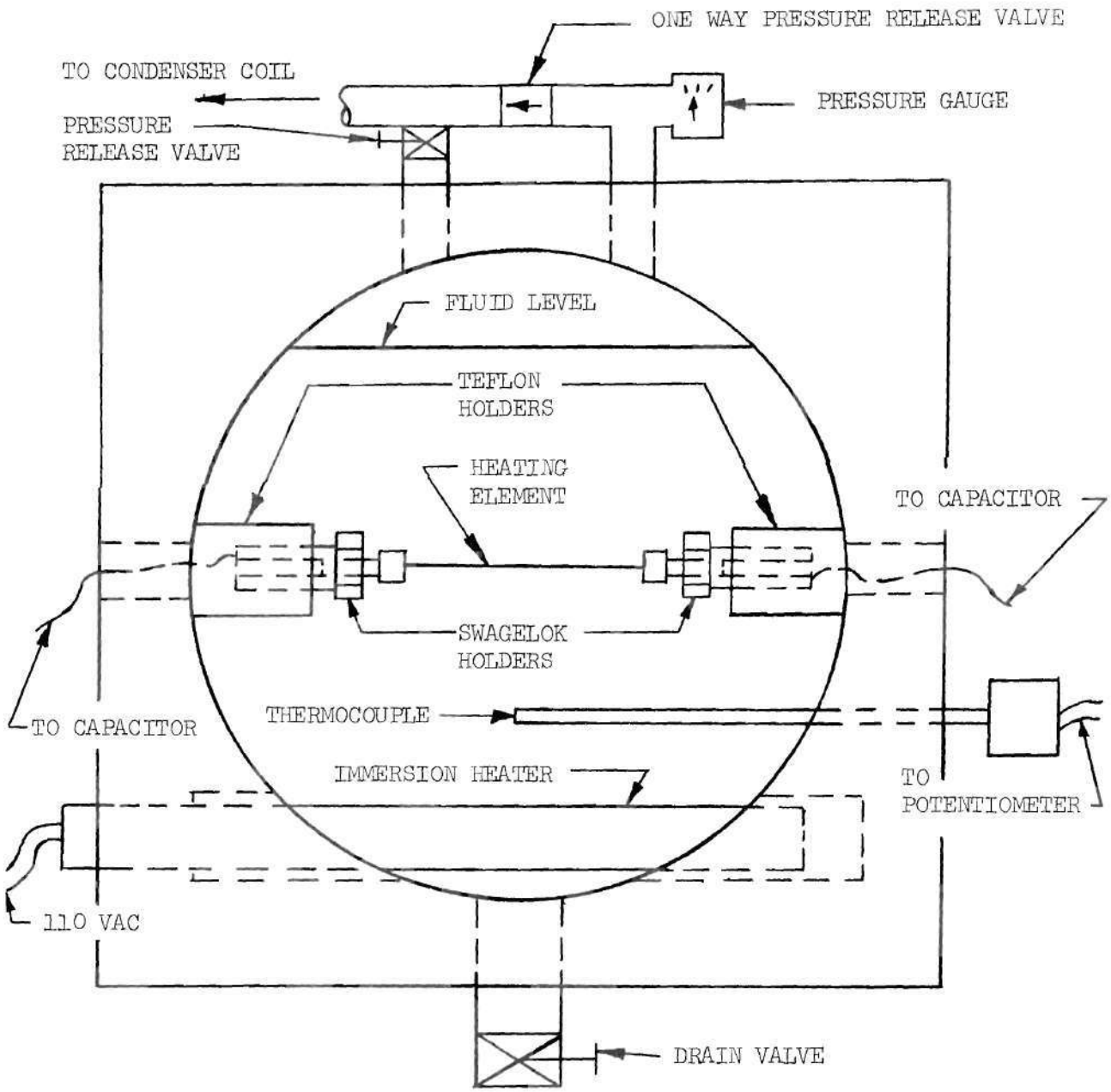

Figure 3. Test Container Design.

monitoring of the pressure within the test container. The fluid vapor that boiled off was condensed in a copper coil immersed in a cooling bath. The whole test tank apparatus was placed inside of an exhaust hood to draw off the toxic vapors that might escape. The one-way pressure release valve was provided as a safety device to insure that excessive pressures did not build up within the test container.

Saturation pool boiling could be obtained by adjusting the energy input through the immersion heater and adjusting the vapor outflow by means of the pressure release valve at the top of the test container. When the pool temperature exceeded slightly the saturation temperature level the pressure gauge would indicate a small excess pressure above atmospheric pressure. The energy input would then be stopped and the test run would be made when the pool cooled to its saturation temperature and had zero pressure.

Heating Wire Selection

Besides the material characteristics such as:

1. Large resistance change with temperature
2. Monotonically increasing resistance change with temperature
3. Good brazing qualities
4. High melting temperature
5. High resistance to corrosion

that were considered by Pitts (2), a high wire emissivity was desired in order to enhance effects of radiation.

After a rather thorough literature search of thermo-physical properties it was decided to investigate Hastelloy C and Nichrome V as

possible heating wires.

Hastelloy C was favored due to its high emissivity after it had been oxidized by heating in air for two hours at 2200° F. The oxidized wire then possessed an emissivity of approximately 0.95 for a wire temperature between 1300 - 1900° F. It was found, however, to give erratic oscilloscope readings after energy had been discharged into it during the course of preliminary runs, and thus was judged unsuitable for use as the heating wire.

Nichrome V may also be oxidized to form a surface with high emissivity at the wire temperature of interest. After oxidization of the very small diameter wire (0.010 inches) was completed the oxide was found to be brittle and subsequently flaked from the wire surface.

Thus, after much preliminary work it was decided to forgo experimental results of the radiation effect and instead analytically predict its effect. Commercially pure platinum wire was selected as the heating wire material because of its proven use in the previous investigations.

Pool Temperature Measurement System

The two main elements of the pool temperature measurement system are:

- Copper-constantan thermocouple mounted inside of one-eighth inch diameter stainless steel tubing
- Leeds and Northrup Potentiometer, Philadelphia, Pennsylvania, Catalog No. 8687, Serial No. 106145

The thermocouple was mounted centrally within the pool, halfway between the immersion pool heater and the heating element, as shown in

Figure 3. The thermocouple emf was read on the potentiometer to determine the pool temperature for each test.

CHAPTER V

EXPERIMENTAL PROCEDURE

Temperature Calibration

Temperature calibration was carried out in a manner described in Chapter III of Reference 2. A total of eight heating elements were calibrated during the course of this investigation. Only five of these elements were actually used during the transient film boiling experiments. Calibration data for these five elements and element descriptive information is given in Appendix G.

Transient Film Boiling Experiments

The general procedure for the film boiling tests may be found in Chapter III of Reference 2. A schematic of the general experiment arrangement may be seen in Figure 4.

The resistance that had been added to the wiring circuit by the heating element holder apparatus introduced a possible source of error. This resistance was measured with a Wheatstone bridge and its effect on the final element temperature was calculated and corrected for. If uncorrected, this resistance could have introduced an error of approximately seven per cent in the element temperature determination.

As calculated in Appendix F, the probable error for a single element temperature measurement, neglecting the effect of the copper lead wires during calibration and the effect of the element holder apparatus during the test runs, was 5.43 per cent.

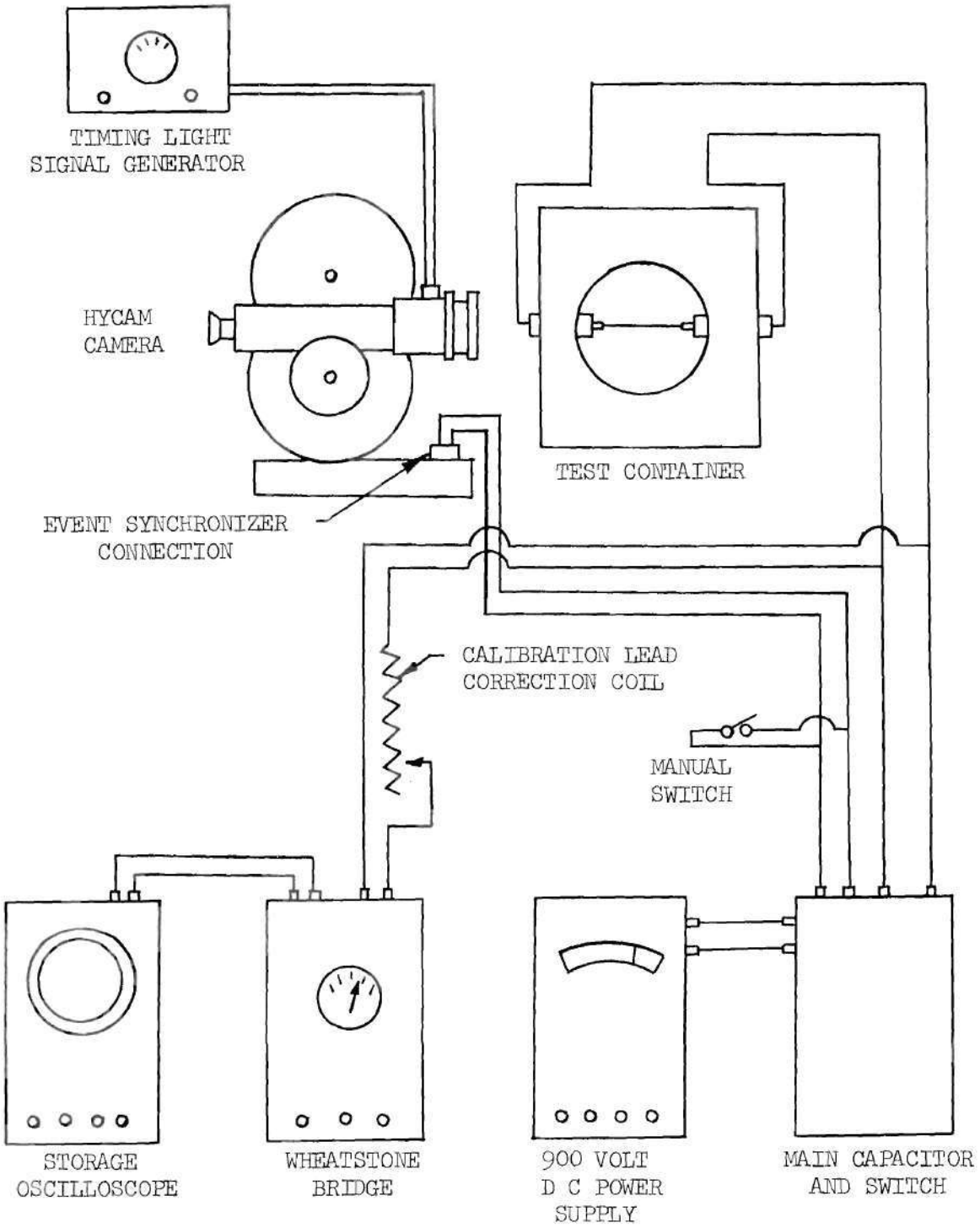

Figure 4. Schematic of General Experiment Arrangement.

Pertinent data from each test are presented in Tables 6 and 7 in Appendix G for the successful experiments.

A total of 26 filmed tests were made. Data were obtained from 18 of these tests and are reported in this thesis. A summary of the tests that did not yield results follows:

Run No. 4 -- This test was conducted with the pool liquid temperature too cold to yield measurable film growth rates.

Run No. 11, 12, 13, and 14 -- The voltage input to the timing signal generator was insufficient to give timing dots on the film.

Run No. 15, 17, and 18 -- Pressure above one atmosphere was developed within the test container. This tended to suppress the vapor growth and did not yield measurable film growth rates.

Data Reduction

Data reduction was accomplished in a manner described in Chapter III of Reference 2. A Bell and Howell model 173 projector was used to project the test film onto a white surface from which vapor film diameter measurements were taken. As calculated in Appendix F, the probable error for a single diameter measurement is 8.7 per cent. This method of diameter determination involved the assumption that the vapor film could be represented as a body of revolution. Thus, the volume could be approximated by measuring the diameter at prescribed intervals along the length of the wire, calculating the area at each

of these stations, multiplying this area by the distances between stations to form a volume, and then summing the total of the incremental volumes thus formed. This may be expressed mathematically as

$$V = \sum_{i=1}^{n} \frac{\pi}{4} D_i^2 \Delta\ell_i$$

where

$$\Delta\ell_1 = \Delta\ell_2 = \ldots.$$

Wire diameter measurements were taken from the last frame of the film with no vapor film present and this was considered to be the zero for the current experiment. Since the framing rate of the camera was approximately 4,000 frames per second, for all tests the zero time location could at most be in error by one-fourth millisecond. The next frame was then analyzed as was each succeeding fourth frame. The analysis was continued until approximately forty frames of film had been analyzed. This covered an interval of about ten milliseconds after which vapor breakaway from the wire began to occur.

CHAPTER VI

DISCUSSION OF RESULTS

The heating element temperature and vapor film growth rate were determined for the fluids used. Both the conductive heat transfer through the vapor phase into the vapor-liquid interface and the convective heat transfer from the vapor-liquid interface into the liquid phase were calculated numerically.

Temperature Determination

The Wheatstone bridge and oscilloscope system (see Chapter IV) provided a means for determining the heating element temperature as a function of time. A typical plot of heating element temperature versus time is presented in Figure 5. The element temperature change was initiated by the capacitor discharge and was better than 99 per cent complete at the end of 145 microseconds.

The recorded temperature data were used to obtain a mean element temperature for each test run. Since the transient film boiling period was ten milliseconds in length the mean temperature was defined as the element temperature at five milliseconds following capacitor discharge. The mean element temperature was then used in the vapor growth rate and heat transfer calculations reported herein.

Experimental Vapor Growth Data

The experimental vapor formation data are summarized in Table 2. The vapor cylinder radius at nine milliseconds is given for each of the

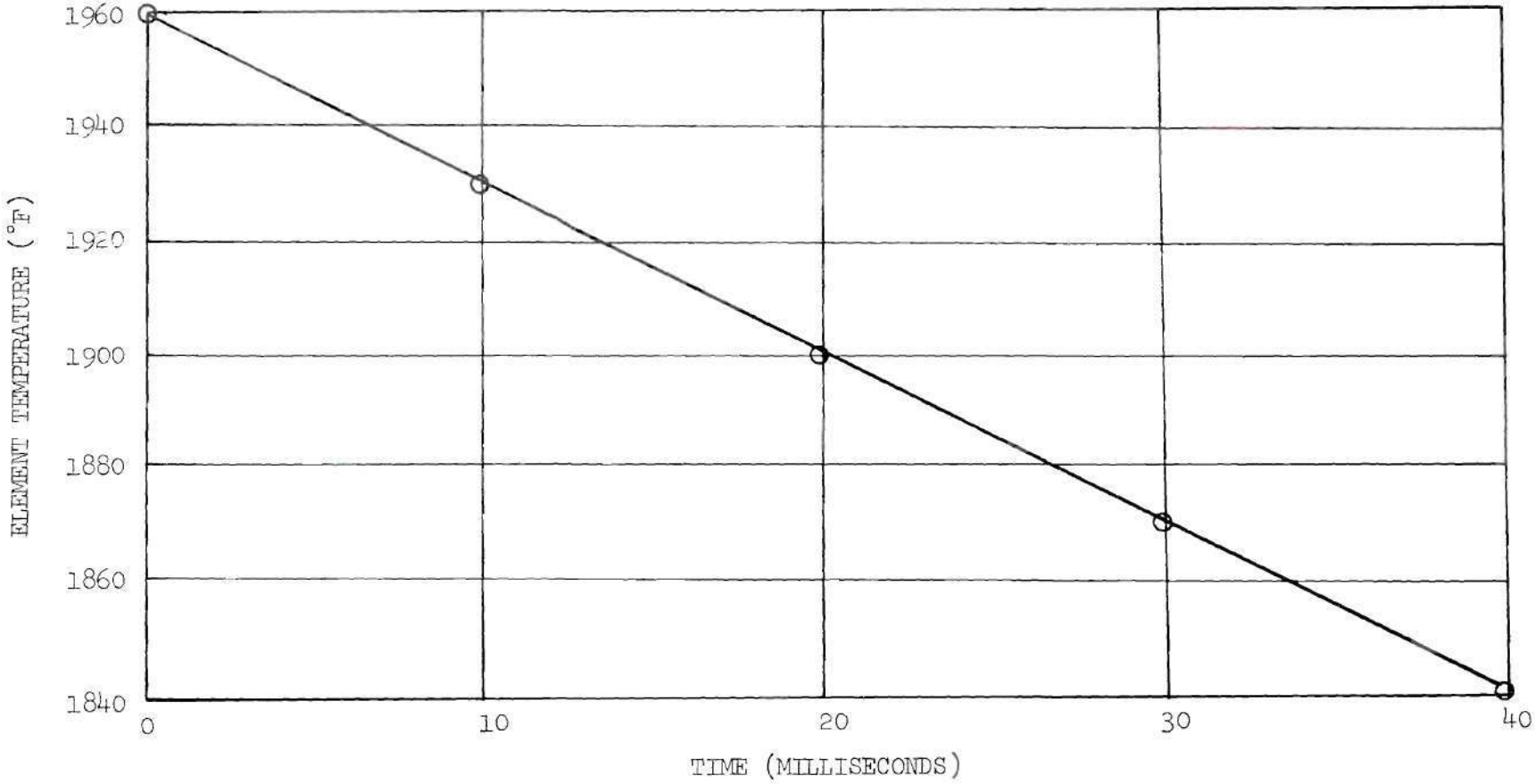

Figure 5. Heating Element Temperature versus Time Recorded During Run No. 1.

Table 2. Experimental Vapor Cylinder Radius Study.

ΔT $(T_W - T_{SAT})$ (°F)	T_∞ (°F)	Wire Diameter (inches)	Run Number	Vapor Cylinder Radius at 9 Millisec. (inches)
Fluid: Carbon Tetrachloride				
1775	170.0	0.010	1	0.0235
1802	157.7	0.010	2	0.0180
1768	153.9	0.010	3	0.0190
1744	168.9	0.010	5	0.0255
1180	168.9	0.010	6	0.0165
1315	169.0	0.010	7	0.0230
1382	169.0	0.010	8	0.0250
1325	164.6	0.010	9	0.0210
1350	163.2	0.010	10	0.0185
Fluid: Water				
1263	212.0	0.010	16	0.0275
1265	210.9	0.0098	5*	0.0255
1468	210.9	0.0098	9*	0.0335
1343	194.0	0.0098	8**	0.0125
1108	205.0	0.0126	20**	0.0165

Table 2. Experimental Vapor Cylinder Radius Study (Continued).

ΔT $(T_w - T_{SAT})$ (°F)	T_∞ (°F)	Wire Diameter (inches)	Run Number	Vapor Cylinder Radius at 9 Millisec. (inches)
Fluid: Freon 113				
1253	111.2	0.010	19	0.0185
1302	111.2	0.010	20	0.0170
1306	104.3	0.010	21	0.0165
1432	116.7	0.010	22	0.0235
1458	117.1	0.010	23	0.0235
1462	103.4	0.010	24	0.0190
1403	102.6	0.010	25	0.0170
1463	110.5	0.010	26	0.0185

*Reference 2.
**Reference 3.

18 film boiling experiments as well as for several runs recorded in References 2 and 3. These data were obtained by drawing a "best fit" curve through the experimental data points.

An initial burst of vapor was observed at the beginning of each of the filmed tests. This vapor was nucleate in character and somewhat opaque while the vapor found later was transparent. It was thus seen that during the initial period nucleate boiling took place. The first frame that showed a transparent vapor was considered to be the start of the transient film boiling process and all numerical calculations were started using the corresponding value of time and vapor radius.

As shown in Figures 6 through 10, and Table 2, many of the tests were made to verify the repeatability of the experimental results under the same conditions. Not all of the test results were compared with numerical solutions. Instead, representative runs were selected to be analytically verified and the comparisons are presented graphically in Figures 13 through 23. Results from References 2 and 3 were also included and are presented in Figures 24 through 27.

Pictures of the vapor film from run number 22 are shown in Figure 11. These pictures show no noticeable end effect near the wire holder. The pictures cover only the first ten milliseconds, since after this initial period is over stable film boiling and film break-away from the wire occurs.

Nusselt-Relation for Convection and its Effect on Vapor Growth

Equation (2.37) was programmed for a Burrough 5500 digital computer and solved by means of Runge-Kutta integration for each

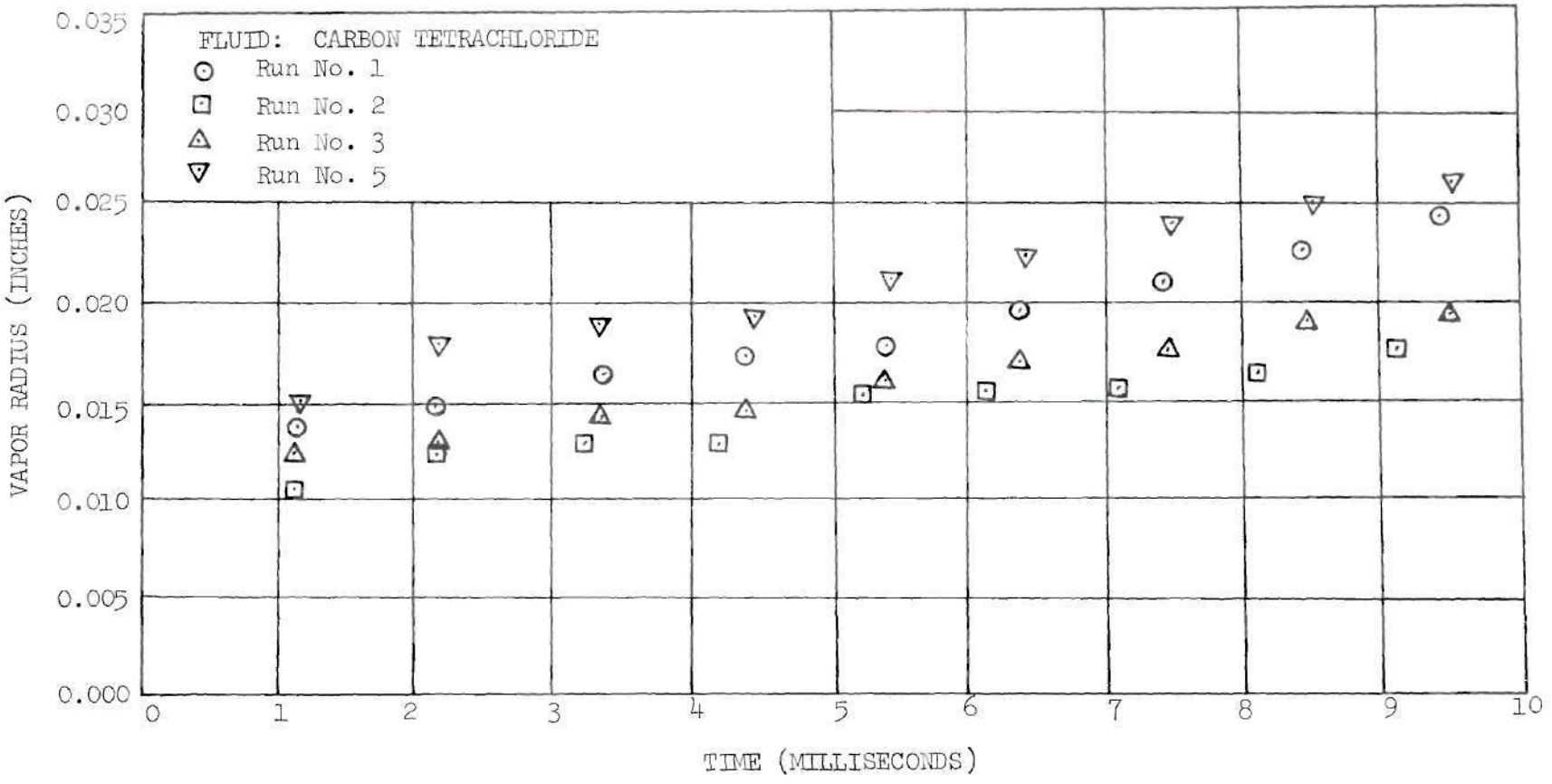

Figure 6. Vapor Radius versus Time for Runs No. 1, 2, 3, and 5 from Experimental Data. $r_w = 0.005$ in.

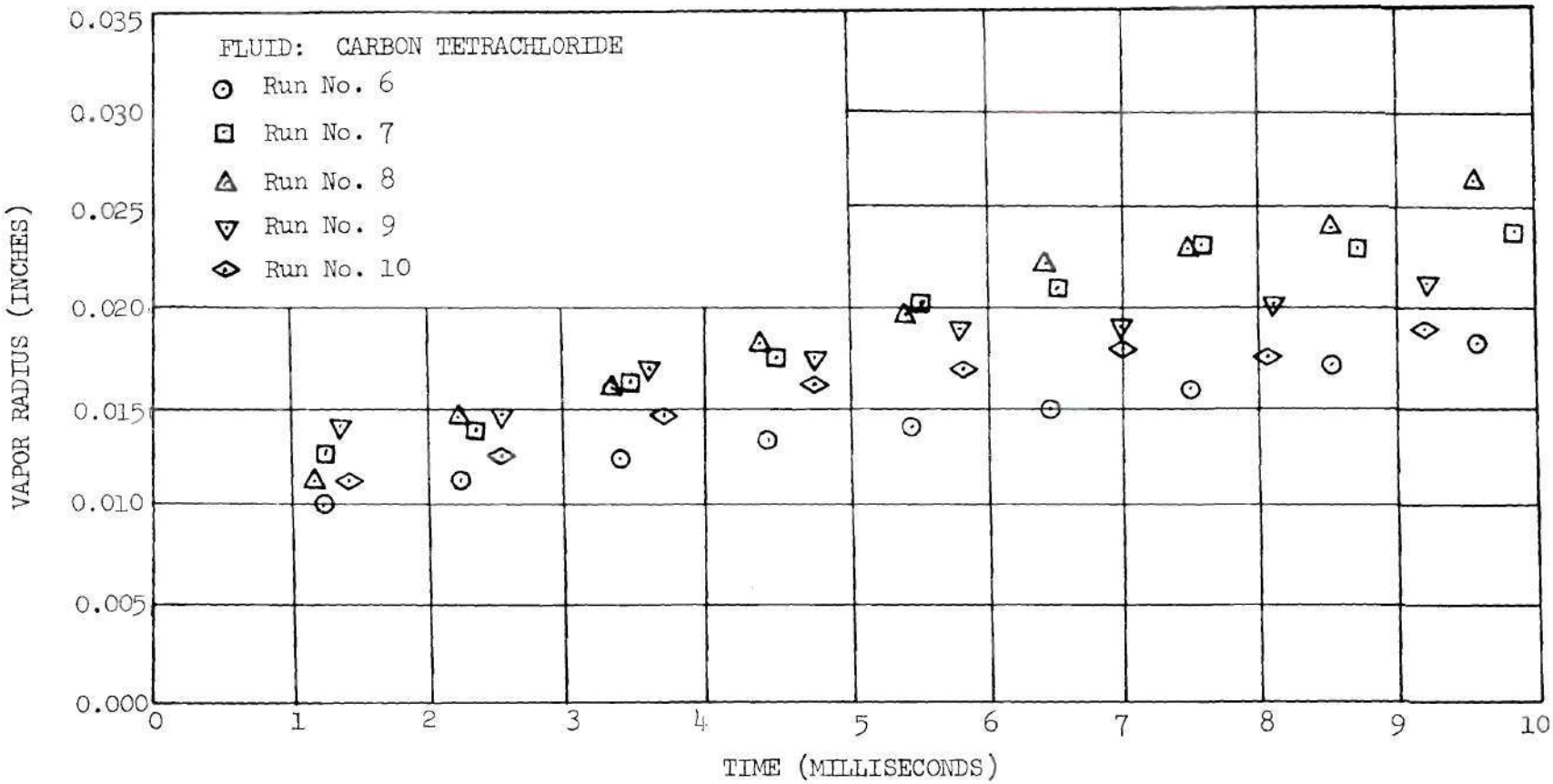

Figure 7. Vapor Radius versus Time for Runs No. 6, 7, 8, 9, and 10 from Experimental Data. $r_w = 0.005$ in.

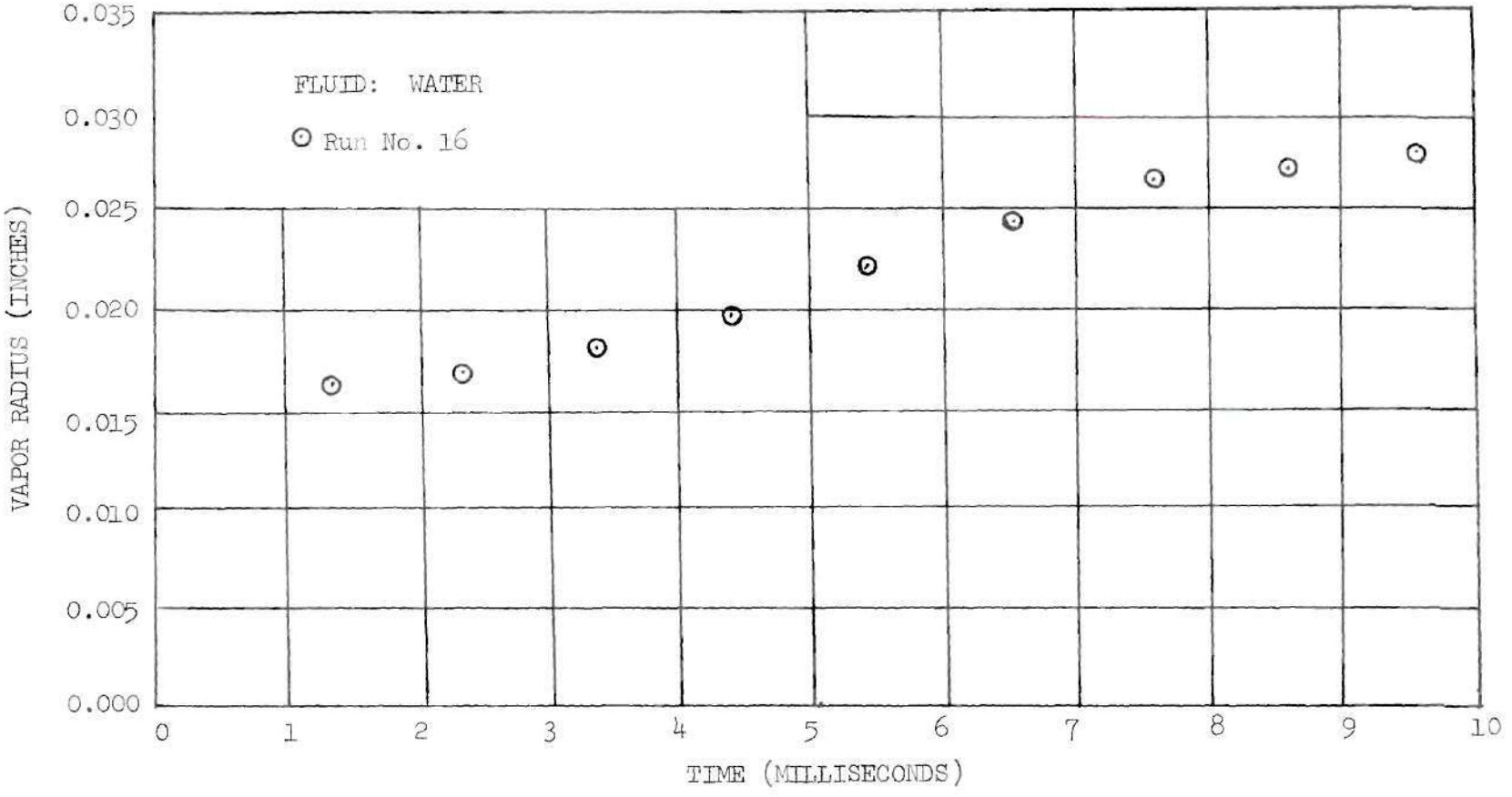

Figure 8. Vapor Radius versus Time for Run No. 16.
$r_w = 0.005$ in.

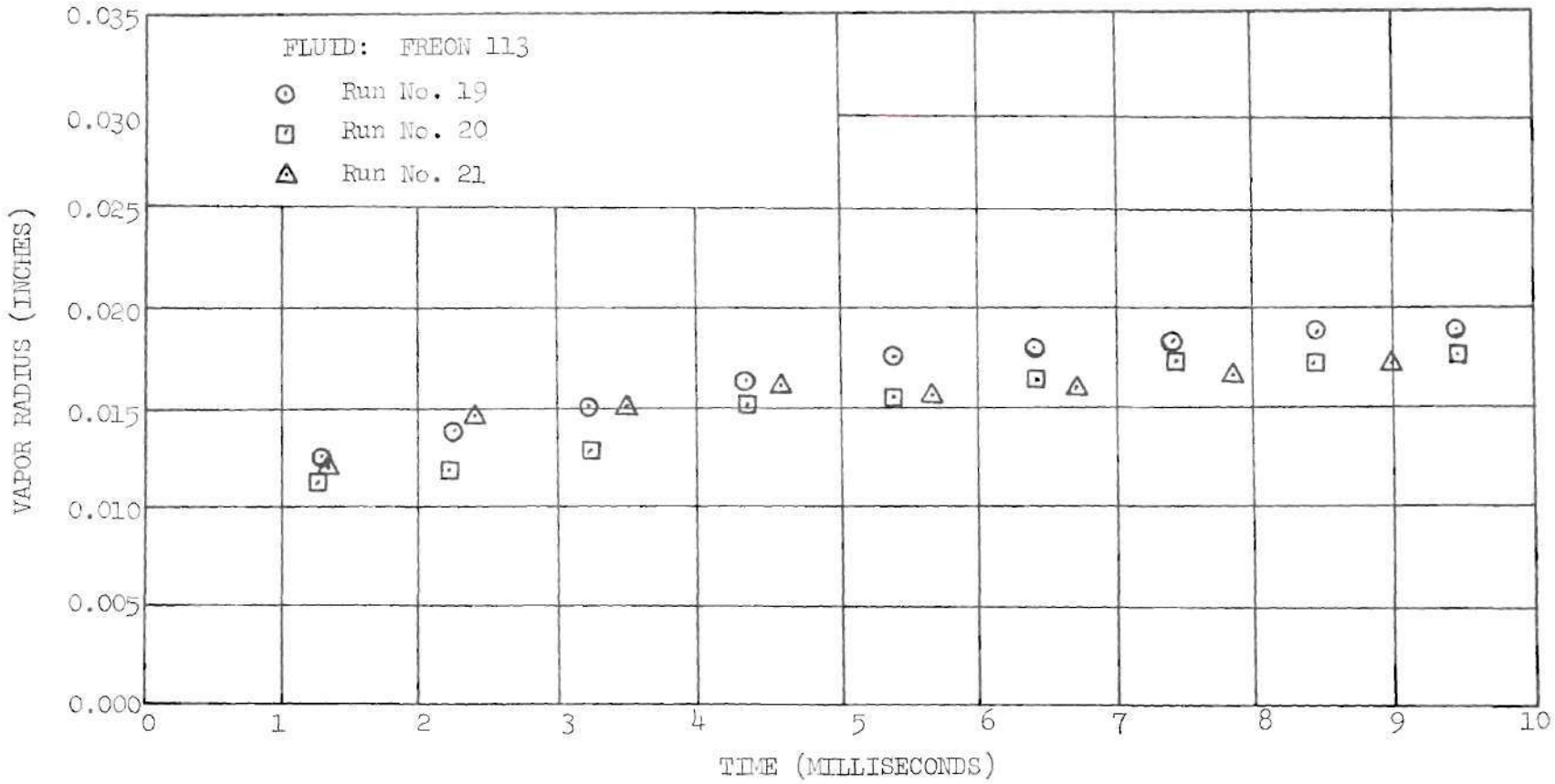

Figure 9. Vapor Radius versus Time for Runs No. 19, 20, and 21 from Experimental Data. $r_w = 0.005$ in.

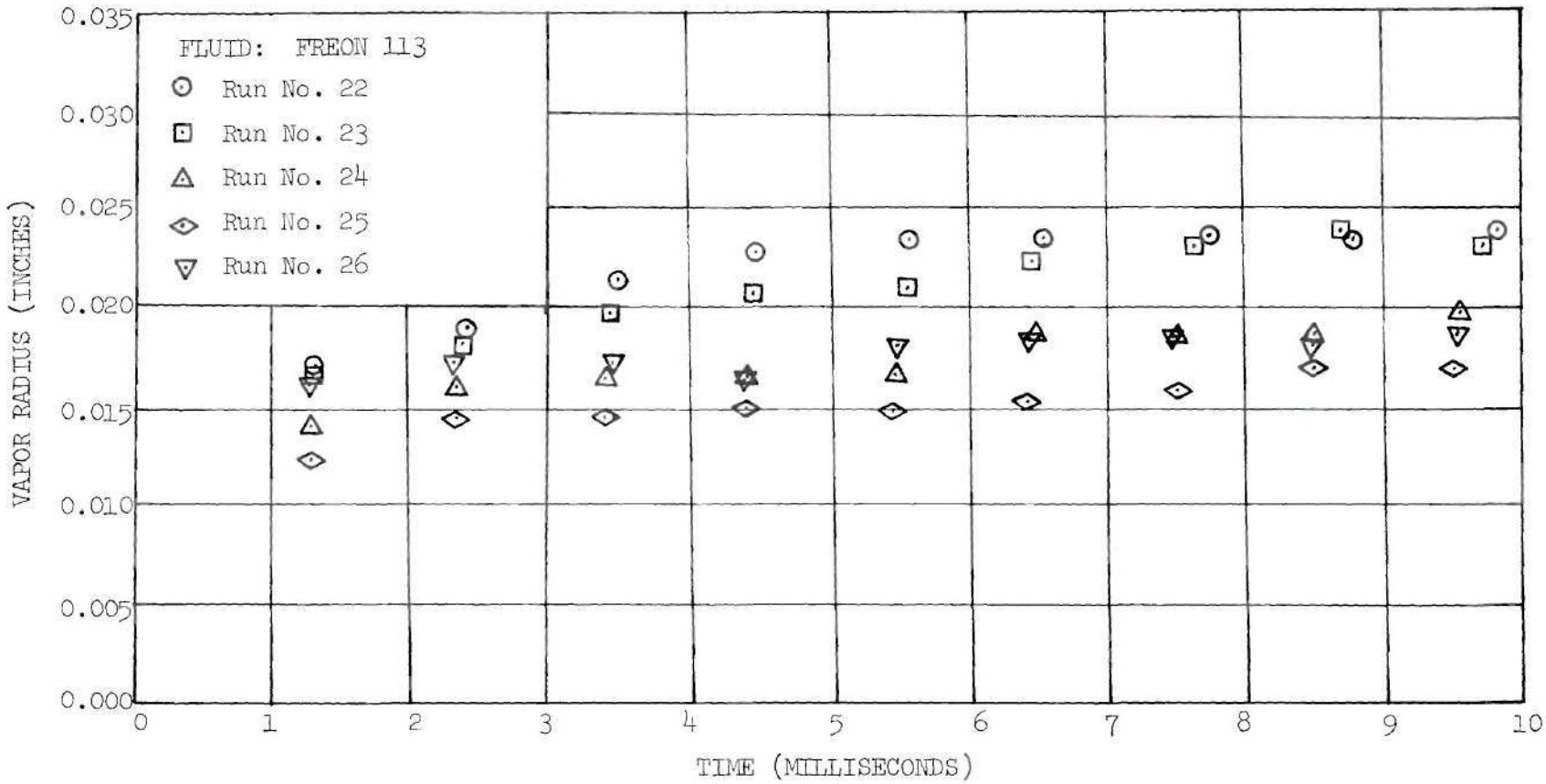

Figure 10. Vapor Radius versus Time for Runs No. 22, 23, 24, 25, and 26 from Experimental Data. $r_w = 0.005$ in.

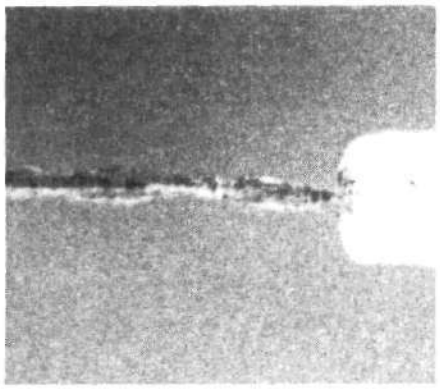

$\theta = 1.334 \times 10^{-3}$ sec

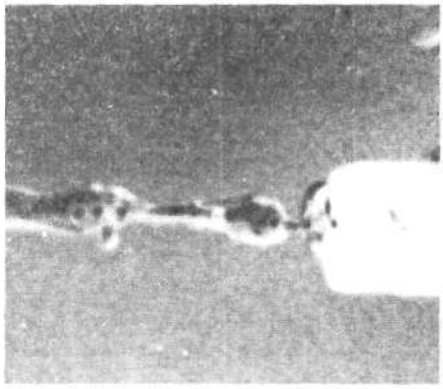

$\theta = 5.334 \times 10^{-3}$ sec

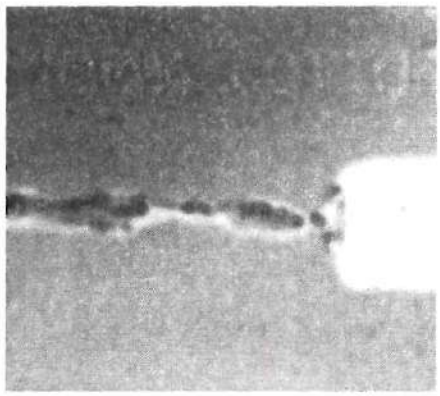

$\theta = 2.667 \times 10^{-3}$ sec

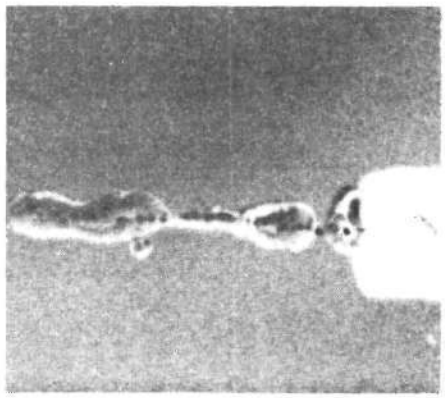

$\theta = 6.668 \times 10^{-3}$ sec

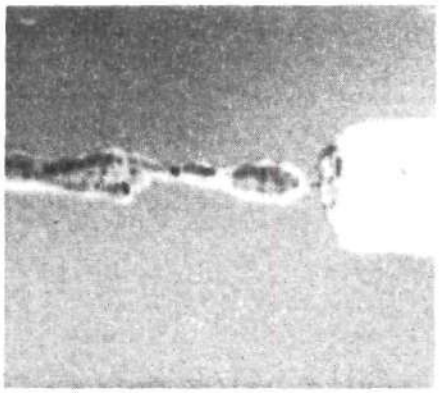

$\theta = 4.001 \times 10^{-3}$ sec

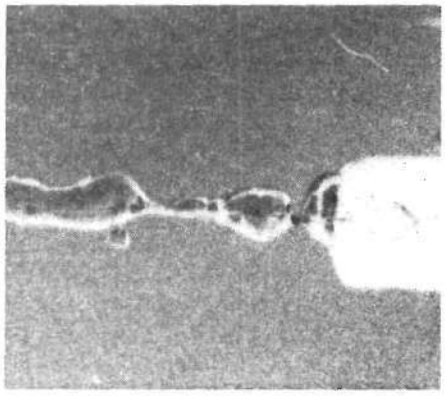

$\theta = 8.001 \times 10^{-3}$ sec

Figure 11. Sequence Photographs Showing Typical End Effects During Transient Film Boiling on a Horizontal Platinum Wire.

representative run of this investigation.

At the start of the numerical solution process the value of c, the coefficient in the Nusselt relationship of Equation (2.29), was varied to determine if some value other than c = 1.2 would yield better agreement between theory and experiment. It was found that the final value of vapor film radius at ten milliseconds depended on c as is shown in Figure 12. The ratio of the analytical to the experimental maximum vapor film radius for the three cases (runs 2, 16, and 23) of essentially saturated pool conditions had an average value of 1.08. Here, c has not effect, since with the present model, the convective heat transfer reduces to zero and thus the ratio should have been 1.0. Because of this the value of c was selected that gave a mean value of 1.08 for all remaining tests. This value was found to be C = 2.2. All test runs were then solved numerically using c = 2.2 and the results are presented in Figures 13 through 27 along with the experimental data. The experimental data shown in Figures 24 through 27 were obtained from References 2 and 3. The mean deviation between theory and experiment was calculated to be approximately 9 per cent.

Thermal Decomposition of Test Fluid

Thermal decomposition was minimal under the conditions encountered in this investigation. The extremely short time period during which the vapor was at its elevated temperature was not long enough to produce the thermal decompositions shown in References 14 and 15. The total time that the heating element temperature was higher than the pool temperature was approximately nine-tenths of a second for a test run.

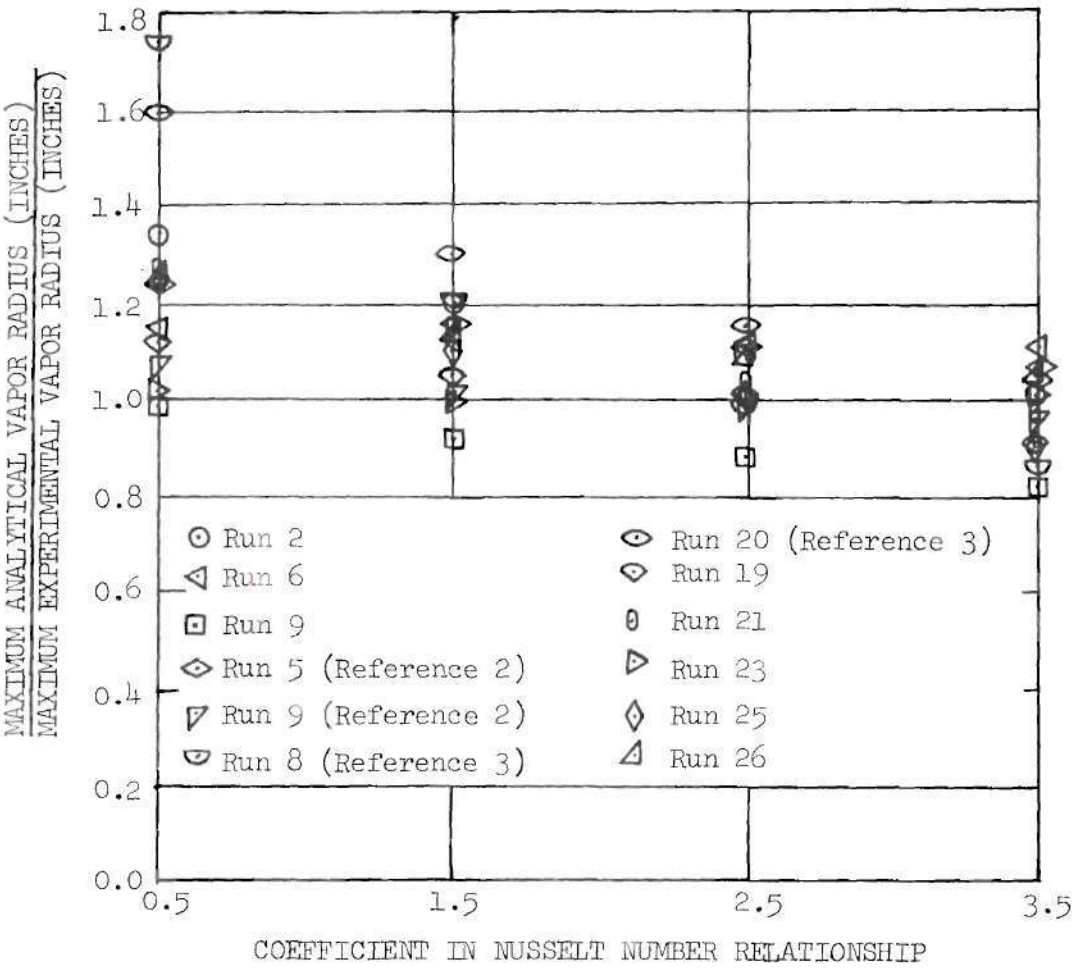

Figure 12. Ratio of Analytical to Experimental Maximum Vapor Film Radius versus Coefficient in Nusselt Number Relationship (COEFOV).

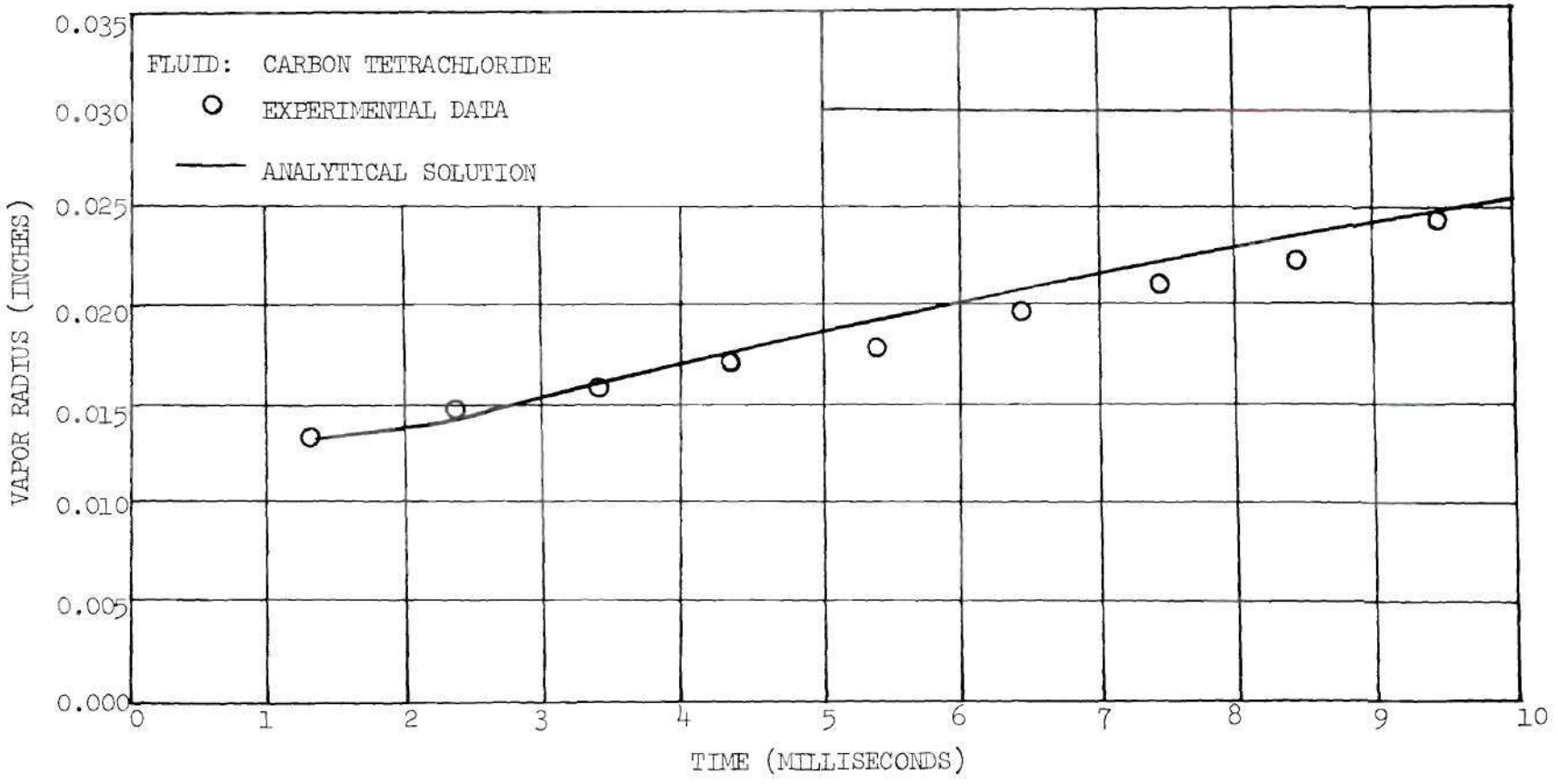

Figure 13. Plot of Vapor Radius as a Function of Time for Run 1.

$T_w = 1945°$ F $\quad T_\infty = 170°$ F

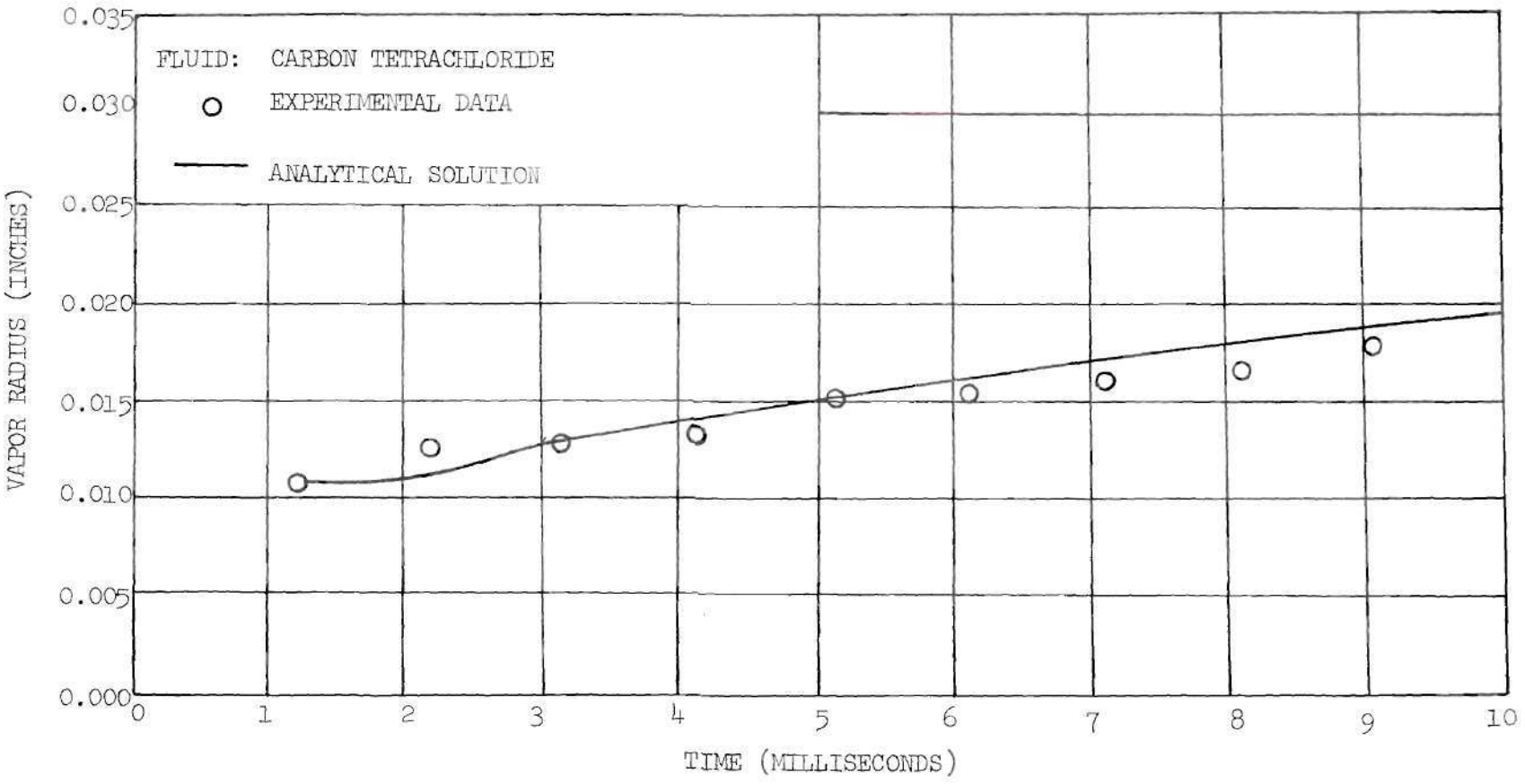

Figure 14. Plot of Vapor Radius as a Function of Time for Run 2.

$T_w = 1972°$ F $\quad T_\infty = 157.7°$ F

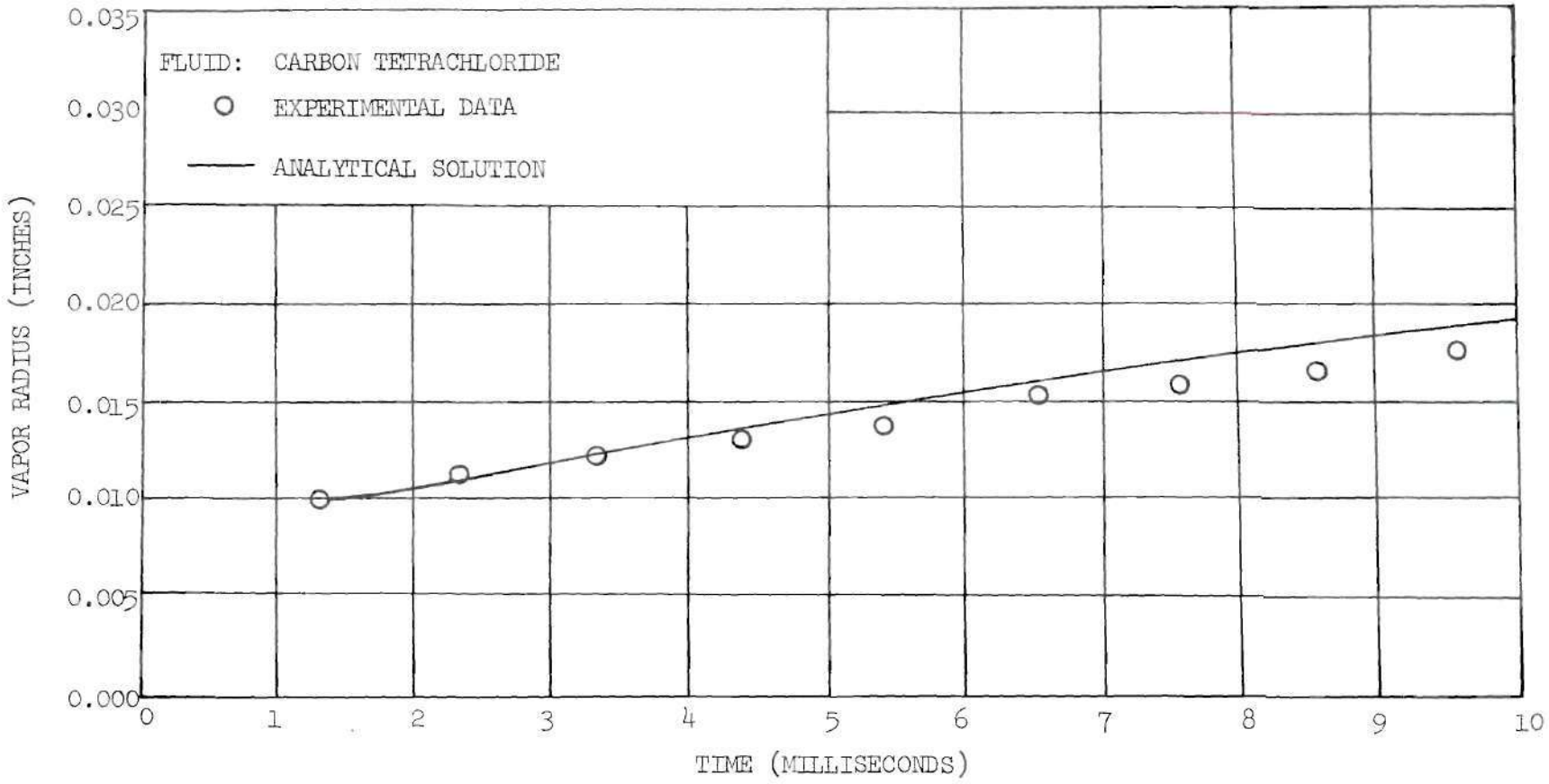

Figure 15. Plot of Vapor Radius as a Function of Time for Run 6.

$T_w = 1350°$ F $\quad T_\infty = 168.9°$ F

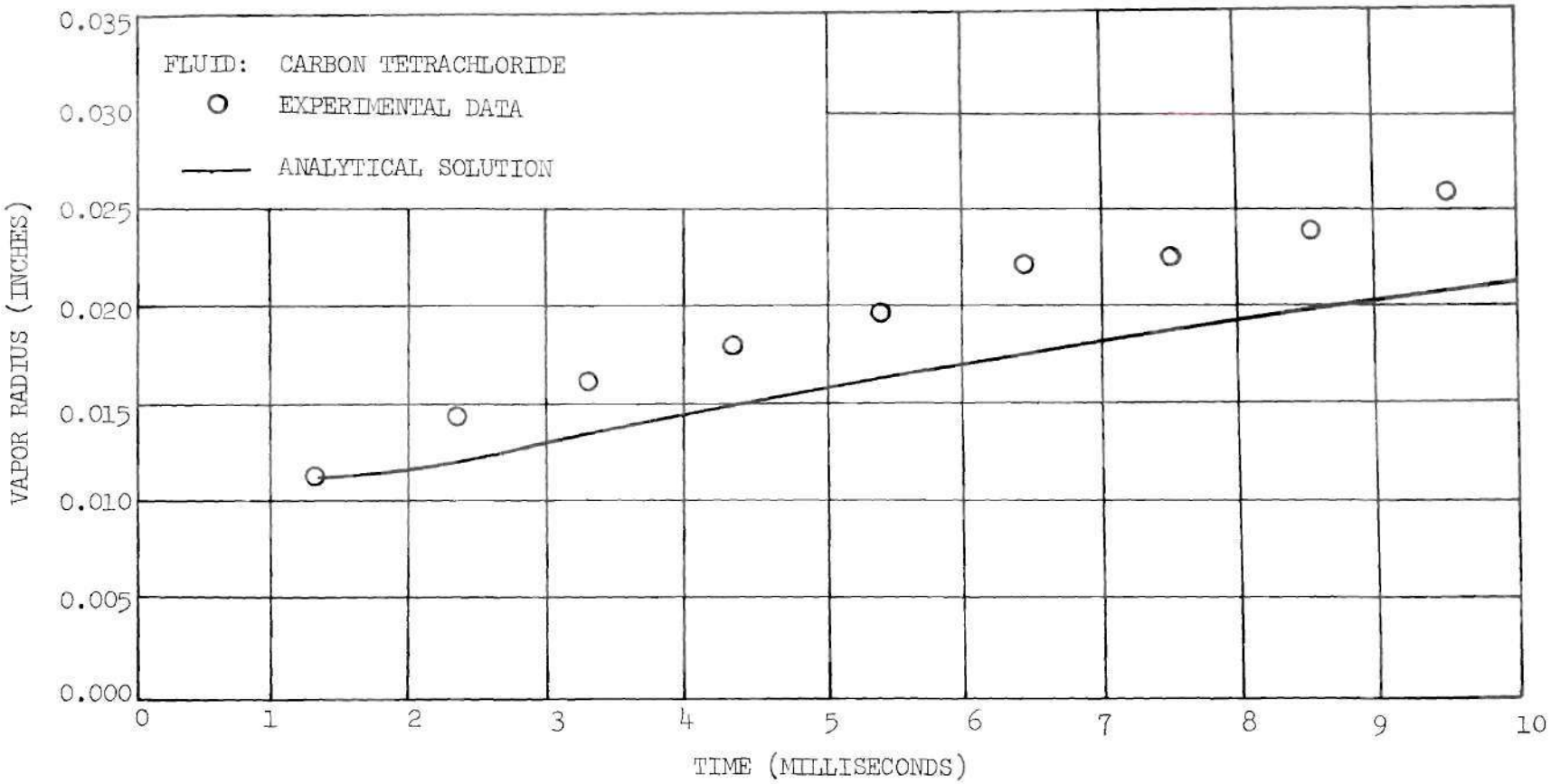

Figure 16. Plot of Vapor Radius as a Function of Time for Run 8.

$T_w = 1552^\circ$ F $T_\infty = 169^\circ$ F

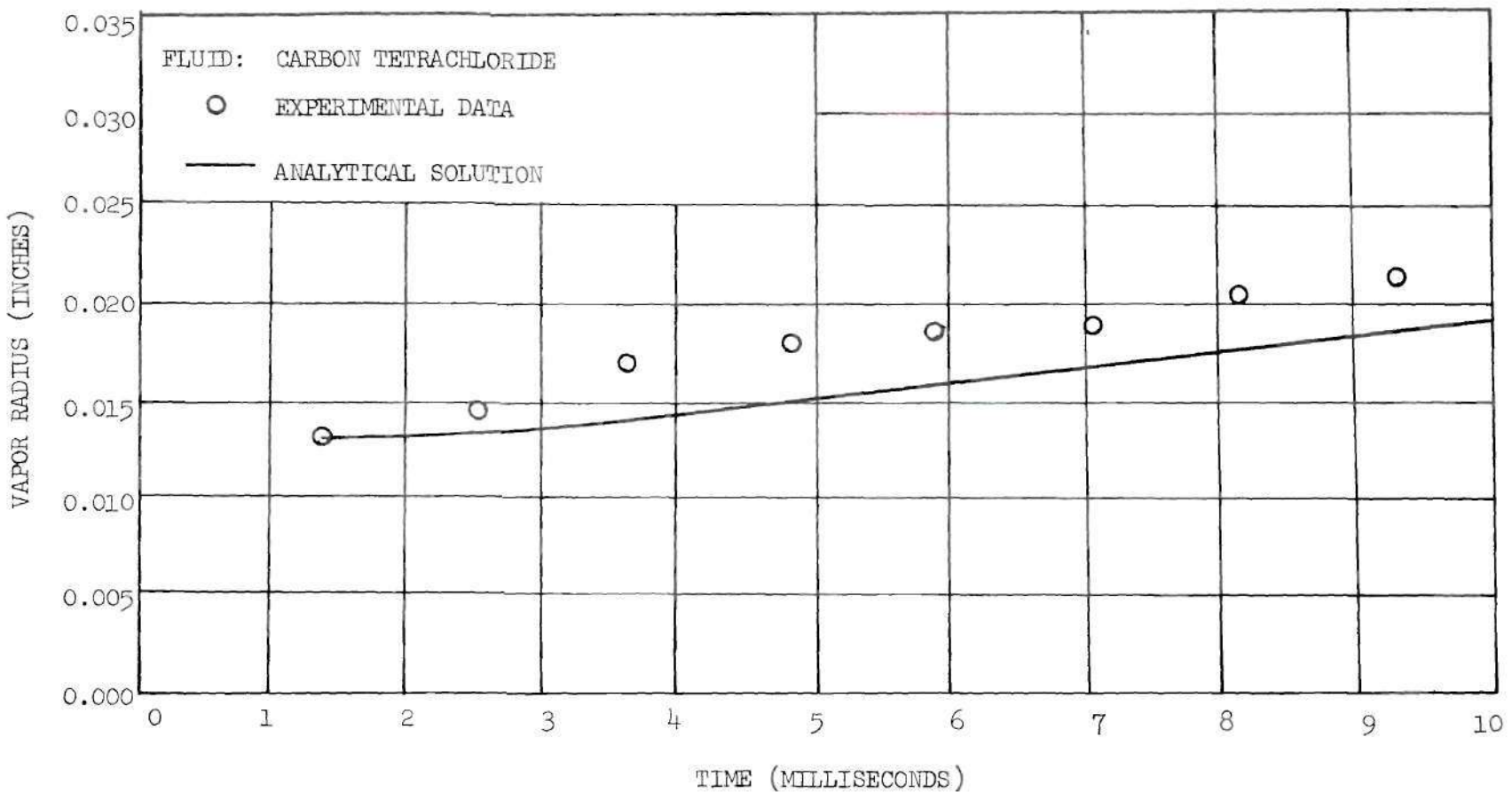

Figure 17. Plot of Vapor Radius as a Function of Time for Run 9.

$T_w = 1495°$ F $\quad T_\infty = 164.6°$ F

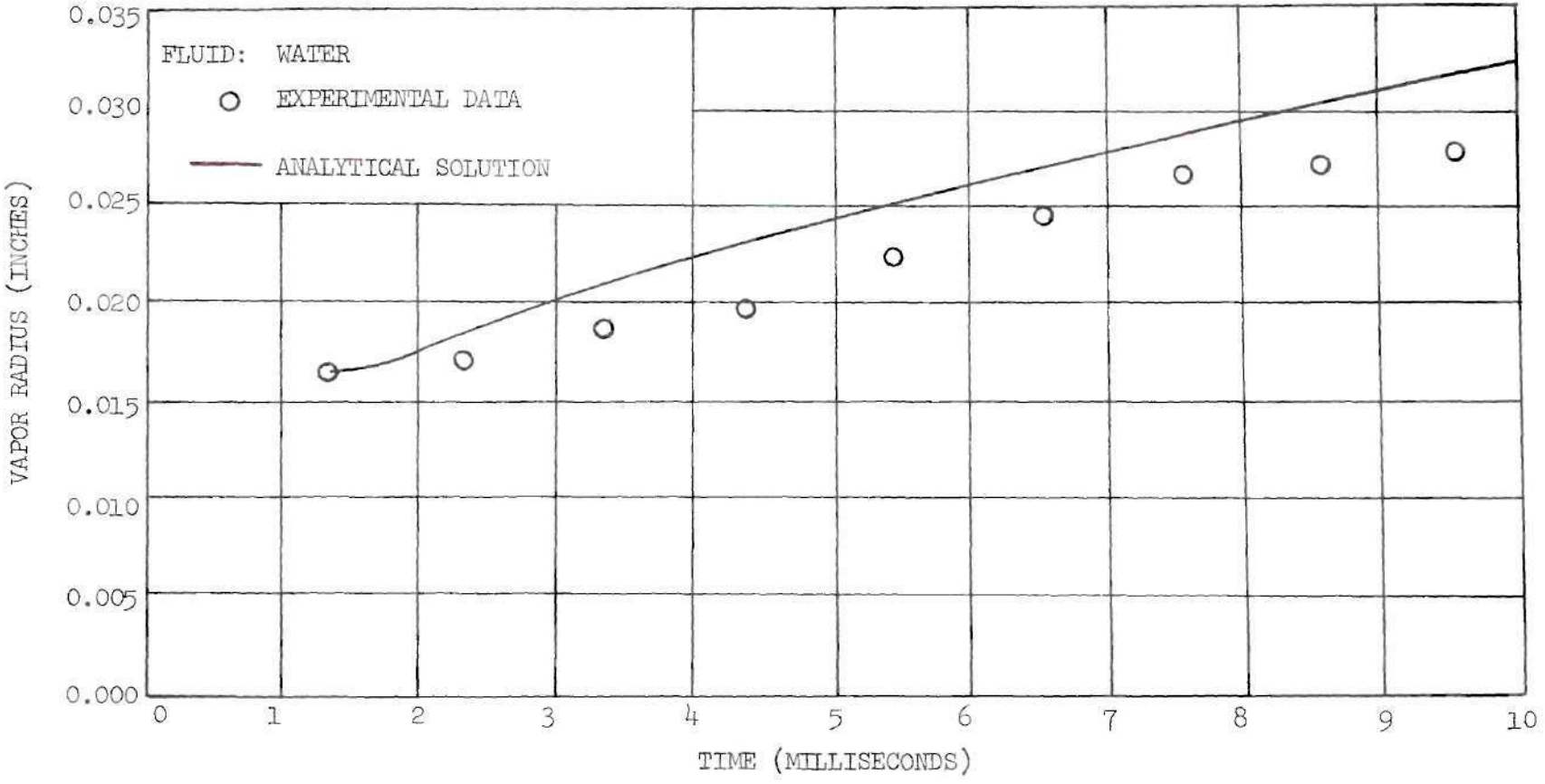

Figure 18. Plot of Vapor Radius as a Function of Time for Run 16.
$T_w = 1475^\circ$ F $\quad T_\infty = 212^\circ$ F

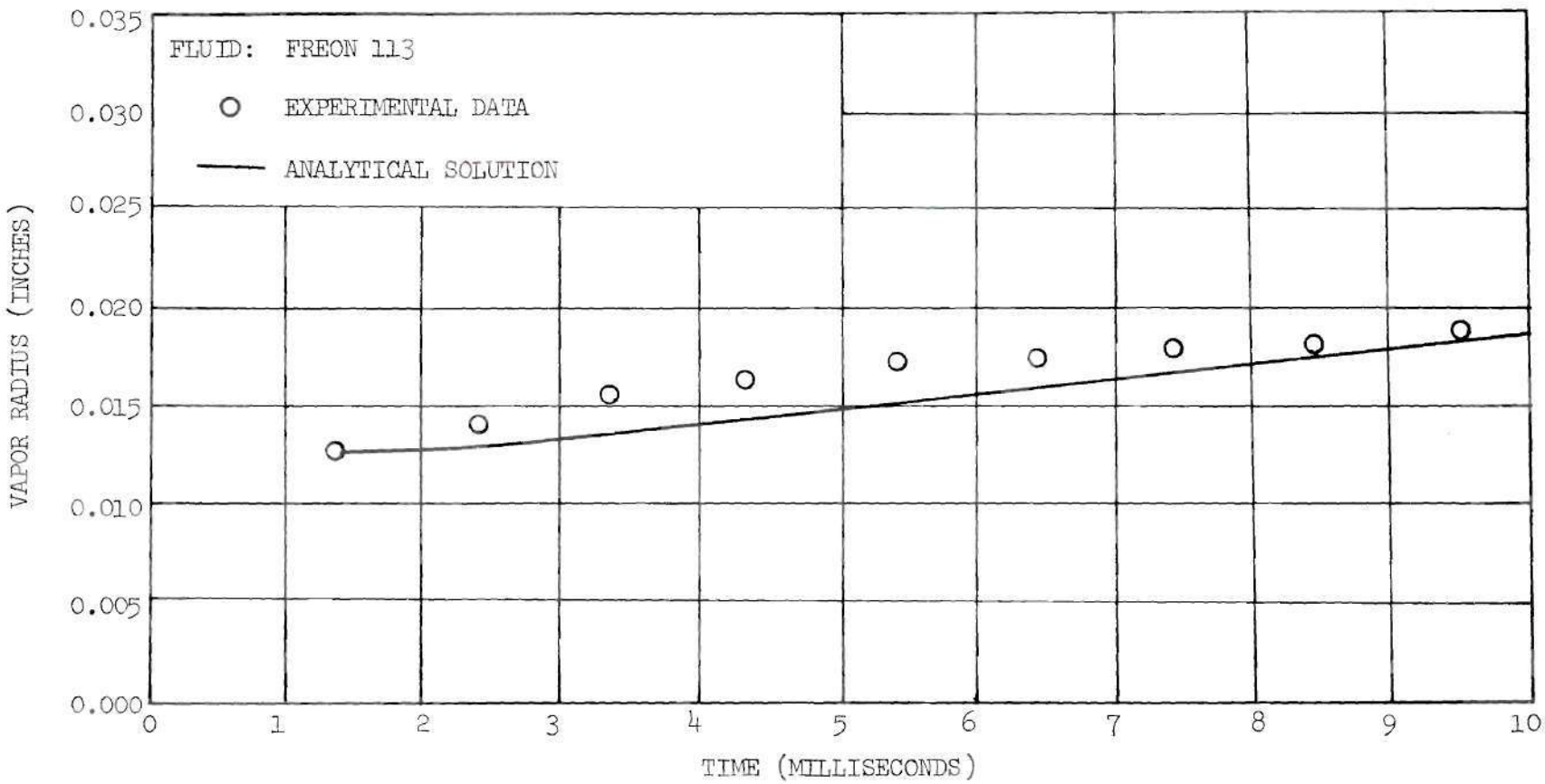

Figure 19. Plot of Vapor Radius as a Function of Time for Run 19.

$T_w = 1370°$ F $\quad T_\infty = 111.2°$ F

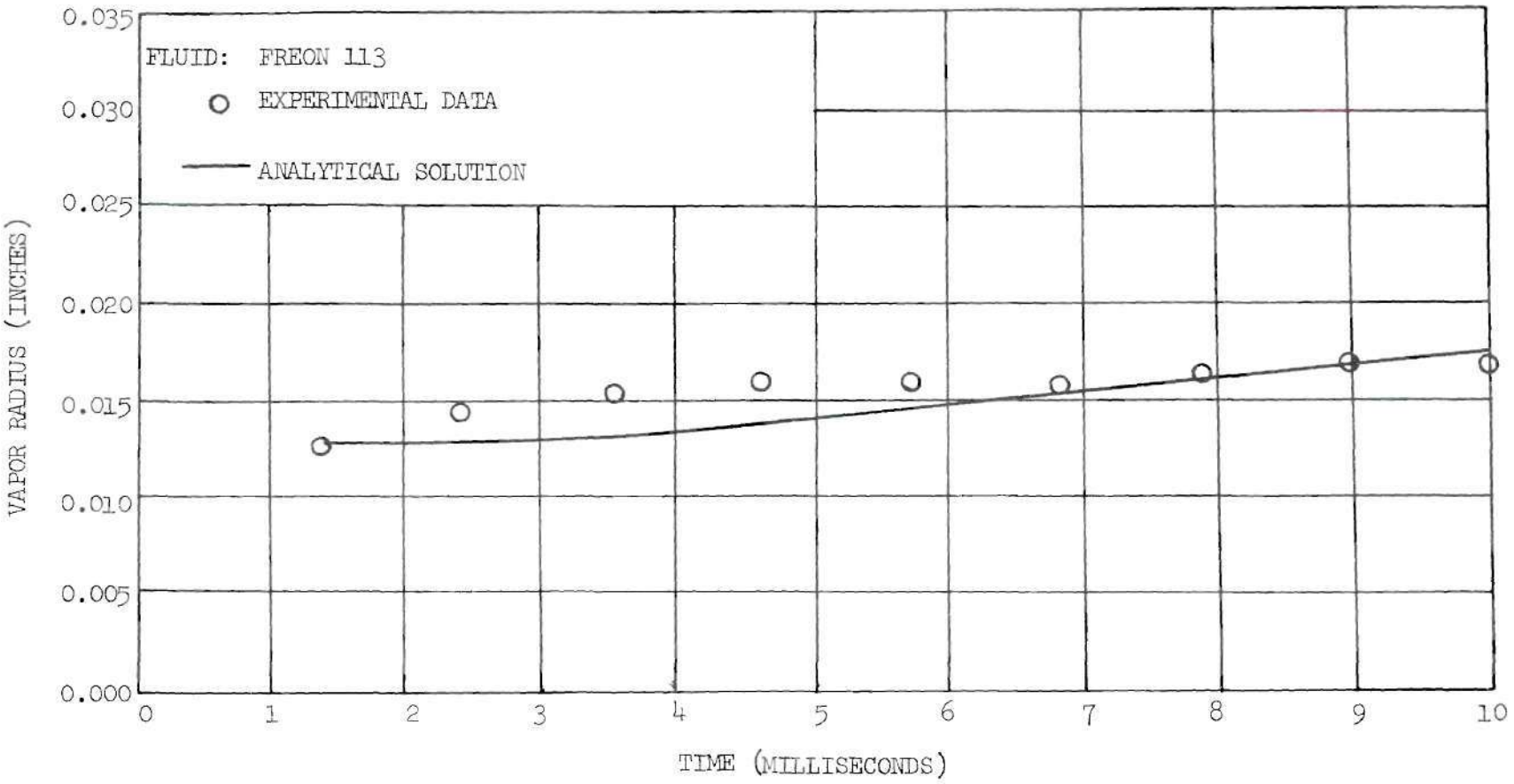

Figure 20. Plot of Vapor Radius as a Function of Time for Run 21.

$T_w = 1423°$ F $\quad T_\infty = 104.3°$ F

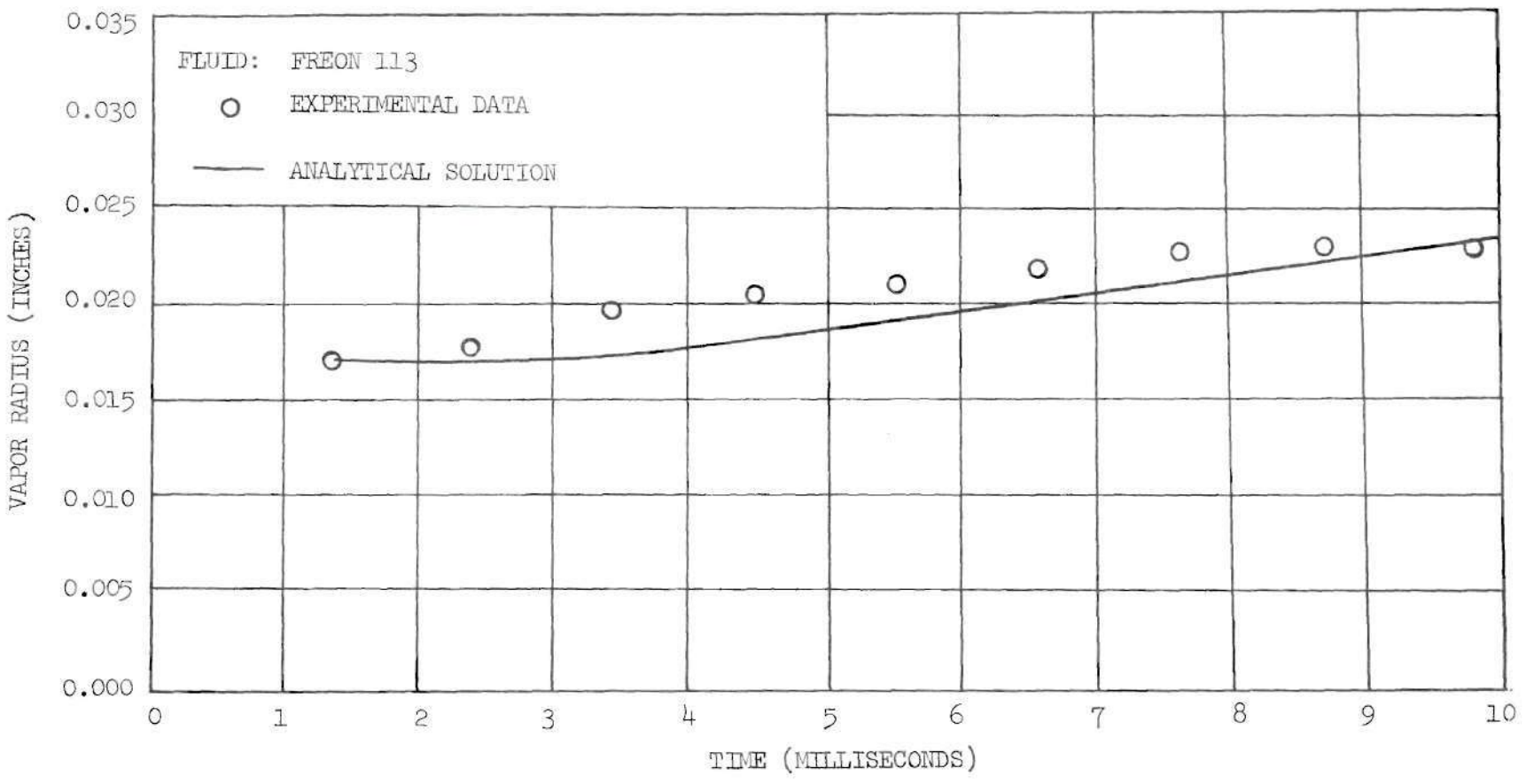

Figure 21. Plot of Vapor Radius as a Function of Time for Run 23.

$T_w = 1575^\circ$ F $\quad T_\infty = 117.1^\circ$ F

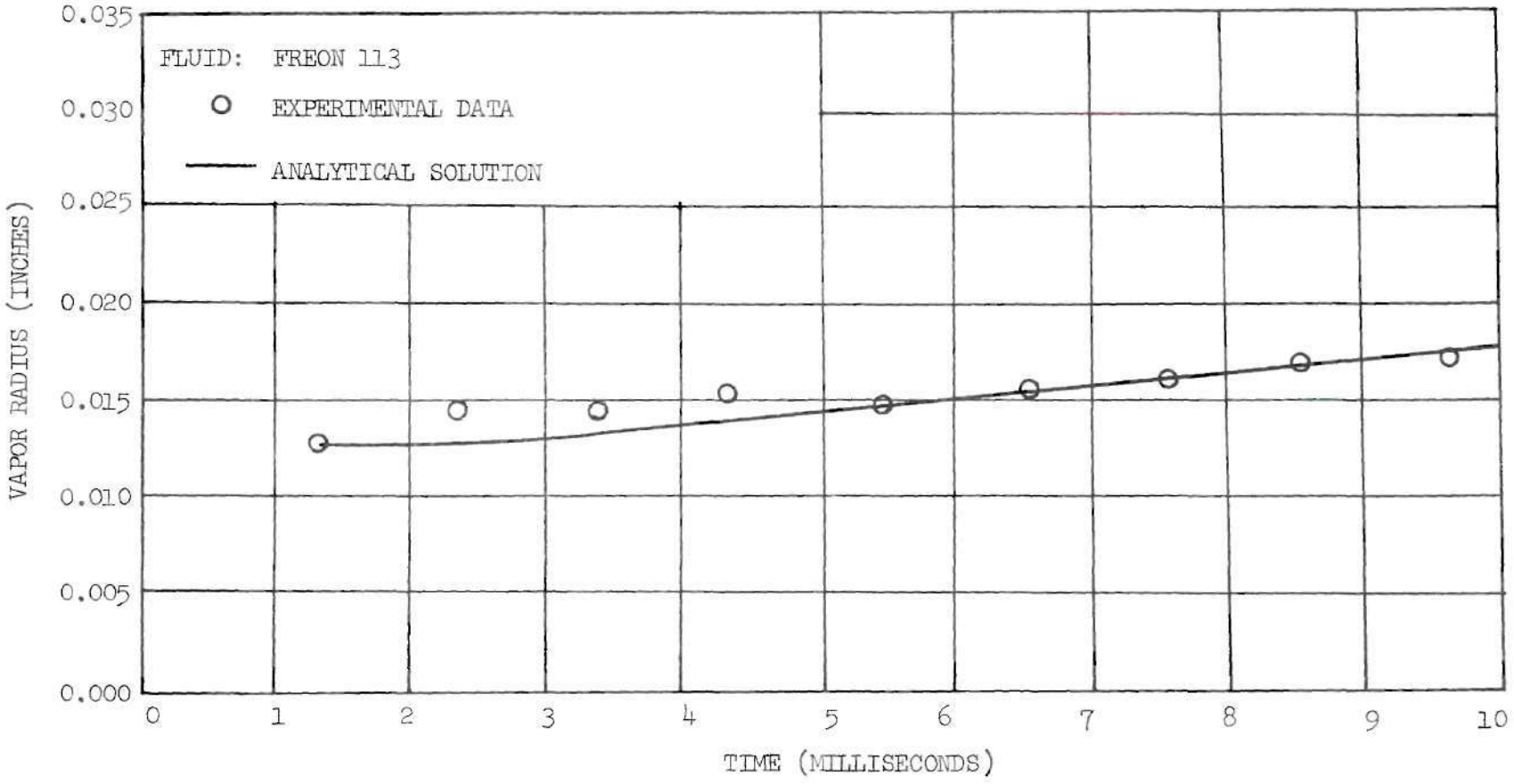

Figure 22. Plot of Vapor Radius as a Function of Time for Run 25.

$T_w = 1520°$ F $\quad T_\infty = 102.6°$ F

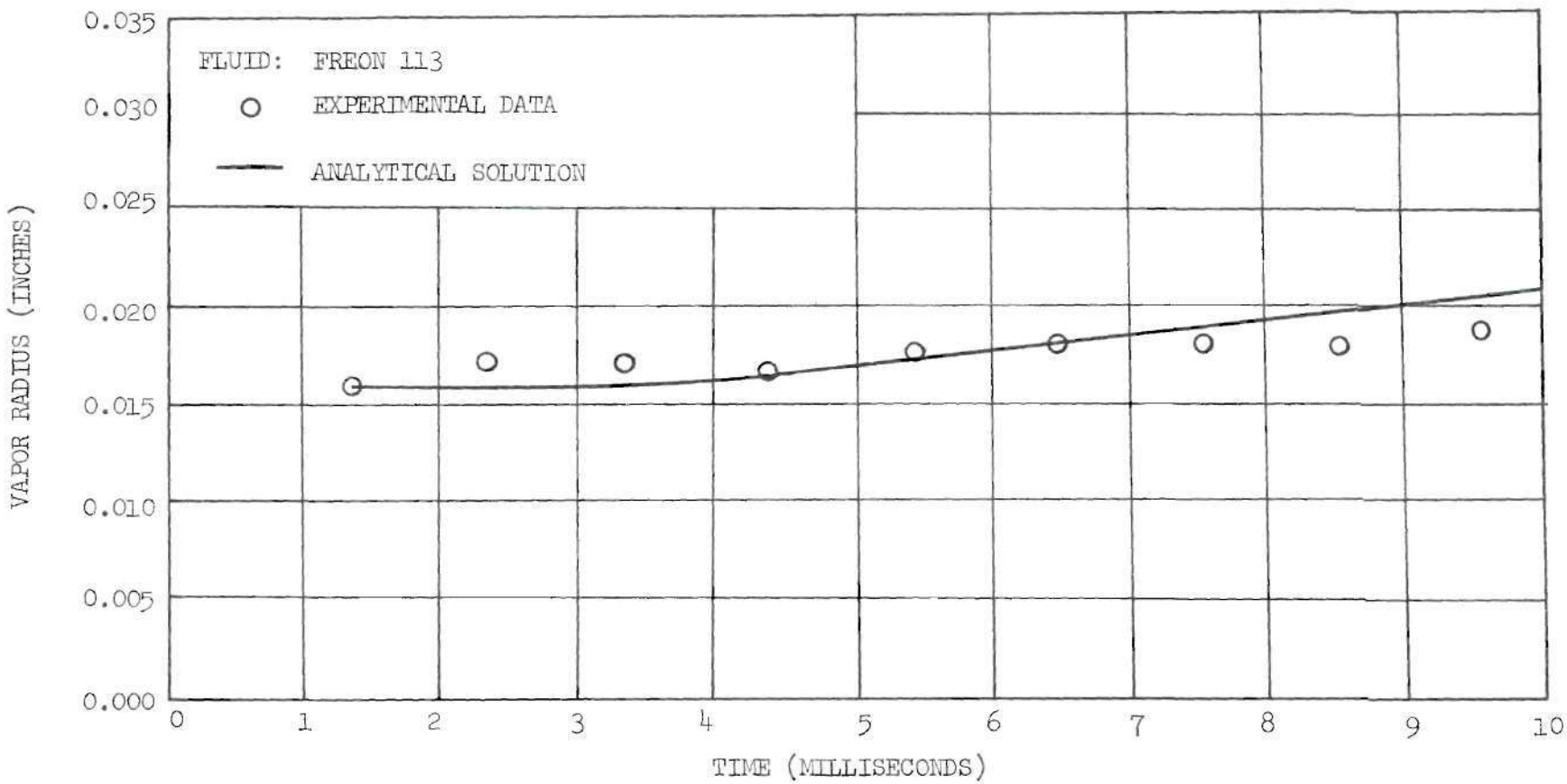

Figure 23. Plot of Vapor Radius as a Function of Time for Run 26.

$T_w = 1580°$ F $\quad T_\infty = 110.5°$ F

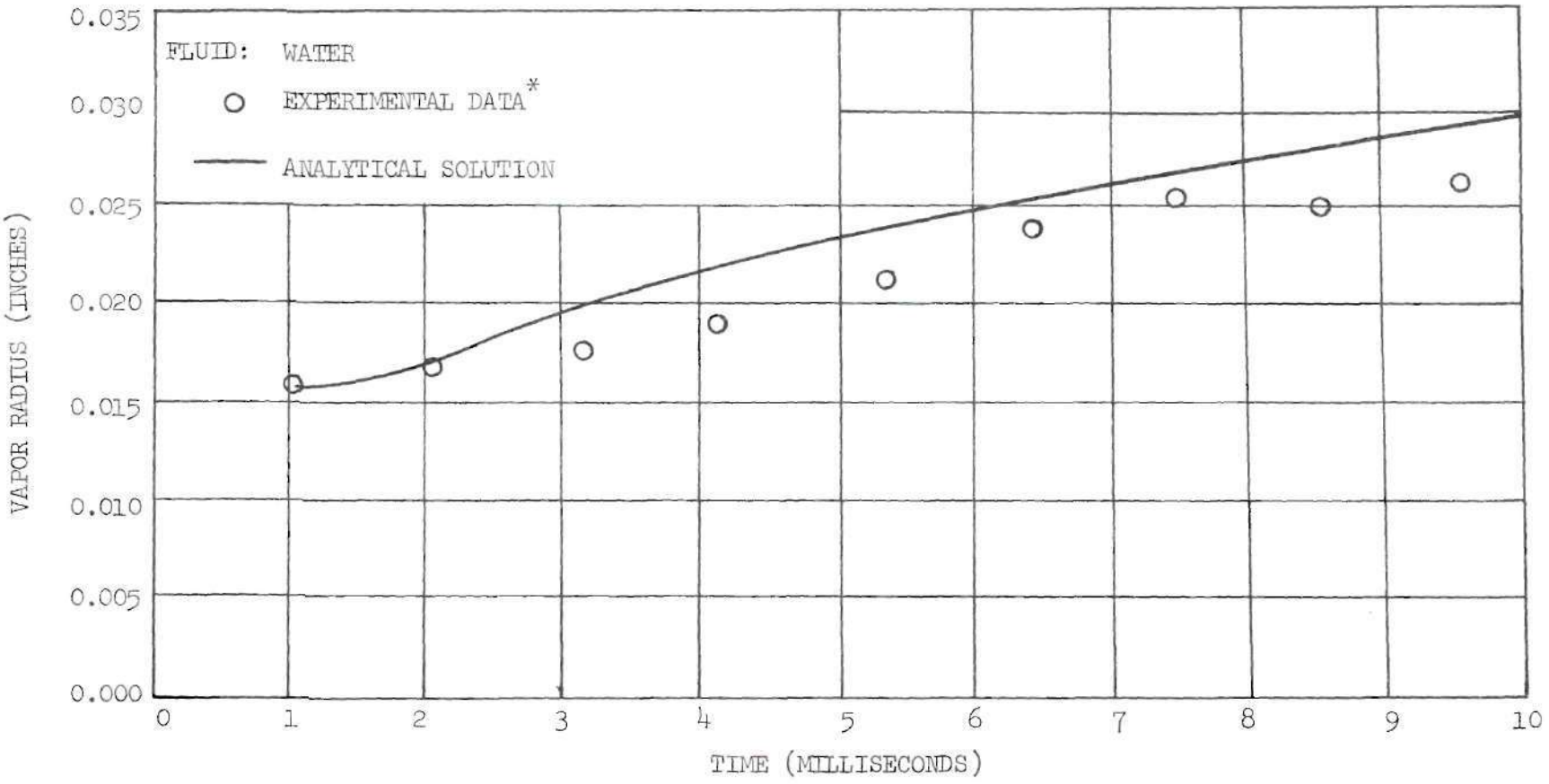

Figure 24. Plot of Vapor Radius as a Function of Time for Run 5.

$T_w = 1477^\circ$ F $\quad T_\infty = 210.9^\circ$ F

*Reference 2.

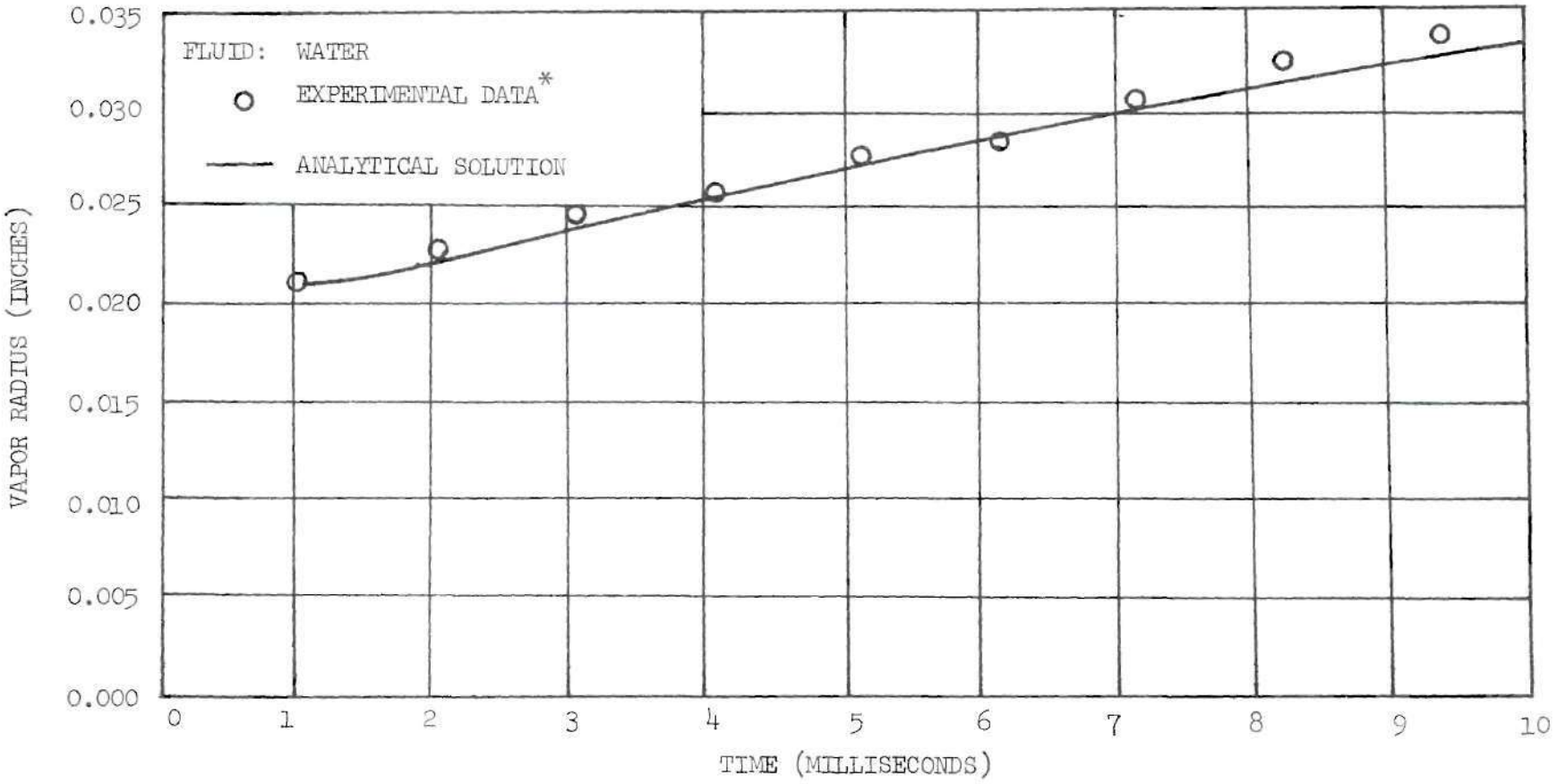

Figure 25. Plot of Vapor Radius as a Function of Time for Run 9.

$T_w = 1680°$ F $\quad T_\infty = 210.9°$ F

*Reference 2.

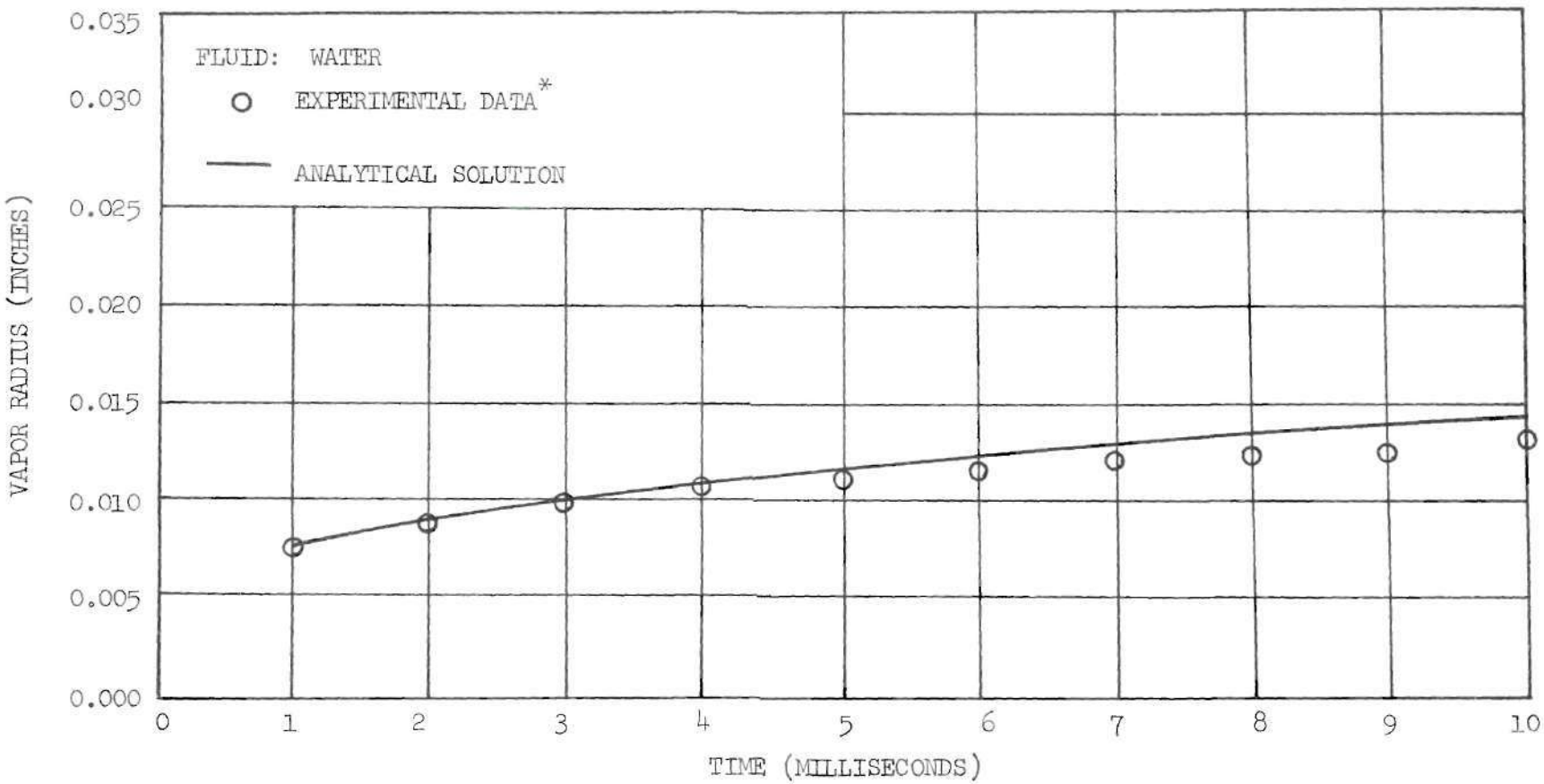

Figure 26. Plot of Vapor Radius as a Function of Time for Run 8.

$T_w = 1555°$ F $\quad T_\infty = 194°$ F

*Reference 3.

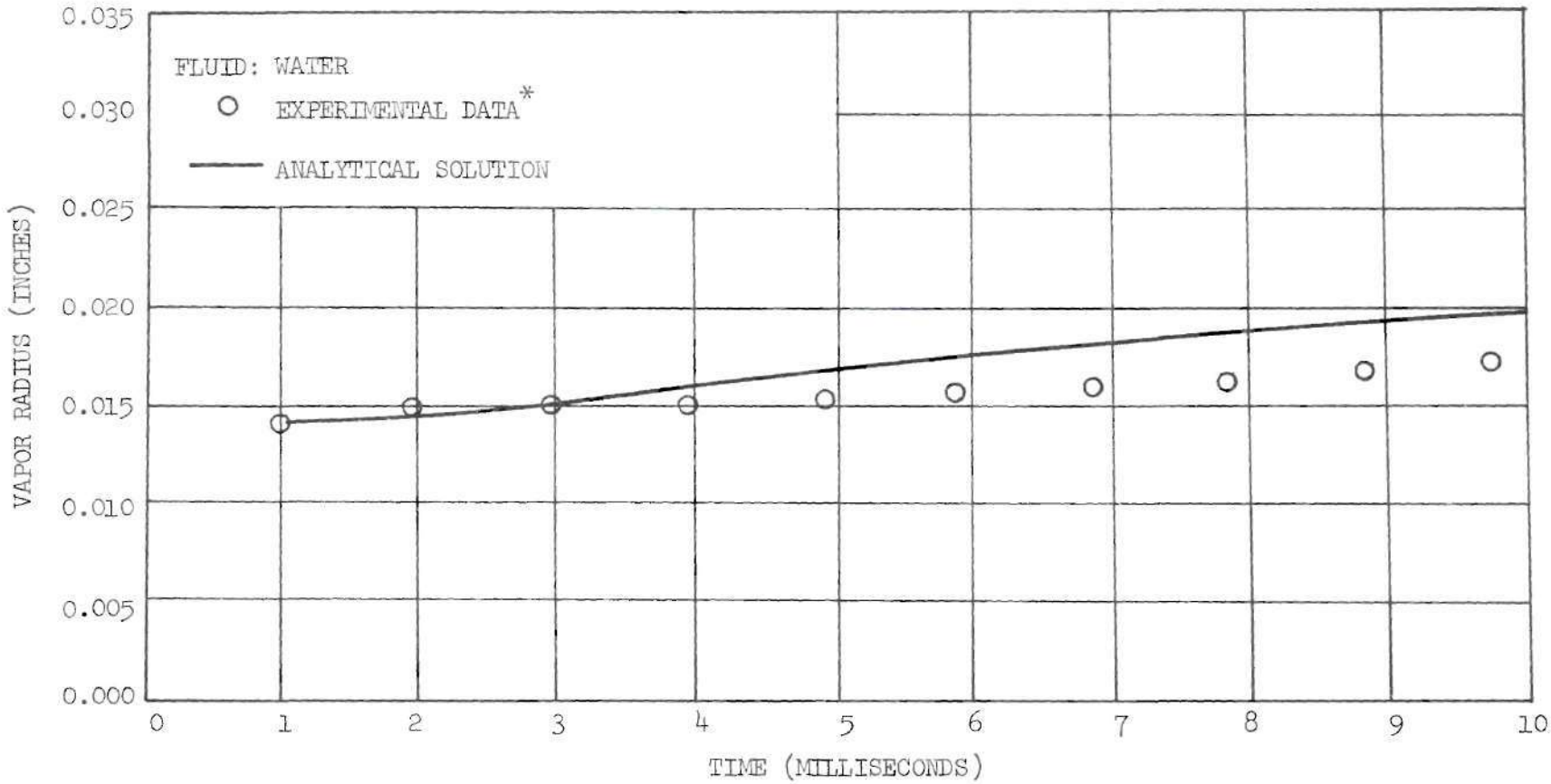

Figure 27. Plot of Vapor Radius as a Function of Time for Run 20.

$T_w = 1320°$ F $\quad T_\infty = 205°$ F

*Reference 3.

To check for possible deposits that may have been left on the wire due to possible decomposition of the fluid, a "Steroscan" Mark II scanning electron microscope (Cambridge Instrument Company) was used to photograph calibrated wire elements that had been used for experimental tests and calibrated element number 9 that had not been exposed to test conditions. As shown in Figures 28 and 29 there are no noticeable differences between the various surfaces.

Conduction Heat Transfer

Graphs of typical numerically calculated conduction heat transfer rates through the vapor into the vapor-liquid interface versus time are given in Figures 30 through 32. From Figure 32 it is seen that for nearly equal wire temperatures the case with the lower liquid pool temperature has the higher conduction heat transfer rate. This is because the vapor film is smaller for the case of the lower liquid pool temperature, hence the smaller insulating effect of the smaller vapor film allows a larger conductive heat transfer to pass through it. From the computer solution of the vapor growth rate and heat transfer effects for runs number 5 and 9 of Reference 2 it is seen that for equal liquid pool temperatures the conduction heat transfer is greatest for the lower wire temperature. The higher wire temperature causes an initial vapor film that is much larger than that for the lower wire temperature. The larger vapor film thickness has an insulating effect that more than offsets the larger driving force due to the higher wire temperature and thus the smaller conduction heat transfer rate results.

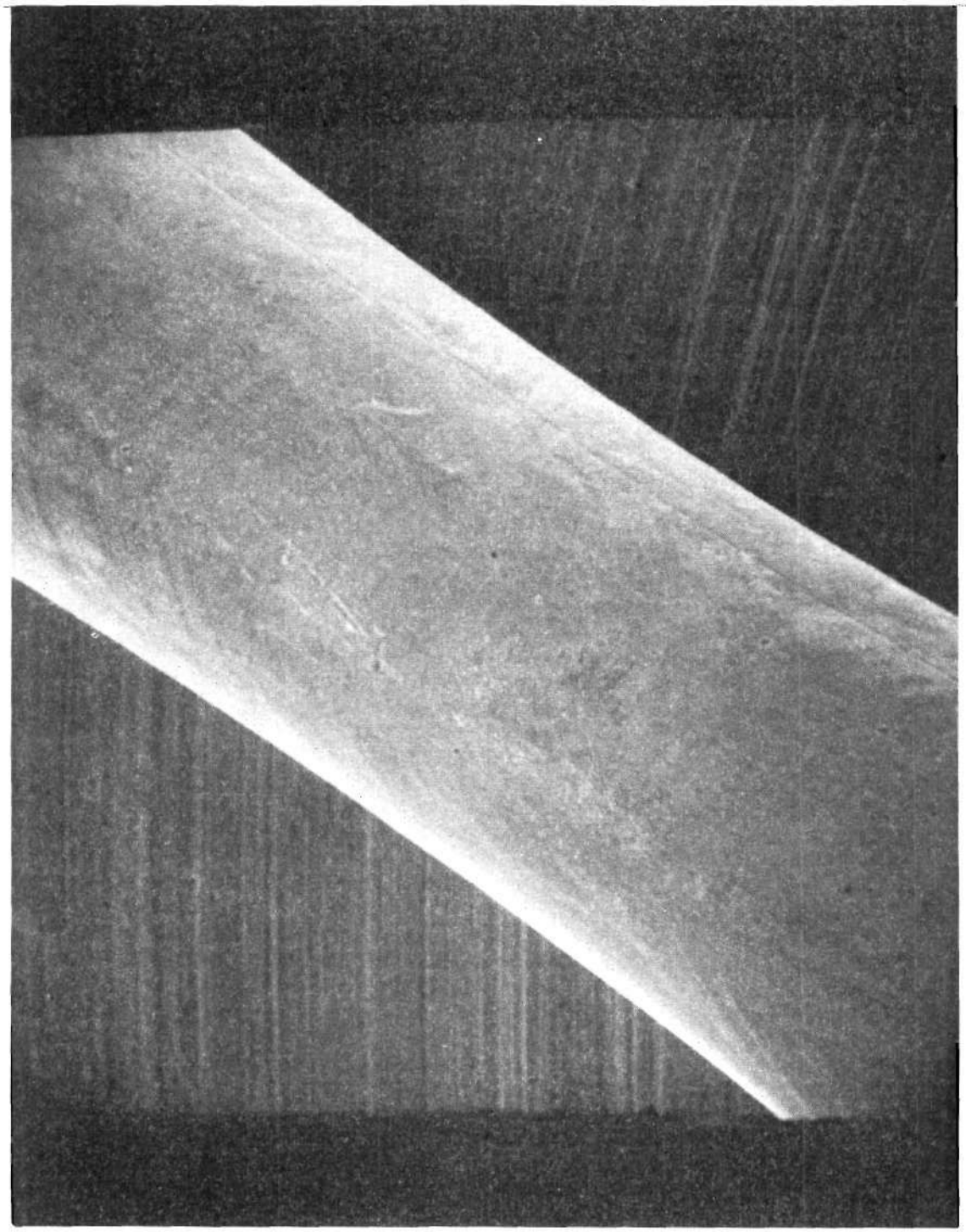

Figure 28. Photograph of Heating Element No. 1 with Magnification of 180X.

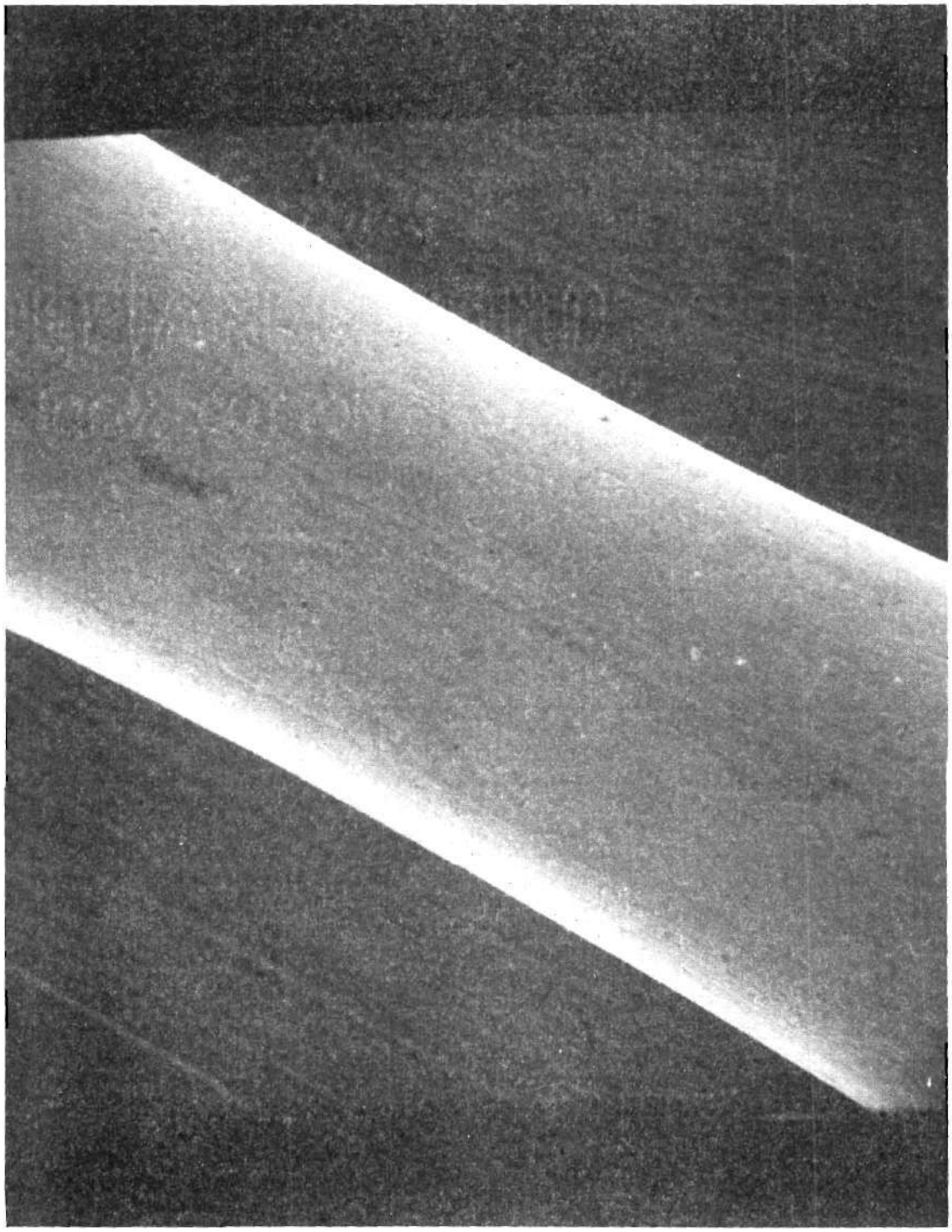

Figure 29. Photograph of Heating Element No. 9 with Magnification of 180X.

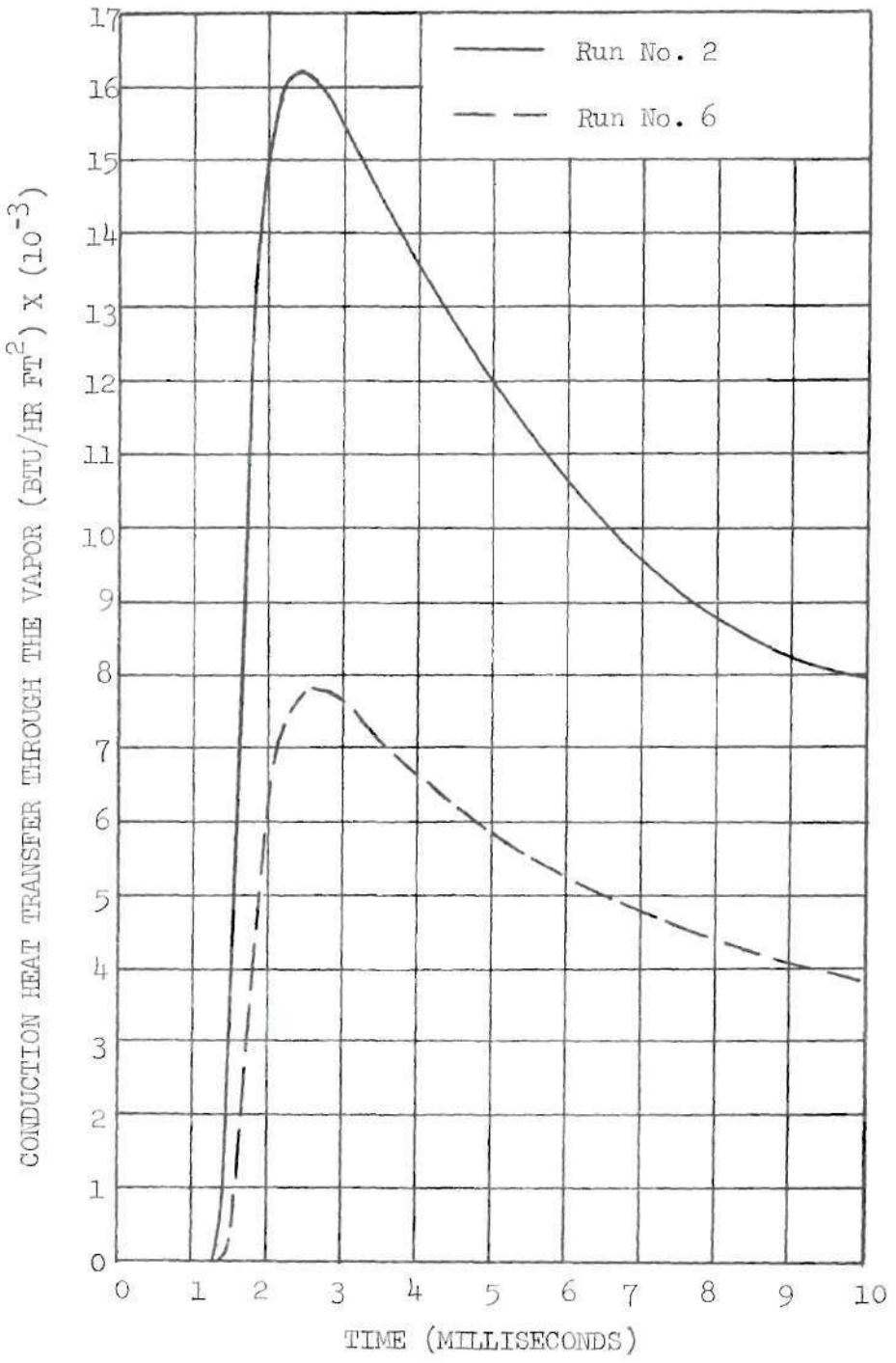

Figure 30. Conduction Heat Transfer Through the Vapor versus Time for Runs No. 2 and 6. Fluid: Carbon Tetrachloride.

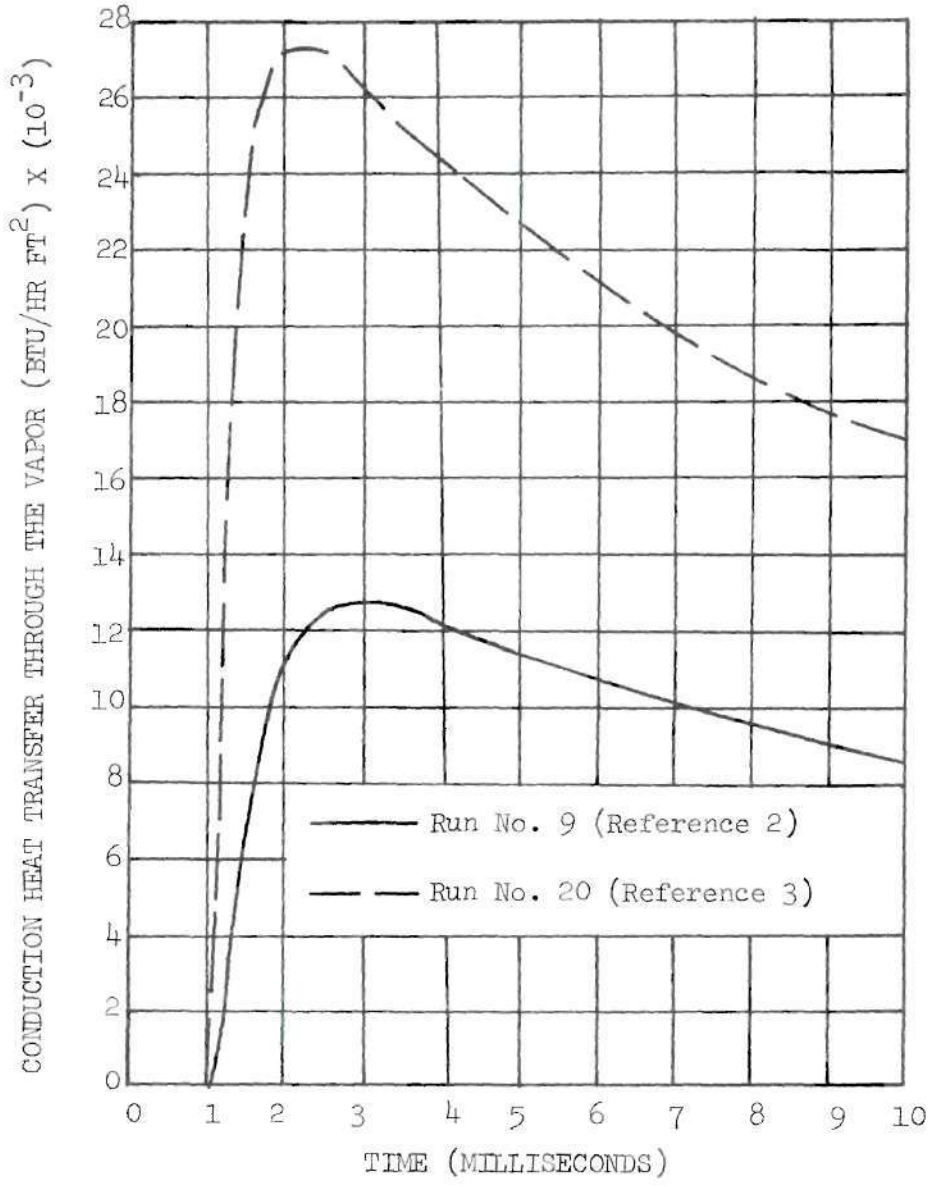

Figure 31. Conduction Heat Transfer Through the Vapor versus Time for Runs No. 9 (Reference 2) and 20 (Reference 3). Fluid: Water.

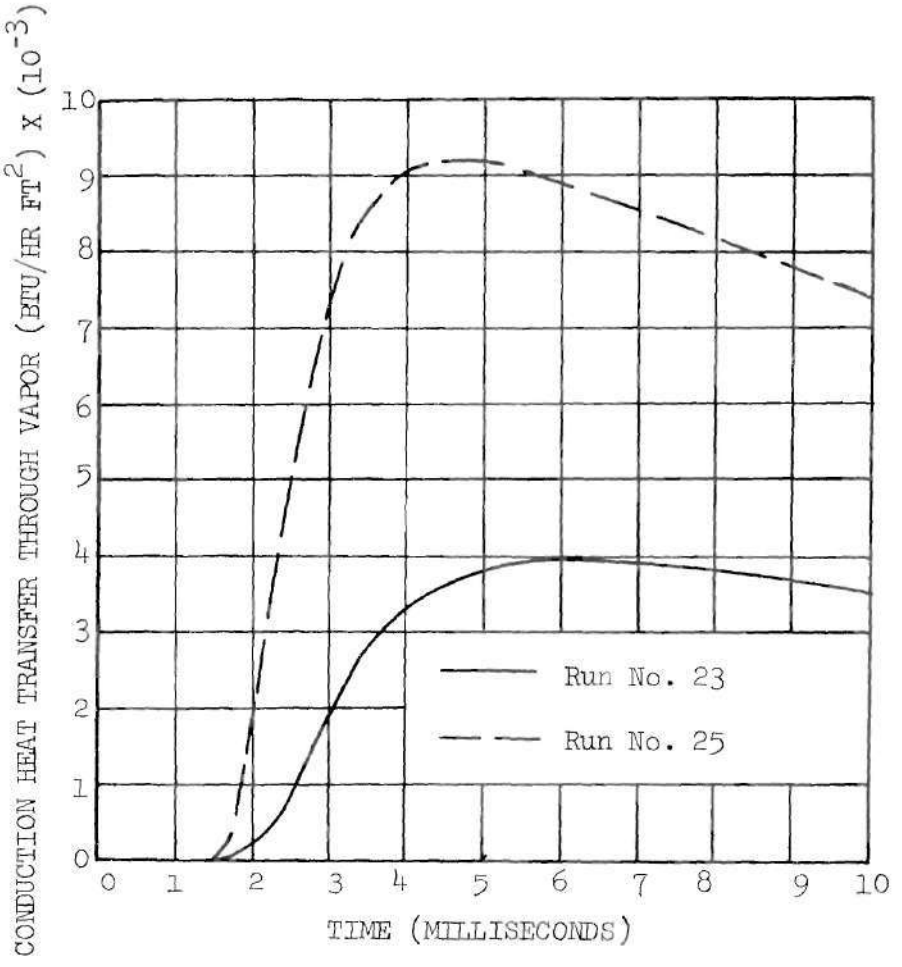

Figure 32. Conduction Heat Transfer Through the Vapor versus Time for Runs No. 23 and 25. Fluid: Freon 113.

Convection Heat Transfer

Graphs of typical numerically calculated convection heat transfer rates into the liquid pool from the vapor-liquid interface versus time are given in Figures 33 through 35. From Figure 35 it is seen that for nearly equal wire temperatures the convection heat transfer is much greater for the case with the lower liquid pool temperature. From the computer solution of the vapor growth rate and heat transfer effects for runs number 5 and 9 of Reference 2 it is seen that for equal liquid pool temperatures convection heat transfer is greater for the lower wire temperature. Again these last two effects show the insulating properties of the larger vapor films which occur for higher wire temperatures and for liquid pools with low subcooling.

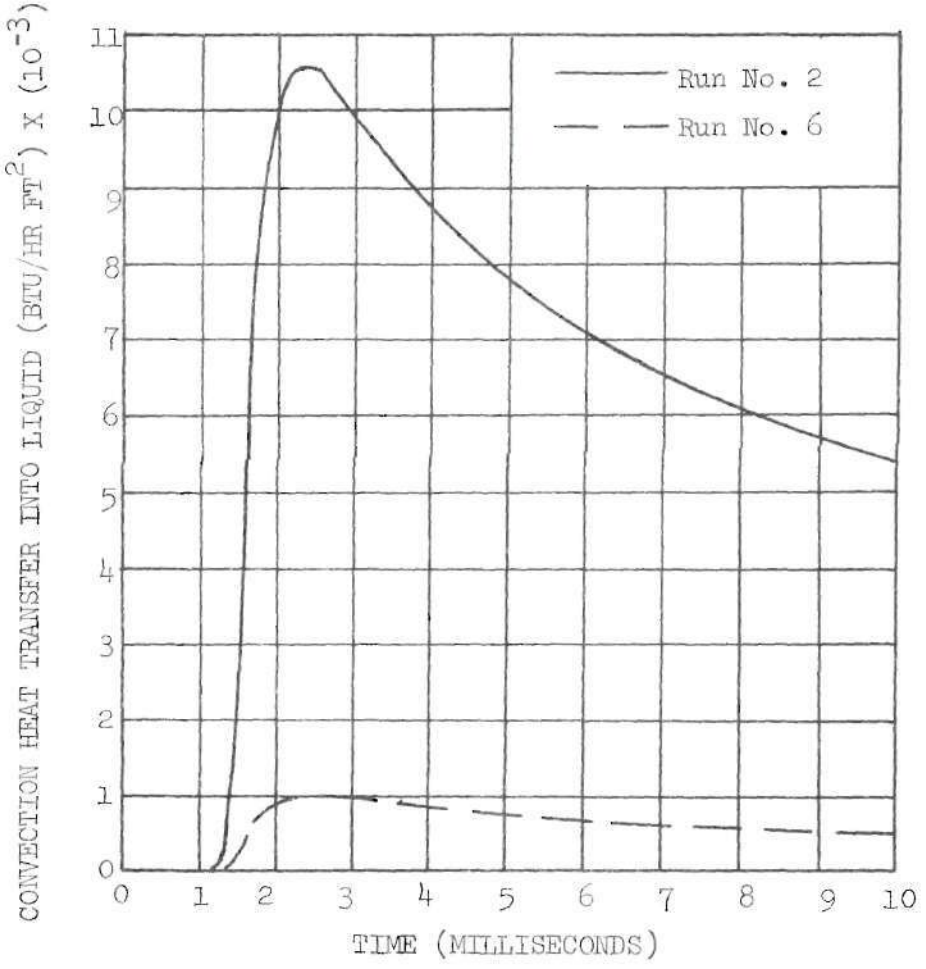

Figure 33. Convection Heat Transfer into the Liquid versus Time for Runs No. 2 and 6. Fluid: Carbon Tetrachloride.

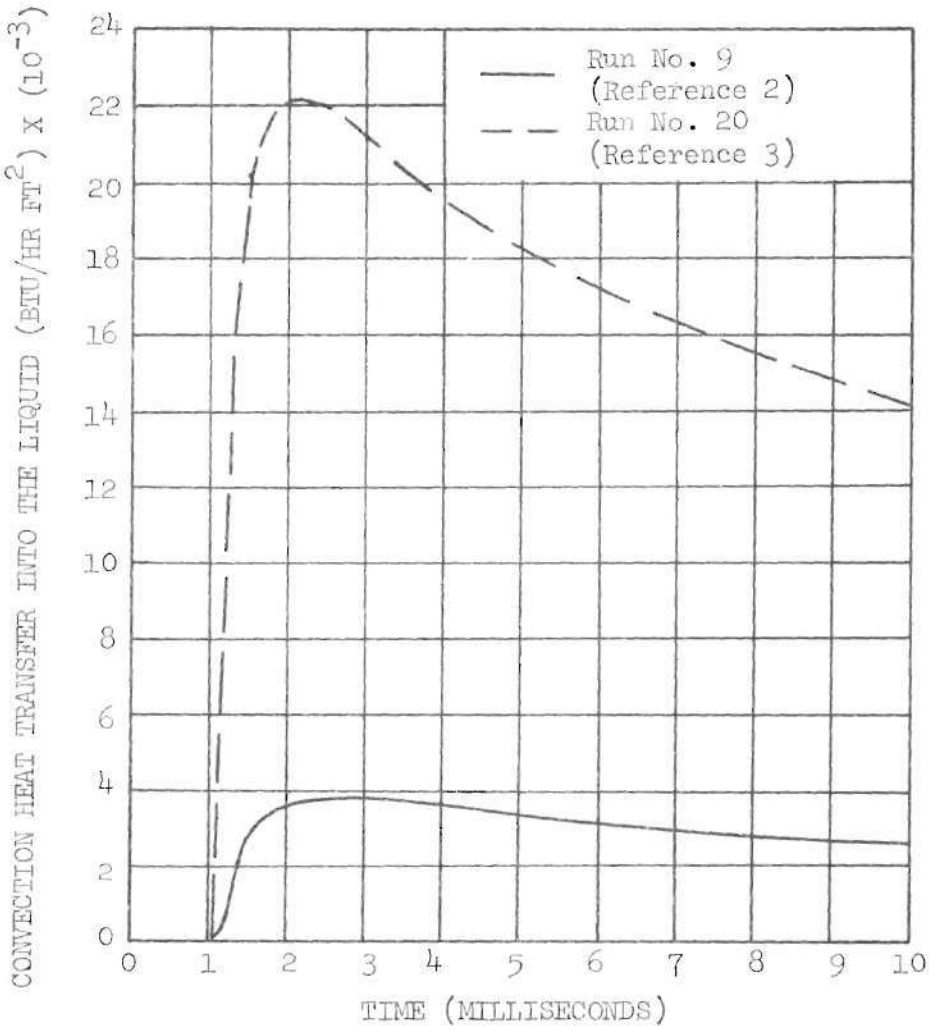

Figure 34. Convection Heat Transfer into the Liquid versus Time for Runs No. 9 (Reference 2) and 20 (Reference 3). Fluid: Water.

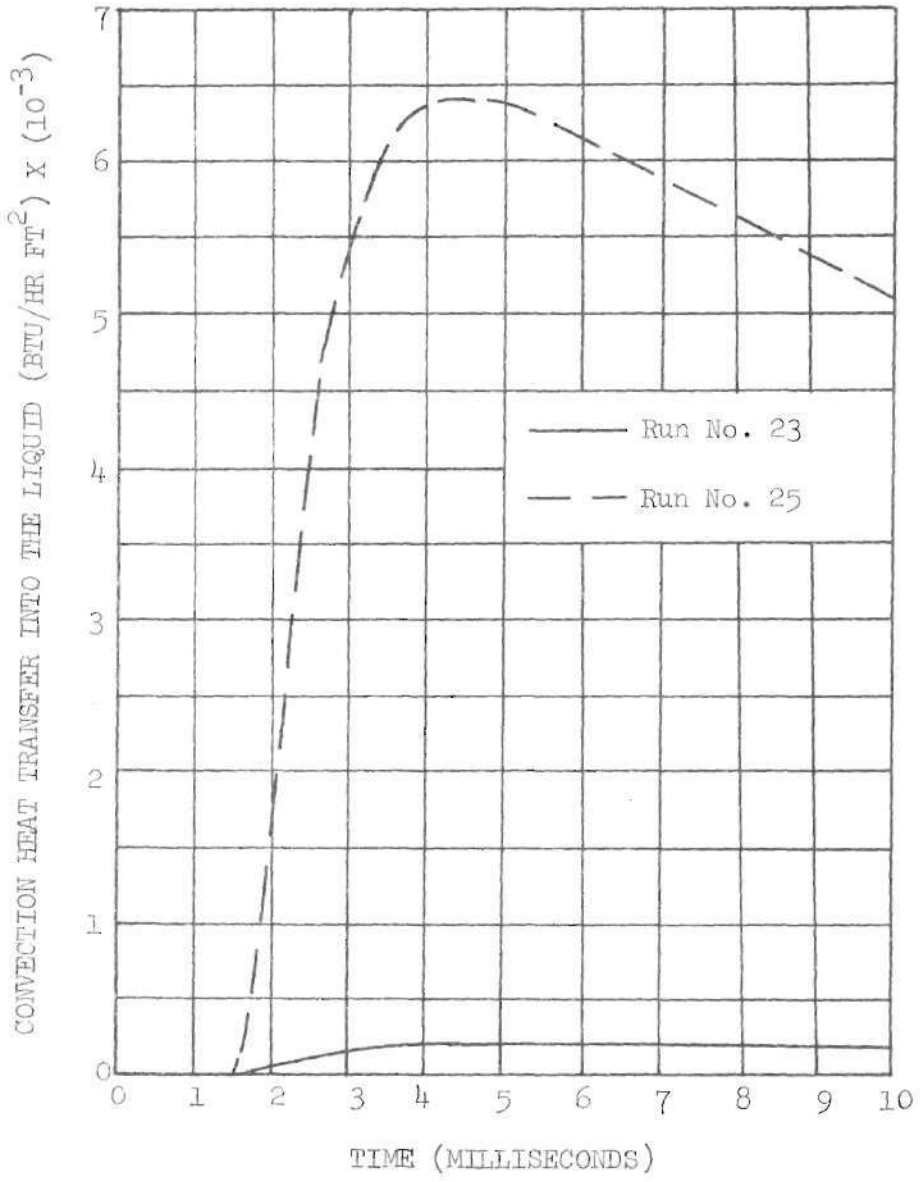

Figure 35. Convection Heat Transfer into the Liquid versus Time for Runs No. 23 and 25. Fluid: Freon 113.

CHAPTER VII

CONCLUSIONS AND RECOMMENDATIONS

Conclusions

Conclusions reached as a consequence of this investigation are as follows:

1. It is not possible to obtain film boiling immediately upon a step change in wire temperature. Initially nucleate type bubbles are formed which quickly unite to form a vapor film. It requires approximately one millisecond for a clear vapor film to form.
2. The transient film boiling process occurs in thermal equilibrium. The vapor-liquid interface is at the saturation temperature corresponding to the external pressure that is present.
3. Liquid inertia effects are negligible during heat transfer controlled transient film boiling.
4. The analytical model presented here gives agreement within 9 per cent of the experimental data if the coefficient $c = 2.2$ in the Nusselt relationship, Equation (2.29). However, the analytical model is hypothetical in other respects (arbitrary starting conditions) and the Nusselt relationship cannot be inferred with confidence, nor can be proven to have constant exponents and coefficients.

Recommendations

Specific recommendations for future research include:

1. The external pressure dependence of the transient film boiling process could be studied to determine the amount of energy input needed to obtain appreciable film growth at external pressures greater than atmospheric.
2. Liquids such as hydrocarbons which have no exact saturation temperature could be investigated analytically and experimentally.
3. Investigation into the initial period of film growth could be made to see if better agreement between theory and experiment may be obtained by some appropriate matching of experimental and analytical vapor-liquid interface velocity at the onset of film boiling.

APPENDIX A

RADIATION EFFECTS

Radiation Effect Within Vapor Phase

Radiation Effect Within Liquid Phase

Radiation Effect Within Vapor Phase

In order to estimate the effect of the vapor on the radiation exchange between the high temperature wire and the saturated vapor-liquid interface the following analysis was performed.

Consider water vapor at a mean temperature of 1460° R, which would be the approximate maximum mean temperature encountered in this investigation, between two infinite parallel plates as an approximation to the actual system to obtain an estimate of the vapor effect. From Hottel (16) it is found that the gas absorptivity, α_g, is

$$\alpha_g = \left(\frac{T_g}{T_w}\right)^{0.45} \epsilon_g \left\{(P_w L)\frac{T_w}{T_g},\ T_w\right\} \tag{A.1}$$

where T_g = gas temperature, °R

T_w = wall temperature, °R

ϵ_g = gas emissivity

P_w = water vapor partial pressure

and

L = mean beam length = 2.0 x (separation distance between plates).

Thus for a maximum separation distance in this investigation of 0.030 in.

$$(P_w L)\frac{T_w}{T_g} = 1 \text{ atm} \times 2.0 \times 3.0 \text{ in} \times \frac{\text{ft}}{12\text{in}} \times \frac{2{,}260^\circ \text{ R}}{1{,}460^\circ \text{ R}} \tag{A.2}$$

$$(P_w L) \frac{T_w}{T_g} = 0.00773 \text{ ft atm.} \tag{A.3}$$

From Figure 6-11 on page 232 of Reference (16) it is found that, at $(P_w L) \frac{T_w}{T_g} = 0.00773$ ft atm and $T_w = 2{,}260°$ R, $\epsilon_g = 0.005$. This value of gas emissivity must then be multiplied by C_w, a *correction factor*, to correct for the departure from an "ideal" state of $P_w = 0$ and $P_{total} = 1.0$ atm. At $(P_w + P_{total})/2 = 1$ atm and $(P_w L)(T_w/T_g) = 0.00773$ ft atm it is found from Figure 6-10 of Reference (16) that $C_w = 1.58$. So the corrected value of gas emissivity is

$$\epsilon_g = 1.58 \times 0.0050 = 0.0079. \tag{A.4}$$

Now to obtain gas absorptivity ϵ_g from Equation (A.4) must be multiplied by $(T_g/T_w)^{0.45}$, as shown in Equation (A.1), to obtain

$$\alpha_g = \left(\frac{1{,}460° \text{ R}}{2{,}260° \text{ R}}\right)^{0.45} \times 0.0079 = 0.0065 \tag{A.5}$$

or 0.65 per cent. If the value of T_g had been 672° R, its lowest temperature, then α_g would equal 0.0083 or 0.83 per cent.

Therefore the absorption of radiant energy by water vapor is negligible and has been ignored in this analysis. As shown in References (17) and (18) the absorption of radiant energy by carbon tetrachloride and Freon 113 is not significantly different from that of water vapor, and so they also will absorb a negligible amount of energy.

Radiation Effect Within Liquid Phase

From References (19) and (20) it is seen that the index of refraction for all fluids investigated is less than 1.5. So from Figure 4-5 of Hottel (16) it is found that α (90°) = ϵ (90°) > 0.95. Negligible radiation enters the liquid at an angle other than 90° to the vapor-liquid interface surface. Thus, essentially all of the incident radiation that reaches the vapor-liquid interface will be absorbed by the liquid and only a very small portion will be reflected from the interface toward the wire or to other points on the interface.

It will now be shown that the absorption of the radiation by the liquid phase is a volume effect and not restricted to the surface.

For liquid water, Coblentz (21) shows an approximate absorption coefficient of 7.13 mm^{-1} for the wire temperatures of interest (less than 2000° F). Thus 95 per cent of the thermal radiation is absorbed in 0.0166 inches of liquid water.

For liquid Freon 113 the approximate absorption coefficient is 1.423 mm^{-1} as presented by Proctor (22). Thus 95 per cent of the thermal radiation is absorbed in 0.083 inches of Freon 113 liquid.

For carbon tetrachloride Coblentz (23) shows an approximate absorption coefficient of 3.15 mm^{-1}. So 95 per cent of the thermal radiation is absorbed in 0.0375 inches of liquid carbon tetrachloride.

Therefore the radiated incident energy does penetrate appreciably into the liquid phase when compared to the typical vapor film radius of 0.025 inch encountered in this investigation. The absorption of radiant energy must be considered as a volume effect and not as a surface effect.

APPENDIX B

DERIVATION OF ENERGY EQUATION FOR THE VAPOR PHASE

Inertia of the Liquid

Surface Tension

Buoyancy

The energy equation for any coordinate system is

$$\rho \frac{Di}{D\theta} - \nabla \cdot (k\nabla T) - \mu\Phi - \frac{DP}{D\theta} - S = 0 \tag{B.1}$$

from Kays (24), where

i = enthalpy = $e + P/\rho$

Φ = dissipation function = $\tau_{ij} \frac{\partial u_i}{\partial u_j}$,

and

S = internal heat source function which includes absorption of radiant energy by the vapor phase.

The first term of Equation (B.1) is

$$\rho \frac{Di}{D\theta} = \rho \left(\frac{\partial i}{\partial \theta} + v_r \frac{\partial i}{\partial r}\right). \tag{B.2}$$

In general

$$\frac{Di}{D\theta} = C_p \frac{DT}{D\theta} + \left(\frac{\partial i}{\partial P}\right)_T \frac{DP}{D\theta}$$

which for the approximation that the vapor phase may be considered to behave as a perfect gas becomes

$$\frac{Di}{D\theta} = C_p \frac{DT}{D\theta} .$$

If the specific heat at constant pressure, C_p is then considered constant and evaluated at the mean vapor film temperature Equation (B.2) becomes

$$\rho \frac{Di}{D\theta} = \rho \; C_p \; (\frac{\partial T}{\partial \theta} + v_r \frac{\partial T}{\partial r}).$$

As shown in Appendix C the convective transport of energy is negligible compared to the conductive transport of energy so

$$\rho \frac{Di}{D\theta} = \rho \; C_p \frac{\partial T}{\partial \theta}.$$

The second term of Equation (B.1) becomes

$$\nabla \cdot (k\nabla T) = k \; (\frac{\partial^2 T}{\partial r^2} + \frac{1}{r} \frac{\partial T}{\partial r}) \qquad (B.3)$$

for constant thermal conductivity, k, that is evaluated at the mean vapor film temperature.

The third term of Equation (B.1) is the viscous dissipation

$$- \mu \Phi$$

which is zero for this investigation in which the vapor velocity is always assumed to be radial and thus perpendicular to any shear planes at the vapor boundary.

The fourth term of Equation (B.1) is

$$- \frac{DP}{D\theta} = - \left[\frac{\partial P}{\partial \theta} + v_r \frac{\partial P}{\partial r} \right]. \qquad (B.4)$$

The pressure at the vapor-liquid interface within the vapor phase will now be shown to vary negligibly from the pressure within the test container above the free surface. Buoyancy forces, which are the only body forces present, will also be shown to be negligible, since they have been ignored in Equation (B.1).

Inertia of the Liquid

For a single vapor cylinder in an incompressible inviscid liquid of finite extent, the equation of motion for the liquid is

$$\rho_\ell \left(\frac{\partial v_r}{\partial \theta} + v_r \frac{\partial v_r}{\partial r}\right) = - \frac{\partial P}{\partial r} .$$

The continuity equation is

$$\frac{1}{r} \frac{\partial}{\partial r} (r\ v_r) = 0.$$

A mass balance at the vapor-liquid interface gives

$$\frac{d}{d\theta} (\pi R^2 L\ \rho_v) = 2\pi\ RL\ (\dot{R} - v_r)\ \rho_\ell$$

where R = vapor-liquid interface radius

L = length of vapor film cylinder considered

$\dot{R}$ = velocity of vapor-liquid interface

v_r = velocity of liquid at vapor-liquid interface

ρ_v = density of vapor

and

ρ_ℓ = density of liquid.

After taking the derivative and then dividing through by 2π RL the mass balance yields

$$\dot{R}\,\rho_v = (\dot{R} - v_r)\,\rho_\ell$$

$$v_r = \dot{R}\,(1 - \frac{\rho_v}{\rho_\ell})$$

and so for $\rho_v \ll \rho_\ell$ the liquid velocity at the interface, v_r, is equal to the vapor-liquid interface velocity, $\dot{R}$. Integration of the continuity equation from the radius of the vapor film interface $R(\theta)$ to r, where $r > R(\theta)$, gives the radial liquid velocity, v_r, in terms of the interface velocity, $\dot{R}$, as

$$r\,v_r = R\,\dot{R}.$$

So $v_r = \dot{R}\,\frac{R}{r}$ within the liquid. Substitution of the liquid velocity into the equation of motion yields

$$\rho_\ell(\frac{(\dot{R})^2 + R\ddot{R}}{r} - \frac{(\dot{R})^2\,R^2}{r^3}) = -\frac{\partial P}{\partial r}$$

which, upon integration from the bubble interface, R, to the liquid free surface height above the vapor cylinder, h, gives

$$\rho_\ell \left\{ \left[(\dot{R})^2 + R\ddot{R} \right] \ln \left(\frac{h}{R}\right) + \frac{1}{2} \left[(\dot{R})^2 \left(\frac{R^2}{h^2} - 1\right) \right] \right\} = - P_\ell (R) - P_\ell (h). \quad (B.5)$$

From the numerical solution to run number 2 (see Chapter III, Table 1)

$R = 0.01043$ in

$\dot{R} = 0.3222$ in/sec

$\ddot{R} = 3.219 \times 10^3$ in/sec^2

$h = 1.0$ in

and $P_\ell (h) = 14.7$ lb$_f$/in^2

at $\theta = 1.557 \times 10^{-3}$ sec.

Substitution of the above values into Equation (B.5) yields

$$\frac{92.75 \frac{lb_m}{ft^3}}{32.17 \frac{lb_m\ ft}{lb_f\ sec} \times 2.08 \times 10^4 \frac{in^4}{ft^4}} \times \left\{ \left[\left(0.322 \frac{in}{sec}\right)^2 + 0.0104 \text{ in} \times 3.22 \times 10^3 \frac{in}{sec^2} \right] \times \ln \left(\frac{1.0 \text{ in}}{0.0104 \text{ in}}\right) + \frac{1}{2} \left[\left(0.322 \frac{in}{sec}\right)^2 \left[\left(\frac{0.0104 \text{ in}}{1.0 \text{ in}}\right)^2 - 1 \right] \right] \right\} =$$

$$P_\ell (R) - 14.7 \frac{lb_f}{in^2}$$

or, the relative excess pressure in the vapor film is

$$\Delta P/P = \frac{0.161}{14.7} = 0.011$$

above the atmospheric pressure. Thus the pressure at the vapor cylinder wall in the liquid differs negligibly from the pressure at the liquid

free surface. Sernas and Hooper (25) also state that for the vapor bubble growth of their investigation the liquid inertia effects were not significant beyond the first fifty microseconds.

Surface Tension

A force balance on the vapor cylinder considering the surface tension yields

$$P_v - P_\ell = \frac{\sigma}{R}$$

where

P_v = vapor pressure at interface

P_ℓ = liquid pressure at interface

σ = liquid surface tension

and

R = vapor cylinder radius.

For the smallest possible vapor cylinder radius obtainable for this investigation $R \geq r_w = 0.005$ in. Thus, for water, which had the highest surface tension of the three liquids considered, the equation yields

$$P_v - P_\ell = \frac{56.89 \frac{\text{dynes}}{\text{cm}} \times 2.54 \frac{\text{cm}}{\text{in}} \times 1 \times 10^{-5} \frac{\text{newton}}{\text{dyne}} \times \frac{\text{lb}_f}{4.45 \text{ newton}}}{0.005 \text{ in}} \qquad \text{(B.6)}$$

$$P_v - P_\ell = 0.065 \text{ lb}_f/\text{in}^2.$$

Now since the pressure within the vapor at the interface differs negligibly from that within the liquid at the interface, and it was shown previously that the liquid pressure at the interface varied negligibly from that of the free surface, it is noted that the pressure in the vapor at the interface is approximately that of the free surface.

Buoyancy

For a typical fluid, say water, the buoyancy force of the vapor is

$$\text{Buoyancy Force} = (g\,\rho_\ell - g\,\rho_v)\,V = g\,\rho_\ell\left(1 - \frac{\rho_v}{\rho_\ell}\right) V$$

where

ρ_ℓ = liquid density

ρ_v = vapor density

and

V = volume of vapor present.

Since $\rho_v \ll \rho_\ell$ the above equation becomes

$$\text{Buoyancy Force} = g\,\rho_\ell\,V.$$

For a typical final vapor diameter of 0.07 inches at 10 milliseconds the buoyancy force becomes

$$\text{Buoyancy Force} = \frac{g}{g_c} \times 62.4\,\frac{lb_m}{ft^3} \times \frac{1.85\text{ in}}{12\text{ in/ft}} \times \pi \times \frac{(.07\text{ in})^2}{4} \times \frac{ft^2}{144\text{ in}^2}$$

$$\text{Buoyancy Force} = 2.57 \times 10^{-4}\ \text{lb}_f.$$

This force yields an "effective *pressure*" *of*

$$\frac{2.57 \times 10^{-4}\text{lb}_f}{1.85\ \text{in} \times .07\ \text{in}} = 1.98 \times 10^{-3}\ \frac{\text{lb}_f}{\text{in}^2}$$

upward on the vapor cylinder. Thus the buoyancy force is negligible.

The pressure could vary greatly within the vapor only if there were large accelerations within the vapor. As stated in Appendix C the probable vapor velocities are two orders of magnitude less than the vapor film interfacial velocity. Therefore for the small vapor velocities and pressure variations present the second term of Equation (B.4) is negligible. Due to the small pressure variations present during the vapor film growth process the change of pressure with respect to time would also be negligible and thus Equation (B.4) would be equal to zero, so

$$\frac{DP}{D\theta} = 0. \tag{B.7}$$

In order to determine if the vaporization at the vapor-liquid interface is taking place in thermal equilibrium it is necessary to estimate the vapor temperature at the interface. The pressure of the liquid and the vapor at the interface can be related to the amount of superheat present by the Clausius-Clapeyron equation

$$\frac{dP}{dT} = \frac{h_{fg}\ J}{v_{fg}\ T}$$

where

P = pressure

T = temperature

h_{fg} = heat of vaporization

and

$v_{fg} = v_g - v_f$ = change in specific volume during phase change.

For the case of $\rho_\ell \gg \rho_v$ the above equation may be expressed in finite difference form as

$$\frac{P_v - P_\ell}{T_v - T_{SAT}} = \frac{h_{fg}\ J\ \rho_v}{T_{SAT}}$$

or

$$T_v - T_{SAT} = \frac{T_{SAT}}{h_{fg}\ J\ \rho_v}\ (P_v - P_\ell).$$

For water this yields

$$T_v - T_{SAT} = \frac{212^\circ\ F \times 0.065\ lb_f/in^2 \times 144\ in^2/ft^2}{970\ Btu/lb_m \times 778\ ft\ lb_f/Btu \times 0.0372\ lb_m/ft^3}$$

$$T_v - T_{SAT} = 0.070^\circ\ F.$$

Thus there is very little liquid superheat and the vaporization process may be considered to be taking place in thermal equilibrium.

As shown in Appendix A the internal source function, S, which includes absorption of radiant energy by the vapor phase, approaches zero for the negligible absorption present in this study.

Substitution of Equations (B.2), (B.3) and (B.7) into Equation (B.1) gives

$$\rho \, C_p \frac{\partial T}{\partial \theta} - k \left(\frac{\partial^2 T}{\partial r^2} + \frac{1}{r}\frac{\partial T}{\partial r}\right) = 0$$

or

$$\frac{\partial T}{\partial \theta} - \alpha \left(\frac{\partial^2 T}{\partial r^2} + \frac{1}{r}\frac{\partial T}{\partial r}\right) = 0 \qquad \text{(B.8)}$$

within the vapor phase. This is Equation (2.1) of Chapter II.

APPENDIX C

CONVECTION EFFECT WITHIN VAPOR PHASE

Convection Effect Within Vapor Phase

In order to estimate the effect of ignoring convection in the energy equation for the vapor phase it is necessary to know the ratio of convective to conductive heat fluxes

$$\frac{\rho_v C_{p_v} v \frac{\partial T}{\partial r}}{k_v \left[\frac{\partial^2 T}{\partial r^2} + \frac{1}{r} \frac{\partial T}{\partial r} \right]} . \tag{C.1}$$

Subject to the case of negligible convection it was found that

$$\frac{\partial T}{\partial r} = K_1 (\theta) \frac{e^{-\frac{r^2}{4\alpha_v \theta}}}{r} \tag{C.2}$$

so

$$\frac{\partial^2 T}{\partial r^2} = K_1 (\theta) e^{-\frac{r^2}{4\alpha_v \theta}} \left(- \frac{1}{r^2} - \frac{1}{2\alpha_v \theta}\right) . \tag{C.3}$$

Substitution of Equations (C.2) and (C.3) into Equation (C.1) gives

$$\frac{\rho_v C_{p_v} v \frac{\partial T}{\partial r}}{k_v \left[\frac{\partial^2 T}{\partial r^2} + \frac{1}{r} \frac{\partial T}{\partial r} \right]} = \frac{\frac{1}{\alpha_v} \frac{v K_1 (\theta) e^{-\frac{r^2}{4\alpha_v \theta}}}{r}}{K_1 (\theta) e^{-\frac{r^2}{4\alpha_v \theta}} \left[\left(- \frac{1}{r^2} - \frac{1}{2\alpha_v \theta}\right) + \frac{1}{r^2} \right]} \tag{C.4}$$

so

$$\frac{\rho_v \, C_{p_v} \, v \, \frac{\partial T}{\partial r}}{k_v \left[\frac{\partial^2 T}{\partial r^2} + \frac{1}{r} \frac{\partial T}{\partial r} \right]} = - \frac{2v\theta}{r} . \tag{C.5}$$

The vapor velocity, v, may be estimated by considering the work of Florschuetz and Chao (26). As stated by them, for equilibrium bubble growth within a liquid of small superheat the bubble wall temperature approaches the saturation value corresponding to the external pressure, and hence the pressure difference approaches zero. The liquid inertia is then negligible and heat transfer is the controlling factor of the bubble growth. This situation is essentially the case for the present investigation after the first few hundred microseconds have passed. Thus the portion of the film growth considered is controlled by heat transfer to the interface through the vapor and convection away from the interface by the liquid.

For heat transfer controlled collapse Florschuetz and Chao (26) found that the velocity, v, at the vapor-liquid interface was two orders of magnitude smaller than the bubble wall velocity, $\dot{R}$. For the case where the growth process may be considered to be the inverse of the collapse process and v is taken to be two orders of magnitude smaller than $\dot{R}$ for both bubble growth and the film growth of the present investigation, Equation (C.5) gives

$$\frac{2v\theta}{r} = \frac{2 \times (\frac{3.87 \text{ in/sec}}{100}) \times 7.33 \times 10^{-4} \text{ sec}}{9.4 \times 10^{-3} \text{ in}} \tag{C.6}$$

$$= 0.00604$$

for run number 2.

Therefore the value of the ratio of convective to conductive heat fluxes is less than one per cent, and the ignoring of convection within the vapor phase is justified.

APPENDIX D

DERIVATION OF THE ENERGY BALANCE AT THE VAPOR-LIQUID INTERFACE

To analyze the energy transfer that is taking place at the vapor-liquid interface region a control volume will be used. The control volume is depicted as shown in the sketch below.

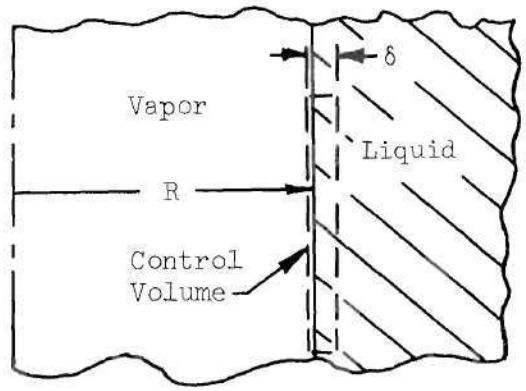

The control volume is of thickness δ and is located at the vapor-liquid interface within the liquid phase. The control volume is considered stationary at some instant in time.

From Hill and Peterson (27), with the addition of an internal heat generation term, the energy equation for the control volume is

$$\int_{CS} \dot{Q}\, dA + \int_{CV} \dddot{q}\, dV = \frac{d}{d\theta} \int_{CV} (e_o\, \rho)\, dV + \int_{CS} (h + \frac{u^2}{2} + gz)\, \rho \vec{u} \cdot \vec{n} dA$$

$$+ P_w + P_s - \int_{CV} \vec{X} \cdot \vec{u}\, dV \qquad \text{(D.1)}$$

where

$\dot{Q}$ = local heat transfer rate (per unit time per unit area), positive into control volume,

$\dddot{q}$ = internal heat generation term,

e_o = total energy per unit mass,

h = $e + P/\rho$ = enthalpy of fluid,

P_w = shaft work done by control volume,

P_s = viscous work done by control volume,

and

$\vec{X}$ = body force per unit volume on fluid within control volume.

The integral

$$\int_{CS} Q \, dA$$

constitutes the heat transfer across the entire control surface surrounding the control volume. For this investigation it yields

$$\int_{CS} Q \, dA = \left[- kv \left.\frac{\partial T}{\partial r}\right|_{r=R} R - h_{\ell m} \left(T_{SAT} - T_{\infty}\right) \left(R + \delta\right)\right] 2 \pi L \qquad (D.2)$$

where the first term on the right side of the equation is the conduction into the control volume from the vapor and the second term is the convection into the liquid from the control volume.

The integral

$$\int_{CV} \dddot{q} \, dV$$

is the internal heat generation as the result of radiant energy absorption within the control volume and so

$$\int_{CV} \dot{q}\, dV = K \; (q_{rad,w}) \; \frac{r_w}{R} \; (2\,\pi L R \delta) \tag{D.3}$$

where K = absorption coefficient of the liquid

$q_{rad,w}$ = radiant energy leaving the wire

and

r_w = radius of the wire.

The total energy for the control volume of mass m is

$$E_o = E + m\frac{u^2}{2} + mgz \tag{D.4}$$

and E_o per unit mass is designated as e_o. The rate of change of the total energy per unit mass within the control volume is therefore

$$\frac{d}{d\theta} \int_{CV} e_o \, \rho \, dV = \frac{d}{d\theta} \left[e_o \, \rho \; 2\,\pi R L \, \delta \right]. \tag{D.5}$$

The transport of enthalpy, kinetic energy, and potential energy is denoted by the integral

$$\int_{CS} \left(h + \frac{u^2}{2} + gz\right) \rho \vec{u} \cdot \vec{n} \; dA. \tag{D.6}$$

For this investigation the kinetic energy and potential energy transfer are negligible and thus Equation (D.6) becomes

$$\int_{C_S} h \rho \vec{u} \cdot \vec{n} \, dA \approx \left[- h_{liquid} (R + \delta) + h_{vapor} R \right] \rho_v \dot{R} \, 2 \pi L. \qquad (D.7)$$

The term P_w is the shaft work done within the control volume and is zero for this investigation.

The velocity of the fluid flow is perpendicular to the control surface and therefore the term P_s for the viscous work is also zero.

The last term of Equation (D.1) which is

$$\int_{CV} \vec{X} \cdot \vec{u} \, dV \qquad (D.8)$$

represents work transfer via body forces. For X_r being the radial component of the body force Equation (D.8) gives

$$\int_{CV} \vec{X} \cdot \vec{u} \, dV = X_r \dot{R} \, 2 \pi RL \, \delta . \qquad (D.9)$$

Substitution of Equations (D.2), (D.3), (D.5), (D.7), and (D.9) into Equation (D.1) then yields

$$\left[- k_v \left. \frac{\partial T}{\partial r} \right|_{r=R} R - h_{\ell m} (T_{SAT} - T_\infty) (R + \delta) \right] 2 \pi L + K (q_{rad,w}) \frac{r_w}{R} (2 \pi LR \, \delta) =$$

$$\left[\frac{d}{d\theta} (e_o \rho) \right] 2 \pi RL \, \delta + \left[-h_{liquid} (R + \delta) + h_{vapor} R \right] \rho_v \dot{R} \, 2 \pi L - X_r \dot{R} \, 2 \pi RL \, \delta . \qquad (D.10)$$

After taking the limit as $\delta \rightarrow 0$ and then dividing through by $2\pi LR$ Equation (D.10) gives

$$- k_v \left.\frac{\partial T}{\partial r}\right|_{r=R} - h_{\ell m} (T_{SAT} - T_\infty) = \rho_v \dot{R} (h_{vapor} - h_{liquid}). \qquad (D.11)$$

Since

$$T(R) = T_{SAT}, \; T(R + \delta) \rightarrow T_{SAT} \quad \text{as} \quad \delta \rightarrow 0.$$

Therefore

$$h_{R + \delta,\ liquid} \rightarrow h_{SAT} \text{ and then } (h_{vapor} - h_{liquid}) = h_{fg}$$

so that Equation (D.11) becomes

$$- k_v \left.\frac{\partial T}{\partial r}\right|_{r=R} - h_{\ell m} (T_{SAT} - T_\infty) = \rho_v \dot{R} h_{fg}. \qquad (D.12)$$

Equation (D.12) is the energy balance at the vapor-liquid interface of the vapor film. It is noted that the absorption of radiant energy goes to zero as the control volume thickness, δ, goes to zero. This is due to the absorption in depth of the radiation within the liquid phase.

APPENDIX E

CALCULATIONS

System Time Constant

Calculation of Adiabatic Wire Temperature

Axial Temperature Distribution Within Wire

Radial Temperature Variation Within Wire

System Time Constant

The electrical charge on a capacitor decreases exponentially with time according to

$$Q = Q_o e^{-t/RC} \tag{E.1}$$

where Q_o is the initial charge, t is the time in seconds, R is the circuit resistance in ohms, and C is the capacitance in farads. The capacitance was 100 microfarads for the investigation. The heating element had an approximate resistance of 0.2510 ohm at an average temperature of 785° F. The copper leads from the capacitor and the heating element holder apparatus contributed resistances of 0.0242 ohm and 0.0388 ohm respectively. Thus the total resistance of the capacitor discharge circuit was approximately 0.3140 ohm.

Approximate the time constant, i.e., the product RC, by the approximate total circuit resistance times the circuit capacitance to obtain

$$RC = 0.3140 \times 100 \times 10^{-6} = 31.40 \times 10^{-6} \text{ seconds.} \tag{E.2}$$

Thus, by Equation (E.1), the discharge of the capacitor is more than 99 per cent complete at the end of 145 microseconds.

Calculation of Adiabatic Wire Temperature

In order to estimate the possible upper limit of the wire temperature the adiabatic wire temperature was calculated. As stated previously

in the calculation of the system time constant a portion of the energy will be dissipated in both the copper leads from the capacitor and the heating element support. Thus the amount of energy that dissipates within the heating element may be approximated as

$$Q = \left(\frac{\text{Resistance of heating element at mean wire temperature}}{\text{Total discharge circuit resistance}}\right) \times \frac{CV^2}{2}$$

which for the case under consideration yields

$$Q = \left(\frac{0.2510\ \Omega}{0.3140\ \Omega}\right) \times \left(\frac{1}{2}\right) \times (0.0001 \text{ farad}) \times (450 \text{ volts})^2$$

$$Q = 1.94 \text{ cal}$$

$$Q = 7.7 \times 10^{-3} \text{ Btu.}$$

Now for the heating element being used

$$Q = m\ C_p\ \Delta T.$$

For the element used the approximate final adiabatic temperature was approximately

$$\Delta T = \frac{Q}{mC_p} = \frac{7.7 \times 10^{-3} \text{ Btu}}{\pi\ (0.005 \text{ in})^2\ (1.85 \text{ in})\ (0.774\ \text{lb}_m/\text{in}^3)\ (0.035\ \text{Btu/lb}_m\ {}^\circ\text{F})}$$

$$\Delta T = 1{,}950^\circ \text{ F}$$

which is a little higher than the average temperature increase obtained in this investigation. Since the copper leads from the capacitor and the heating element holder apparatus had such relatively large masses in

comparison to the heating element, any temperature rise within them should be negligible.

Axial Temperature Distribution Within Wire

The time varying axial temperature distribution was approximated by a region $-\ell < x < \ell$ with zero surface temperature, zero initial temperature, and heat production at the rate $A_o e^{-\lambda\theta}$ per unit volume for $\theta > 0$. The differential equation was then

$$\frac{\partial^2 T}{\partial x^2} - \frac{1}{\alpha}\frac{\partial T}{\partial \theta} = - \frac{A_o e^{-\lambda\theta}}{k} \tag{E.3}$$

with the initial condition

$$T\ (x,\ 0) = 0 \tag{E.4}$$

and boundary conditions

$$T\ (-\ \ell,\ \theta) = 0 \tag{E.5}$$

and

$$T\ (\ell,\ \theta) = 0. \tag{E.6}$$

The solution to Equation (E.3) with the given initial and boundary conditions may be found on page 132 of reference (28) to be

$$T = \frac{\alpha A_o}{\lambda k}\left(\frac{\cos x\,(\lambda/\alpha)^{1/2}}{\cos \ell\,(\lambda/\alpha)^{1/2}} - 1\right) e^{-\lambda\theta}$$

$$+ \frac{4\,\alpha A_o}{\pi \lambda k} \sum_{n=0}^{\infty} \frac{(-1)^n e^{-\alpha\left[(2n+1)^2 \pi^2\theta/4\ell^2\right]} \cos (2n+1)\,\pi\, x/2\ell}{(2n+1)\left\{1 - \left[(2n+1)^2 \pi^2\alpha/4\,\lambda\ell^2\right]\right\}} .$$

The above equation was solved for a typical case in this investigation and the results are plotted in Figure 36. It may be noted that the mean temperature is again approximately 1950° F above the initial wire temperature which was the value calculated previously for the adiabatic wire. This case, like that of the adiabatic wire, again neglects any energy lost radially from the wire.

Radial Temperature Variation Within Wire

From Kreith (29) it is found that for a cylinder the error introduced by the assumption of uniform temperature will be less than 5 per cent when the internal resistance is less than 10 per cent of the external surface resistance, i.e., when the Biot number, Bi, is

$$Bi = \frac{\bar{h}r}{kz} < 0.1 \qquad (E.7)$$

where

$\bar{h}$ = average unit-surface conductance

$\frac{r}{2}$ = characteristic length

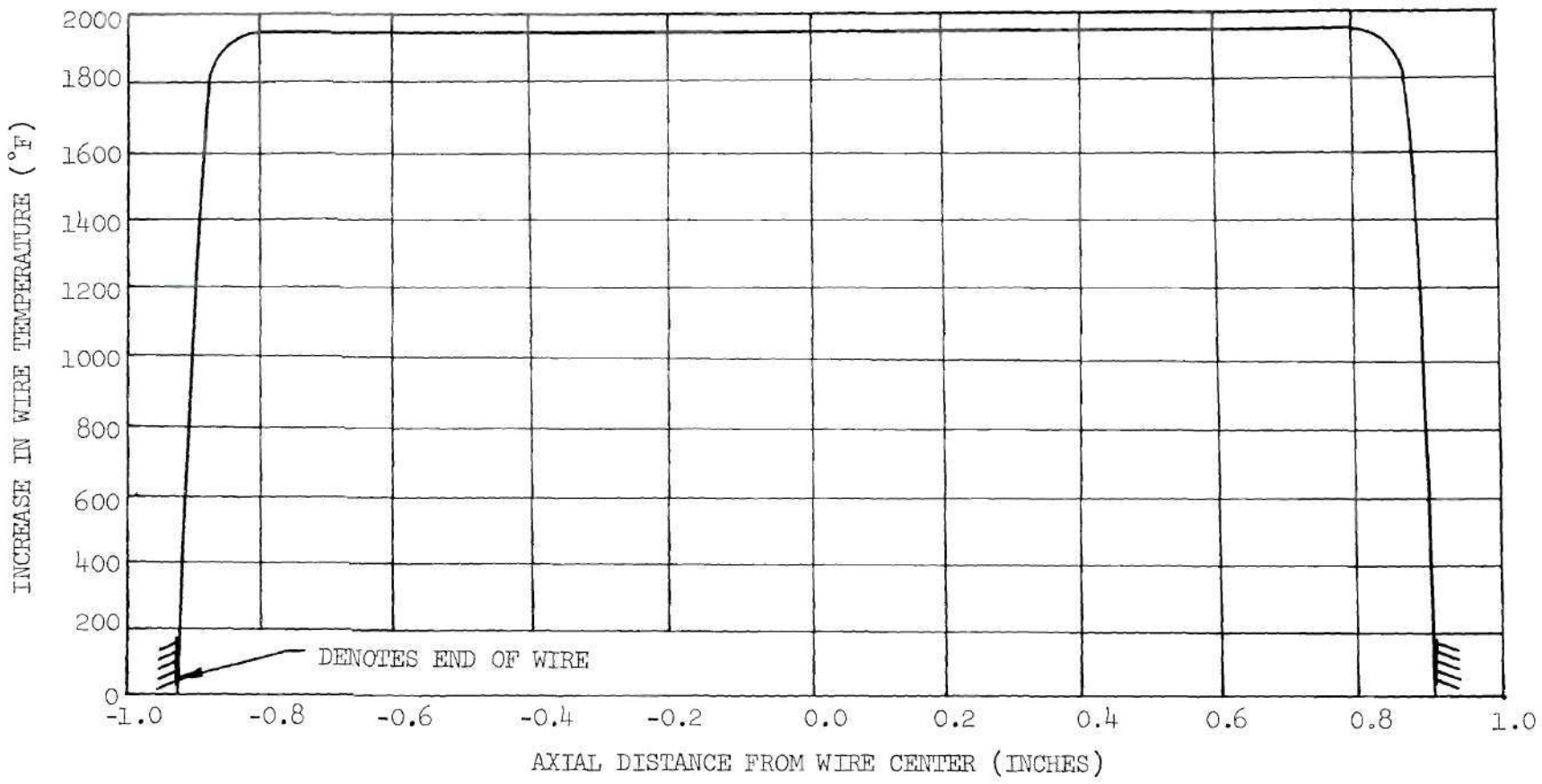

Figure 36. Increase in Wire Temperature versus Axial Distance From Wire Center. Time = 0.010 sec. Platinum Wire. Wire Diameter = 0.010 in.

and

k = thermal conductivity of the wire.

For a typical case consider run number 2 where

$$\bar{h} = \frac{1300 \text{ Btu/hr ft}^2}{1770^\circ \text{ F}} = 7.35 \frac{\text{Btu}}{\text{hr ft}^2 \ ^\circ\text{F}}$$

$$\frac{r}{2} = \frac{0.005 \text{ in}}{2 \times 12 \text{ in/ft}}$$

and

$$k = 40 \text{ Btu/hr ft } ^\circ \text{ F}.$$

Thus Equation (E.7) gives

$$Bi = \frac{7.35 \frac{\text{Btu}}{\text{hr ft}^2 \ ^\circ\text{F}} \times \left(\frac{0.005 \text{ in}}{2 \times 12 \text{ in/ft}}\right)}{40 \text{ Btu/hr ft } ^\circ\text{F}}$$

$$= 3.83 \times 10^{-5}$$

and therefore the radial temperature gradient is negligible within the wire.

APPENDIX F

ERROR ANALYSIS

Vapor Cylinder Radius Determination

Element Temperature Measurement

Vapor Cylinder Radius Determination

The diameter of the test wire was measured prior to the test runs. Each experimentally obtained vapor film was then related to the test wire as a ratio of their respective projected diameters. Thus the vapor film thickness was obtained in terms of its diameter. The error in the determination of the vapor film radius is then equal to the error in the determination of the vapor film diameter, since the radius is merely one-half of the diameter.

For an arbitrary function A the error associated with its determination is given by

$$\Delta A = \sum_i \frac{\partial A}{\partial m_i} \Delta m_i \tag{F.1}$$

where the m_i's are the variables of measurement. For the vapor cylinder diameter the variables of measurement are:

(1) Individual projection station diameter

(2) Actual wire diameter

(3) Projected wire diameter

(4) Defining of vapor-liquid interface

In terms of the above four variables Equation (F.1) becomes

$$\frac{\Delta D}{D} = \frac{\partial D}{\partial d_1} \frac{\Delta d_1}{D} + \frac{\partial D}{\partial d_2} \frac{\Delta d_2}{D} + \frac{\partial D}{\partial d_3} \frac{\Delta d_3}{D} + \frac{\partial D}{\partial d_4} \frac{\Delta d_4}{D} . \tag{F.2}$$

A typical projected vapor-liquid interface diameter was 1.30

centimeters. This was measured to an accuracy of 0.025 centimeters. Thus the error from the individual projection station diameter is

$$\frac{\partial D}{\partial d_1} \frac{\Delta d_1}{D} = \frac{1.30}{1.30} \times \frac{0.025}{1.30} = 0.0192. \qquad (F.3)$$

The actual wire diameter was measured and found to be 0.010 plus or minus .00025 inches. Therefore the error resulting from an actual wire diameter determination was

$$\frac{\partial D}{\partial d_2} \frac{\Delta d_2}{D} = \frac{1.30/2.54}{0.010} \times \frac{.00025}{1.30/2.54} = 0.025. \qquad (F.4)$$

A typical projected wire diameter was 0.35 centimeters. The projected wire diameter was measured to an accuracy of 0.025 centimeters. The error resulting from this source was

$$\frac{\partial D}{\partial d_3} \frac{\Delta d_3}{D} = \frac{1.30}{0.35} \times \frac{0.025}{1.30} = 0.0715. \qquad (F.5)$$

The vapor-liquid interface could be located with an accuracy of 0.05 centimeters to give an error of

$$\frac{\partial D}{\partial d_4} \frac{\Delta d_4}{D} = \frac{1.30}{1.30} \times \frac{0.05}{1.30} = 0.0384. \qquad (F.6)$$

Substitution of Equation (F.3), (F.4), (F.5), and (F.6) into Equation (F.2) yields a typical vapor cylinder diameter error of

$$\frac{\Delta D}{D} = 0.0192 + 0.025 + 0.0715 + 0.0384 = 0.1541 \qquad (F.7)$$

or approximately 15.4 per cent.

If a normal (Gaussian) distribution of errors is assumed, then the probable error becomes

$$\frac{\Delta D_P}{D} = \left[\frac{\partial D}{\partial d_1}\ \frac{\Delta d_1}{D}^2 + \frac{\partial D}{\partial d_2}\ \frac{\Delta d_2}{D}^2 + \frac{\partial D}{\partial d_3}\ \frac{\Delta d_3}{D}^2 + \frac{\partial D}{\partial d_4}\ \frac{\Delta d_4}{D}^2\right]^{1/2}. \qquad (F.8)$$

Substitution of Equation (F.3), (F.4), (F.5), and (F.6) into Equation (F.8) yields a probable error of

$$\frac{\Delta D_P}{D} = \left[(0.0192)^2 + (0.025)^2 + (0.0715)^2 + (0.0384)^2\right]^{1/2} = 0.087 \quad (F.9)$$

or approximately 8.7 per cent for one station.

Element Temperature Measurement

The variables of measurement are:

1. Bridge current, I
2. Oscilloscope gain, G
3. Oscilloscope drift between reference reading and data reading, B

4. Oscilloscope reading error, S
5. Potentiometer error, H
6. Standard platinum versus platinum plus 10 per cent rhodium thermocouple error, P.

Items one through three occur twice in any temperature measurement, once during calibration and once during the boiling experiment. Item four also occurred twice for each temperature measurement, once during calibration and once during the boiling experiment. Also two readings were required for each temperature measurement, i.e., bridge unbalance voltage and bridge unbalance at zero bridge current. From Equation (F.1) the maximum error in element temperature measurement becomes

$$\Delta T = 2 \frac{\partial T}{\partial I} \Delta I + 2 \frac{\partial T}{\partial G} \Delta G + 2 \frac{\partial T}{\partial B} \Delta B$$

$$+ 4 \frac{\partial T}{\partial S} \Delta S + \frac{\partial T}{\partial H} \Delta H + \frac{\partial T}{\partial P} \Delta P. \qquad \text{(F.10)}$$

The bridge current was adjusted to within one-half milliampere for each reading. The current was 100 milliamperes for all tests, so the error for one milliampere at a typical heating element temperature of 1500° F would be

$$\frac{\Delta T}{\Delta I} = \frac{1}{100} \times 1500 = 15^\circ \text{ F/milliampere} \qquad \text{(F.11)}$$

which yields

$$2 \frac{\partial T}{\partial I} \Delta I = 15^\circ \text{ F.} \tag{F.12}$$

The oscilloscope gain was adjusted and controlled to within one-tenth of the smallest grid division on the scope screen. Twenty of these divisions represented about 1500° F. Thus,

$$\frac{\Delta T}{\Delta G} = \frac{1}{20} \times 1500 = 75^\circ \text{ F/division} \tag{F.13}$$

and

$$2 \frac{\partial T}{\partial G} \Delta G = 2 \times 75 \times \frac{1}{10} = 15^\circ \text{ F.} \tag{F.14}$$

The oscilloscope drift was checked before every reading during both the calibrations and the actual tests. This was accomplished by triggering the scope at a sensitivity five times as great as the one used during the actual tests and then observing any drift that may have occurred. Thus, the drift could be held to within one-fourth of the smallest grid division. So

$$2 \frac{\partial T}{\partial B} \Delta B = 2 \times \frac{1500}{20} \times \frac{1}{4} = 24^\circ \text{ F.} \tag{F.15}$$

The oscilloscope reading error was held to within one-fourth of the smallest grid division for each reading. Thus,

$$\frac{\Delta T}{\Delta S} = \frac{1500}{20} = 75^\circ\text{/division} \tag{F.16}$$

and

$$4 \frac{\partial T}{\partial S} \Delta S = 4 \times 75 \times \frac{1}{4} = 75^\circ \text{ F.} \tag{F.17}$$

The manufacturer's stated error for the K-3 potentiometer is 0.015 per cent plus 0.5 microvolts. The emf error at 1500 degrees Fahrenheit is approximately

$$\Delta H \approx .00015 \times 7.498 + 0.5 \times 10^{-6} \approx 1.6 \times 10^{-3} \text{ millivolt} \tag{F.18}$$

and

$$\frac{\partial T}{\partial H} \approx \frac{1500}{7.498} \approx 200^\circ \text{ F/millivolt} \tag{F.19}$$

so,

$$\frac{\partial T}{\partial H} \Delta H \approx 200 \times 1.6 \times 10^{-3} \approx 0.32^\circ \text{ F.} \tag{F.20}$$

The stated error for the platinum versus platinum plus 10 per cent rhodium thermocouple, that had been calibrated by Leeds and Northrup, is 0.75 degrees Centigrade in the range 0 to 1100 degrees Centigrade. So,

$$\frac{\partial T}{\partial P} \Delta P = 1 \times (0.75 \times 1.8) = 1.35^\circ \text{ F.} \tag{F.21}$$

Hence, by Equation (F.10) the maximum error in a heating element temperature measurement is

$$\Delta T = 15 + 15 + 24 + 75 + 0.32 + 1.35 = 130.67^\circ \text{ F} \tag{F.22}$$

and the maximum per cent error is

$$\frac{\Delta T}{T} = \frac{130.67}{1500} = 8.7 \text{ per cent.} \tag{F.23}$$

Applying Equation (F.8) to the element temperature yields a probable error of

$$\Delta T_P = \left[(15)^2 + (15)^2 + (24)^2 + (75)^2 + (0.32)^2 + (1.35)^2 \right]^{1/2} = 81.5^\circ \text{ F} \tag{F.24}$$

so the probable per cent error is

$$\frac{\Delta T_P}{T} = \frac{81.5}{1500} = 5.43 \text{ per cent} \tag{F.25}$$

for a single temperature determination.

APPENDIX G

DATA

Descriptive and Calibration Data for Heating Elements

General Test Data for each Transient Boiling Experiment

Heating Element Temperature History Data

Vapor Growth Rate Data

Table 3. Heating Element Descriptive Data

Element	Description
1	Commercially pure platinum wire, 0.010 inch in diameter, 1.85 inches long.
2	Commercially pure platinum wire, 0.010 inch in diameter, 1.83 inches long.
5	Commercially pure platinum wire, 0.010 inch in diameter, 1.85 inches long.
6	Commercially pure platinum wire, 0.010 inch in diameter, 1.80 inches long.
7	Commercially pure platinum wire, 0.010 inch in diameter, 1.85 inches long.

Table 4. Temperature Calibration Data for All Heating Elements.

Element	Date	Thermocouple EMF (Millivolts)	Wire Temperature (°F)	Bridge Unbalance (Millivolts)	Bridge Current (Milliamps)
1	5-8-69	0.135	74.5	8.70	100
1	5-8-69	.0.918	277	11.00	100
1	5-8-69	2.100	529	12.80	100
1	5-8-69	3.331	767	15.00	100
1	5-8-69	4.529	988	16.90	100
1	5-8-69	5.698	1195	18.40	100
1	5-8-69	6.523	1337	19.80	100
1	5-8-69	7.873	1562	21.50	100
2	5-10-69	0.201	94	8.50	100
2	5-10-69	1.260	354	10.90	100
2	5-10-69	2.741	655	13.50	100
2	5-10-69	4.001	892	15.50	100
2	5-10-69	5.572	1173	17.50	100
2	5-10-69	6.519	1336	18.90	100
2	5-10-69	7.876	1562	20.50	100
5	7-1-69	2.225	554	14.00	100
5	7-1-69	3.641	825	16.30	100
5	7-1-69	5.201	1108	19.10	100
5	7-1-69	6.308	1300	21.30	100
5	7-1-69	7.669	1528	23.50	100
6	7-8-69	0.166	84	9.10	100
6	7-8-69	1.430	390.6	12.10	100
6	7-8-69	2.950	694.9	15.10	100
6	7-8-69	4.540	990	17.60	100
6	7-8-69	6.090	1262.9	20.00	100
6	7-8-69	7.680	1529.9	22.20	100
7	7-10-69	0.230	102.6	9.40	100
7	7-10-69	2.120	533	13.70	100
7	7-10-69	3.890	871.3	16.70	100
7	7-10-69	5.490	1158.7	18.70	100
7	7-10-69	7.650	1525	22.40	100

Table 5. Temperature Recalibration Data for Heating Element Number 2.

Date	Thermocouple EMF (Millivolts)	Wire Temperature (°F)	Bridge Unbalance (Millivolts)	Bridge Current (Milliamps)
8-23-69	0.140	76.1	8.50	100
8-23-69	1.427	390	11.70	100
8-23-69	3.055	714.5	14.50	100
8-23-69	5.030	1077.7	17.80	100
8-23-69	6.240	1288.6	18.80	100
8-23-69	7.350	1475.5	20.00	100

Table 6. General Data for Transient Boiling Tests

Run No.	Fluid Type	Bulk Fluid Temperature (°F)	Fluid Depth (in.)	Film Type	Lens f/stop	Barometer Pressure (mm Hg.)
1	CCl_4	170.0	1.00	Kodak 4-X	1.8	743.00
2	CCl_4	157.5	1.00	Kodak 4-X	1.8	743.00
3	CCl_4	153.9	1.00	Kodak 4-X	1.8	743.00
5	CCl_4	168.9	1.00	Kodak 4-X	1.8	743.00
6	CCl_4	168.9	1.75	Kodak 4-X	1.8	740.10
7	CCl_4	169.0	1.75	Kodak 4-X	1.8	740.10
8	CCl_4	169.0	1.50	Kodak 4-X	1.8	740.10
9	CCl_4	164.6	1.50	Kodak 4-X	1.8	740.10
10	CCl_4	163.2	1.50	Kodak 4-X	1.8	740.10
16	H_2O	212.0	2.00	Kodak 4-X	1.8	742.40
19	Freon	111.2	2.00	Kodak 4-X	1.8	741.00
20	Freon	111.2	2.00	Kodak 4-X	1.8	741.00
21	Freon	104.3	2.00	Kodak 4-X	1.8	741.00
22	Freon	116.7	2.50	Kodak 4-X	1.8	738.00
23	Freon	117.1	2.50	Kodak 4-X	1.8	738.00
24	Freon	103.4	2.50	Kodak 4-X	1.8	738.00
25	Freon	102.6	2.50	Kodak 4-X	1.8	738.00
26	Freon	110.5	2.50	Kodak 4-X	1.8	738.00

Table 7. Heating Element Temperature Data for Transient Boiling Tests

Run No.	Element	Capacitor Voltage	Time Millisec.	Bridge Unbalance - Millivolts 0	10	20	30	40
1	2	450		24.75	24.50	24.25	24.00	23.75
2	2	450		25.00	24.70	24.40	24.05	23.70
3	2	450		24.75	24.40	24.10	23.80	23.45
5	2	450		24.50	24.25	24.00	23.75	23.50
6	1	410		20.80	20.60	20.40	20.20	20.00
7	1	430		21.95	21.70	21.55	21.30	21.00
8	1	450		22.50	22.25	22.05	21.85	21.65
9	1	450		22.00	21.80	21.60	21.45	21.30
10	1	450		22.20	22.00	21.80	21.60	21.40
16	5	450		23.95	23.55	23.30	22.90	22.45
19	6	432		21.75	21.55	21.35	21.10	20.90
20	6	432		22.25	21.90	21.60	21.10	20.65
21	6	432		22.25	21.95	21.65	21.40	21.00
22	7	450		23.75	23.30	22.90	22.50	22.05

(continued)

Table 7. (Continued)

Run No.	Element	Capacitor Voltage	Time Millisec.	Bridge Unbalance - Millivolts 0	10	20	30	40
23	7	450		24.00	23.50	23.05	22.65	22.45
24	7	450		24.00	23.45	23.00	22.55	22.25
25	7	450		23.45	23.00	22.75	22.40	22.05
26	7	450		24.05	23.50	23.10	22.75	22.45

Table 8. Film Growth Rate Data for Run Number 1

	Vapor Film Projected Diameter - Centimeters											
Frame Station	1 13	2 14	3 15	4 16	5 17	6 18	7 19	8 20	9 21	10 22	11	12
Wire	.35 .35	.35 .35	.35 .35	.35 .35	.35 .35	.35 .35	.35 .35	.35 .35	.35 .35	.35 .35	.35	.35
Frame No. 1	.55 .65	.55 .70	.55 .75	.55 .70	.55 .65	.55 .80	.55 .75	.55 .60	.60 .65	.65 .75	.65	.65
5	1.05 .70	1.10 1.15	1.10 1.10	.90 .85	.70 .60	.55 1.50	.55 1.05	.55 .35	.75 1.15	.95 1.35	1.00	.85
9	1.10 .85	1.00 1.35	1.00 1.35	.95 .70	.85 .70	.80 2.00	.75 .95	.65 .55	.80 1.10	1.00 1.30	1.30	.75
13	1.25 .95	1.10 1.40	1.00 1.40	1.00 .75	1.15 1.00	1.00 1.80	.90 1.20	.85 .50	.85 1.50	1.05 1.75	1.40	.80
17	1.10 .85	1.05 1.50	1.00 1.55	1.10 .60	1.15 1.10	1.10 2.00	1.00 1.50	.85 .50	.85 1.65	1.10 1.70	1.35	.65
21	1.00 .70	.90 1.65	1.00 1.65	1.15 .55	1.30 1.20	1.30 2.20	1.05 1.60	.85 .40	.80 1.80	1.05 1.95	1.25	.65
25	.95 .50	1.00 1.80	1.20 1.95	1.25 .50	1.35 1.50	1.35 2.50	1.25 1.90	1.00 .40	.80 1.70	1.15 2.10	1.35	.85

(continued)

Table 8. (Continued)

	Vapor Film Projected Diameter - Centimeters											
Frame Station	1 13	2 14	3 15	4 16	5 17	6 18	7 19	8 20	9 21	10 22	11	12
Frame No. 29	1.00 .40	1.20 1.95	1.30 2.10	1.35 .50	1.50 1.40	1.45 2.70	1.25 1.85	1.10 .40	.90 1.90	1.20 2.30	1.50	.65
33	1.20 .50	1.30 2.00	1.30 2.05	1.40 .45	1.60 1.50	1.50 2.80	1.35 1.90	1.20 .50	1.05 2.00	1.35 2.80	1.55	.50
37	1.30 .40	1.50 2.20	1.60 2.10	1.50 .35	1.65 2.00	1.55 3.00	1.50 2.10	1.25 .40	1.10 1.85	1.50 3.00	1.75	.40
41	1.35 .40	1.65 2.10	1.65 2.30	1.75 .45	1.75 1.85	1.60 3.00	1.65 2.30	1.10 .40	1.05 1.80	1.65 3.20	1.75	.50

Framing Rate = 43 frames/11 millisec. = 3,910 frames/sec

Table 9. Film Growth Rate Data for Run Number 2

	Vapor Film Projected Diameter - Centimeters											
Frame Station	1 13	2 14	3 15	4 16	5 17	6 18	7 19	8 20	9 21	10	11	12
Wire	.55 .35	.45 .35	.45 .35	.40 .35	.40 .35	.45 .35	.45 .35	.40 .35	.40 .35	.40	.35	.40
Frame No. 1	.65 .65	.55 .55	.55 .70	.50 .60	.55 .75	.60 .85	.55 .70	.55 .65	.60 .65	.70	.70	.70
5	.90 .80	.70 1.05	.65 1.00	.65 .50	.70 .90	.60 1.55	.60 .50	.60 .65	.80 1.00	1.00	.95	.60
9	1.10 1.00	1.00 1.30	.75 1.05	.85 .65	.90 .90	.85 1.70	.85 .60	.75 .50	.95 1.05	1.20	1.20	.65
13	1.25 .90	.95 1.40	.60 1.30	.90 .75	.95 .75	1.05 1.50	1.00 .50	.65 .50	.75 1.30	1.10	1.20	.50
17	1.30 .65	.90 1.50	.55 1.25	.95 .55	1.15 .90	1.15 1.75	1.05 .50	.75 .50	.75 1.60	.75	1.35	.40
21	1.25 .85	.65 1.75	.55 1.25	1.05 .50	1.45 1.40	1.45 2.00	1.15 .40	.75 .50	.85 1.90	1.70	1.45	.40
25	1.35 .60	.55 1.75	.45 .90	1.10 .65	1.45 1.40	1.55 2.00	1.20 .50	.60 .50	1.00 2.05	1.55	1.25	.50

(continued)

Table 9. (Continued)

	Vapor Film Projected Diameter - Centimeters											
Frame Station	1 13	2 14	3 15	4 16	5 17	6 18	7 19	8 20	9 21	10	11	12
Frame	1.50	.45	.65	1.20	1.50	1.60	1.25	.60	1.10	1.65	1.10	.55
No. 29	.75	1.85	.90	.60	1.35	2.00	.40	.40	2.10			
33	1.60	.45	.70	1.30	1.60	1.75	1.25	.45	1.10	1.80	1.20	.55
	.65	1.95	1.00	.50	1.60	2.25	.40	.50	2.05			
37	1.90	.60	.90	1.20	1.70	1.70	1.45	.45	1.20	1.90	1.25	.50
	.65	2.10	1.30	.55	1.90	2.50	.40	.50	2.05			
41	2.00	.50	1.05	.50	1.80	1.80	1.50	.55	1.15	2.00	1.30	.50
	.60	2.20	1.25	.55	2.20	2.60	1.00	.50	1.90			

Framing Rate = 57 frames/14 millisec. = 4,070 frames/sec

Table 10. Film Growth Rate Data For Run Number 3

	Vapor Film Projected Diameter - Centimeters												
Frame Station	1 14	2 15	3 16	4 17	5 18	6 19	7 20	8 21	9 22	10 23	11 24	12 25	13
Wire	.30 .30	.30 .30	.30 .30	.30 .30	.30 .30	.30 .30	.30 .30	.30 .30	.30 .30	.30 .30	.30 .30	.30 .30	.30
Frame No. 1	.55 .65	.65 .70	.60 .75	.65 .65	.70 .60	.70 .65	.70 .75	.65 .75	.55 .80	.55 .70	.65 .60	.70 .60	.65
5	.45 .80	.55 .90	.85 .75	.85 .35	.90 .40	.95 .30	.95 .80	.70 1.25	.40 1.20	.45 .70	.60 .60	.60 .40	.75
9	.65 1.15	.55 1.10	.60 1.05	.70 .55	.90 .50	1.10 .40	1.05 .50	.90 .80	.60 1.15	.50 .50	.55 .50	.65 .50	.90
13	.70 1.40	.55 1.25	.50 .90	.60 .35	.95 .45	1.05 .40	1.20 .60	.95 1.25	.50 1.50	.35 .60	.40 .50	.75 .50	1.05
17	.80 1.40	.55 1.35	.50 .70	.70 .45	.95 .55	1.15 .50	1.25 .60	1.00 1.30	.60 1.55	.35 .60	.45 .40	.70 .50	1.20
21	.50 1.65	.40 1.30	.50 .55	.90 .40	1.20 .45	1.45 .45	1.30 .85	.75 1.65	.30 1.55	.50 .75	.30 .35	1.00 .45	1.50
25	.45 1.60	.50 1.25	.35 .55	.85 .40	1.50 .75	1.40 .40	1.30 .95	.75 1.75	.35 1.85	.70 1.05	.40 .55	.65 .50	1.50

(continued)

Table 10. (Continued)

	Vapor Film Projected Diameter - Centimeters												
Frame Station	1 14	2 15	3 16	4 17	5 18	6 19	7 20	8 21	9 22	10 23	11 24	12 25	13
Frame No. 29	.50 1.55	.55 1.15	.45 .45	.75 .60	1.50 .50	1.55 .50	1.35 1.25	.60 1.80	.35 1.85	.65 1.20	.30 .60	.60 .45	1.65
33	.45 1.70	.60 1.20	.45 .50	.50 .55	1.55 .65	1.85 .55	1.60 1.40	.70 1.85	.35 2.00	.65 1.70	.60 .45	.50 .55	1.60
37	.45 1.80	.65 1.15	.45 .50	.50 .55	1.50 .70	1.95 .60	1.65 1.40	.75 1.90	.40 2.00	.60 1.65	.40 .45	.60 .45	1.55
41	.45 1.75	.65 1.35	.40 .50	.60 .40	1.50 .50	2.10 .60	1.85 1.45	.80 2.05	.50 2.05	.55 1.65	.45 .90	.80 .60	1.70

Framing Rate = 58 frames/15 millisec. = 3,870 frames/sec

Table 11. Film Growth Rate Data For Run Number 5

	Vapor Film Projected Diameter - Centimeters												
Frame Station	1 14	2 15	3 16	4 17	5 18	6 19	7 20	8 21	9 22	10 23	11 24	12 25	13
Wire	.30 .30	.30 .30	.30 .30	.30 .30	.30 .30	.30 .30	.30 .30	.30 .30	.30 .30	.30 .30	.30 .30	.30 .30	.30
Frame No. 1	.65 .60	.60 .70	.60 .70	.55 .70	.60 .75	.65 .80	.65 .75	.65 .70	.75 .55	.70 .60	.85 .70	.70 .80	.70
5	.80 .55	.75 .70	.80 .55	.75 .60	.75 1.00	.85 1.25	1.05 1.10	1.05 .65	1.10 .65	1.15 .80	1.10 1.20	.95 1.20	.60
9	1.10 .70	1.00 .90	.85 1.20	.80 1.40	.70 1.50	.80 1.45	1.00 .80	1.15 .45	1.30 .65	1.30 1.00	1.25 1.35	.95 1.50	.70
13	1.25 .55	1.20 .90	1.15 1.15	.90 1.35	.75 1.40	.80 1.45	1.05 .95	1.20 .40	1.40 .40	1.45 1.10	1.25 1.35	1.05 1.70	.65
17	1.30 .55	1.30 .75	1.15 1.25	.95 1.50	.85 1.65	.75 1.55	.85 1.20	1.10 .50	1.35 .45	1.50 1.30	1.40 1.45	1.10 1.90	.70
21	1.35 .40	1.35 .70	1.30 1.25	1.05 1.70	1.00 1.80	.85 1.70	.85 1.20	1.15 .50	1.40 .40	1.55 .40	1.65 1.70	1.40 1.95	.80
25	1.50 .30	1.65 .30	1.50 1.20	1.25 1.70	1.05 1.95	.90 1.75	1.00 1.20	1.20 .45	1.50 .50	1.75 .40	1.75 1.75	1.35 2.00	.70

(continued)

Table 11. (Continued)

	Vapor Film Projected Diameter - Centimeters												
Frame Station	1 14	2 15	3 16	4 17	5 18	6 19	7 20	8 21	9 22	10 23	11 24	12 25	13
Frame No. 29	1.60 .35	1.60 .35	1.50 1.00	1.30 1.80	1.00 2.20	.90 1.90	1.05 1.15	1.35 .50	1.75 .60	1.80 .40	1.80 2.10	1.45 2.40	.50
33	1.85 .40	1.75 .50	1.65 1.50	1.30 2.05	1.00 2.25	1.00 1.75	1.25 .80	1.70 .40	1.95 .60	2.00 .40	1.95 2.10	1.35 2.40	.40
37	1.80 .65	1.80 .50	1.70 1.20	1.35 2.10	1.05 2.15	1.00 1.75	1.20 .75	1.70 .50	2.00 .50	2.05 1.10	1.65 2.70	.95 2.60	.50
41	1.90 .40	1.80 .55	1.75 1.40	1.45 1.90	1.10 2.35	.95 1.80	1.10 .85	1.60 .60	2.10 .55	2.10 .50	1.65 2.30	1.00 2.50	.45

Framing Rate = 31 frames/8 millisec. = 3,880 frames/sec

Table 12. Film Growth Rate Data for Run Number 6

	Vapor Film Projected Diameter - Centimeters												
Frame Station	1 14	2 15	3 16	4 17	5 18	6 19	7 20	8 21	9 22	10 23	11 24	12 25	13
Wire	.35 .40	.35 .40	.40 .40	.40 .40	.40 .40	.40 .40	.40 .40	.40 .40	.40 .40	.40 .40	.40 .40	.40 .40	.40
Frame No. 1	.70 .70	.65 .70	.65 .70	.60 .70	.60 .70	.60 .70	.60 .70	.65 .65	.60 .60	.65 .65	.65 .60	.60 .70	.70
5	1.00 1.00	1.00 .55	1.05 .75	1.00 .65	1.00 .65	.95 .70	.80 .70	.55 .80	.50 .80	.60 .65	.65 .60	.70 .60	.90
9	1.05 1.00	1.20 1.00	1.10 .85	.95 .65	.90 .55	.80 .60	.80 .75	.55 .95	.55 1.00	.65 1.00	.80 1.00	.95 .90	1.10
13	1.05 1.25	1.00 1.20	1.05 .95	.90 .85	.90 .85	.90 .70	.90 .85	.75 .75	.75 .90	.75 1.00	1.15 1.00	1.25 .95	1.20
17	1.10 1.60	.95 1.45	.85 1.25	.85 1.00	.75 .85	.80 .75	.75 .80	.75 .80	.95 .90	1.00 1.05	1.10 1.15	1.45 1.10	1.65
21	.80 1.75	.80 1.55	.85 1.30	.90 1.30	.90 .95	.80 .50	.80 .40	.90 .70	1.10 .75	1.10 .85	1.35 1.05	1.50 1.00	1.85
25	.85 2.00	.85 1.75	1.00 1.60	1.15 1.25	1.20 .85	.90 .40	.90 .40	1.00 .60	1.10 .85	1.30 .95	1.45 1.00	1.70 1..0	2.00

(continued)

Table 12. (Continued)

		Vapor Film Projected Diameter - Centimeters												
Frame Station		1 14	2 15	3 16	4 17	5 18	6 19	7 20	8 21	9 22	10 23	11 24	12 25	13
Frame No.		.95	1.00	1.20	1.35	1.30	.80	.95	.95	.90	1.30	1.60	1.90	2.10
	29	2.00	1.90	1.55	1.10	.50	.50	.50	.40	.95	1.15	1.15	1.10	
	33	1.20	1.20	1.20	1.20	1.20	1.00	.85	.85	1.00	1.30	1.80	2.00	2.20
		2.20	2.05	1.65	1.10	.45	.60	.50	.40	.75	1.20	1.35	1.25	
	37	1.20	1.05	1.20	1.20	1.35	.90	.80	.90	1.30	1.70	2.10	2.40	2.50
		2.50	2.20	1.75	.50	.50	.75	.50	.40	.75	1.50	1.50	1.40	
	41	1.20	1.10	1.10	1.10	1.30	1.05	.75	.75	1.30	1.70	2.20	2.30	2.60
		2.60	2.20	1.80	.50	.60	.90	.65	.40	.55	1.30	1.60	1.50	

Framing Rate = 23 frames/6 millisec. = 3,840 frames/sec

Table 13. Film Growth Rate Data for Run Number 7

	Vapor Film Projected Diameter - Centimeters												
Frame Station	1 14	2 15	3 16	4 17	5 18	6 19	7 20	8 21	9 22	10 23	11 24	12 25	13
Wire	.30 .30	.30 .30	.30 .30	.30 .30	.30 .30	.30 .30	.30 .30	.30 .30	.30 .30	.30 .30	.30 .30	.30 .30	.30
Frame No. 1	.65 .60	.60 .70	.70 .70	.60 .65	.60 .65	.60 .65	.60 .70	.65 .70	.65 .65	.60 .65	.70 .70	.70 .70	.65
5	.85 .80	.80 .85	.75 .75	.80 .75	.70 .70	.70 .70	.80 .75	.75 .75	.75 .70	.80 .65	.80 .70	.80 .75	.80
9	.85 .95	.80 .75	.75 .65	.70 .70	.75 .70	.80 .75	.90 .70	.95 .70	1.00 .70	1.05 .70	1.00 .80	1.00 .85	1.00
13	.80 .95	.80 .80	.90 .70	.85 .75	.90 .80	1.05 .80	1.20 .90	1.25 .90	1.25 .90	1.30 .90	1.30 .90	1.25 .90	1.10
17	.90 .95	.70 .95	.50 .65	.75 .50	.80 .65	1.00 .80	1.25 .90	1.40 1.00	1.60 1.00	1.40 .90	1.50 .90	1.40 .90	1.20
21	.75 1.15	.40 .75	.70 .40	1.10 .50	1.15 .85	1.35 .95	1.50 1.10	1.75 1.15	1.90 1.15	1.80 1.10	1.70 1.05	1.55 1.10	1.30
25	.60 1.25	.40 .60	.75 .50	.70 .50	1.35 .65	1.55 .90	1.65 1.20	1.75 1.20	1.90 1.20	1.90 1.10	1.80 1.10	1.55 1.10	1.40

(continued)

Table 13. (Continued)

	Vapor Film Projected Diameter - Centimeters												
Frame Station	1 14	2 15	3 16	4 17	5 18	6 19	7 20	8 21	9 22	10 23	11 24	12 25	13
Frame	.40	.40	.90	.50	1.35	1.70	1.90	2.10	2.20	2.25	2.10	1.90	1.70
No. 29	1.50	.70	.50	.75	.40	1.00	1.20	1.35	1.35	1.25	1.20	1.10	
33	.50	.50	.70	.90	.40	1.90	1.90	2.20	2.25	2.20	2.00	1.95	1.70
	1.25	.50	.60	.60	.50	.75	1.30	1.35	1.20	1.15	1.15	1.00	
37	.65	.90	1.10	.95	.50	1.95	2.00	2.20	2.30	2.35	2.10	1.95	1.70
	.60	.55	.95	.85	.60	.55	1.30	1.40	1.30	1.20	1.15	1.05	

Framing Rate = 30 frames/8 millisec. = 3,750 frames/sec

Table 14. Film Growth Rate Data for Run Number 8

	Vapor Film Projected Diameter - Centimeters												
Frame Station	1 14	2 15	3 16	4 17	5 18	6 19	7 20	8 21	9 22	10 23	11 24	12 25	13
Wire	.30 .30	.30 .30	.30 .30	.30 .30	.30 .30	.30 .30	.30 .30	.30 .30	.30 .30	.30 .30	.30 .30	.30 .30	.30
Frame No. 1	.45 .45	.45 .40	.50 .40	.45 .40	.45 .40	.50 .45	.45 .45	.50 .45	.50 .45	.50 .45	.45 .45	.45 .45	.45
5	.60 .55	.60 .50	.60 .60	.65 .50	.65 .50	.65 .45	.65 .70	.75 1.00	.75 1.10	.70 .75	.65 .60	.60 .60	.60
9	.90 .60	.95 .60	.95 .60	.95 .65	.95 .50	1.00 .40	1.00 .80	1.00 1.50	1.00 1.65	.75 .90	.50 .60	.50 .60	.65
13	.95 .75	1.05 .75	1.30 .75	1.45 .80	1.35 .65	1.25 .60	1.15 1.00	1.00 1.60	.85 1.30	.80 .90	.60 .50	.50 .70	.65
17	1.05 .85	1.25 1.00	1.40 1.10	1.50 .95	1.60 .50	1.50 .50	1.40 1.10	1.15 1.55	.95 1.50	.95 1.00	.40 .60	.60 .55	.70
21	1.10 .90	1.35 1.30	1.55 1.30	1.65 .85	1.70 .55	1.65 .65	1.40 1.05	1.25 1.75	1.05 1.65	.35 1.30	.40 .75	.50 .65	.60
25	1.20 .85	1.30 1.30	1.60 1.50	1.80 1.20	1.90 .70	1.80 .60	1.80 1.10	1.45 1.60	1.20 2.00	.40 1.60	.60 1.10	.65 .65	.40

(continued)

Table 14. (Continued)

	Vapor Film Projected Diameter - Centimeters												
Frame Station	1 14	2 15	3 16	4 17	5 18	6 19	7 20	8 21	9 22	10 23	11 24	12 25	13
Frame	1.30	1.50	1.60	2.00	2.10	2.10	1.80	1.50	.80	.40	.80	.80	.30
No. 29	.50	1.20	1.40	.90	.70	.70	1.10	1.65	2.10	1.80	1.20	.70	
33	1.50	1.70	1.75	2.10	2.30	2.00	1.75	1.50	.40	.60	1.00	.75	.40
	.50	1.30	1.25	.90	.65	.90	1.50	1.95	2.10	1.90	1.30	.85	
37	1.50	1.85	2.00	2.40	2.40	2.20	1.95	.50	.40	.90	1.10	.75	.40
	.85	1.40	1.25	.90	.75	1.30	1.95	2.15	2.25	2.05	1.35	1.00	
41	1.40	2.20	2.20	2.30	2.30	2.30	2.00	.35	.45	.95	1.25	.80	.35
	.70	1.30	1.40	.90	.95	1.50	2.00	2.30	2.30	2.10	1.65	1.05	

Framing Rate = 27 frames/7 millisec. = 3,860 frames/sec

Table 15. Film Growth Rate Data for Run Number 9

	Vapor Film Projected Diameter - Centimeters												
Frame Station	1 14	2 15	3 16	4 17	5 18	6 19	7 20	8 21	9 22	10 23	11 24	12 25	13
Wire	.30 .30	.30 .30	.30 .30	.30 .30	.30 .30	.30 .30	.30 .30	.30 .30	.30 .30	.30 .30	.30 .30	.30 .30	.30
Frame No. 1	.65 .65	.60 .60	.50 .65	.50 .60	.50 .50	.50 .50	.50 .50	.55 .60	.55 .50	.60 .50	.55 .80	.50 .95	.60
5	.75 .60	.70 .40	.80 .50	.90 .60	.85 .60	.90 .60	.95 .60	1.00 .60	1.00 .50	1.05 .50	.95 1.10	.90 1.40	.80
9	.60 .75	.60 .65	.70 .45	.75 .55	.90 .65	1.10 .70	1.25 .80	1.30 .70	1.30 .55	1.05 .40	1.05 .70	.95 1.40	.90
13	.45 .80	.60 .45	.35 .55	.65 .65	1.00 .80	1.20 1.05	1.35 1.20	1.45 1.10	1.50 .55	1.40 .40	1.25 .95	1.10 1.40	1.00
17	.55 .40	.35 .50	.40 .40	.35 .50	.90 .85	1.35 1.00	1.60 1.30	1.55 .90	1.55 .55	1.50 .50	1.45 .80	1.10 1.60	.60
21	.50 .55	.45 .60	.50 .60	.45 .40	1.00 .90	1.20 1.30	1.70 1.35	1.90 1.15	1.95 .65	1.75 .60	1.50 .95	1.00 1.60	.40
25	.40 .70	.65 .80	.85 .50	.50 .40	1.40 .95	1.30 1.30	1.65 1.30	1.90 .95	1.85 .55	1.70 .60	1.30 1.25	.40 1.70	.45

(continued)

Table 15. (Continued)

	Vapor Film Projected Diameter - Centimeters												
Frame Station	1 14	2 15	3 16	4 17	5 18	6 19	7 20	8 21	9 22	10 23	11 24	12 25	13
Frame No. 29	.60 1.00	.90 .95	.85 .35	.60 .40	.30 1.25	1.75 1.40	1.90 1.35	2.00 .85	1.90 .60	1.70 1.00	1.00 1.60	.30 1.80	.70
33	.60 1.20	1.05 1.10	1.20 .50	.85 .35	.35 .95	1.80 1.50	1.95 1.40	2.10 .95	2.00 .70	1.95 1.00	.70 1.50	.30 1.80	.65
37	.50 1.20	.95 1.40	1.40 .70	1.05 .30	.40 .55	1.20 1.35	2.00 1.55	2.20 .95	2.05 .90	2.00 .95	1.20 1.30	.40 1.70	.50
41	.55 1.35	1.20 1.40	1.55 .75	1.15 .30	.40 .70	.35 1.30	2.20 1.50	2.25 1.00	2.05 .95	2.05 1.05	.40 1.30	.30 1.55	.70

Framing Rate = 39 frames/11 millisec. = 3,550 frames/sec

Table 16. Film Growth Rate Data for Run Number 10

	Vapor Film Projected Diameter - Centimeters												
Frame Station	1 14	2 15	3 16	4 17	5 18	6 19	7 20	8 21	9 22	10 23	11 24	12 25	13
Wire	.30	.30	.30	.30	.30	.30	.30	.30	.30	.30	.30	.30	.30
	.30	.30	.30	.30	.30	.30	.30	.30	.30	.30	.30	.30	
Frame	.50	.45	.40	.45	.45	.45	.55	.50	.50	.50	.50	.50	.50
No. 2	.50	.50	.45	.40	.40	.40	.45	.40	.40	.50	.70	.70	
5	.60	.50	.50	.65	.70	.75	.80	.80	.70	.70	.65	.70	.70
	.50	.50	.45	.50	.50	.50	.50	.50	.40	.70	1.10	1.05	
9	.50	.55	.65	.75	.90	1.05	1.05	1.10	1.05	.90	.90	.70	.60
	.45	.40	.40	.60	.70	.70	.60	.50	.40	.70	1.30	.85	
13	.35	.40	.65	.90	1.10	1.25	1.25	1.25	1.10	1.00	.95	.85	.60
	.45	.50	.60	.75	.95	1.00	.85	.50	.40	.95	1.35	1.00	
17	.70	.45	.30	.85	1.20	1.45	1.45	1.50	1.40	1.30	1.00	.55	.35
	.40	.45	.55	.80	1.00	1.15	.90	.55	.50	.90	1.45	1.20	
21	.45	.35	.30	.30	1.10	1.35	1.65	1.75	1.65	1.35	1.05	.45	.45
	.50	.50	.50	.60	1.15	1.15	1.00	.65	1.00	.60	1.25	1.55	
25	.45	.40	.55	.40	1.35	1.35	1.75	1.90	1.75	1.50	1.05	.35	.55
	.55	.55	.45	.75	1.15	1.30	1.10	.80	.45	.75	1.50	1.65	

(continued)

Table 16. (Continued)

	Vapor Film Projected Diameter - Centimeters												
Frame Station	1 14	2 15	3 16	4 17	5 18	6 19	7 20	8 21	9 22	10 23	11 24	12 25	13
Frame	.35	.45	.60	.55	.30	1.20	1.85	1.90	1.80	1.40	.40	.30	.70
No. 29	.80	.70	.30	.65	1.25	1.35	1.20	.60	.50	.95	1.40	1.60	
33	.45	.65	.90	.65	.35	1.80	1.75	2.05	1.85	1.05	.30	.45	.95
	1.00	.50	.30	.80	1.45	1.45	1.20	.60	.65	1.10	1.50	1.55	
37	.50	.90	1.15	.85	.35	1.85	2.05	1.90	1.90	.70	.30	.45	1.15
	1.20	.55	.30	.60	1.35	1.50	1.15	.70	.75	1.00	1.25	1.25	
41	.45	1.05	1.25	.85	.30	2.20	2.20	2.05	1.90	.55	.30	.55	1.30
	1.25	.60	.30	.60	1.35	1.60	1.10	.90	.80	1.10	1.40	1.30	

Framing Rate = 32 frames/9 millisec. = 3,550 frames/sec

Table 17. Film Growth Rate Data for Run Number 16

Frame Station	Vapor Film Projected Diameter - Centimeters											
	1	2	3	4	5	6	7	8	9	10	11	12
Wire	.35	.35	.30	.30	.30	.30	.30	.35	.35	.40	.40	.40
Frame No. 1	1.00	1.10	1.00	1.00	1.00	1.00	.95	.95	1.05	1.05	1.25	1.15
5	1.40	1.35	1.00	1.00	1.05	.85	.95	1.00	1.35	1.35	1.05	.95
9	1.40	1.35	1.05	.90	.90	.85	.65	1.00	1.45	1.60	1.30	1.10
13	1.80	1.80	1.25	1.15	1.00	.55	.55	1.05	1.60	1.45	1.40	1.30
17	2.10	1.75	1.50	.90	.90	.50	.50	.50	1.50	1.75	1.50	1.50
21	2.25	2.05	1.65	1.50	.45	.65	1.20	.35	1.50	1.80	2.00	1.60
25	2.50	2.20	1.80	1.60	.40	.65	1.50	.50	1.55	2.15	2.00	1.80
29	2.55	2.50	2.10	1.20	.75	.50	1.90	.60	1.80	2.10	2.10	2.00
33	2.60	2.60	2.20	.55	1.20	.60	1.90	.55	.50	2.30	2.40	2.35

(continued)

Table 17. (Continued)

Frame Station	Vapor Film Projected Diameter - Centimeters											
	1	2	3	4	5	6	7	8	9	10	11	12
Frame No. 37	2.75	2.75	2.30	.90	.80	1.10	2.05	.60	.40	2.40	2.50	2.10
41	3.00	3.00	2.40	.60	.40	1.50	2.05	.60	.65	2.20	2.70	2.10

Framing Rate = 23 frames/6 millisec. = 3,830 frames/sec

Table 18. Film Growth Rate Data for Run Number 19

	Vapor Film Projected Diameter - Centimeters											
Frame Station	1 13	2 14	3 15	4 16	5 17	6 18	7 19	8 20	9 21	10	11	12
Wire	.35 .25	.35 .30	.35 .25	.35 .30	.30 .30	.30 .30	.30 .30	.30 .30	.30 .35	.25	.30	.30
Frame No. 1	.65 .60	.65 .60	.55 .65	.65 .65	.65 .60	.65 .60	.65 .60	.55 .65	.55 .65	.60	.65	.60
5	.70 .70	.65 .50	.60 .90	.80 .80	.95 .90	.90 .60	.65 .85	.70 .95	.80 .90	.80	.70	.70
9	.75 .80	.75 .40	.70 .90	.90 1.10	1.15 .85	1.15 .55	.70 .95	.65 1.20	.70 .95	.85	.85	.85
13	.75 .85	.70 .35	.80 1.00	.85 1.20	1.20 .80	1.25 .65	.80 1.05	.90 1.35	1.10 .85	1.10	.70	.85
17	.80 .85	.80 .45	.90 1.20	.90 1.45	1.10 1.05	1.15 .70	.75 1.05	.95 1.45	1.15 .90	1.15	.75	.85
21	1.00 1.00	1.00 .30	1.05 1.15	.90 1.45	1.20 1.10	1.15 .60	.60 1.10	1.10 1.35	1.40 .85	1.30	.80	1.00
25	1.05 1.25	1.00 .35	1.10 1.05	1.00 1.45	1.20 .70	1.00 .60	.55 1.20	1.15 1.40	1.55 .90	1.35	.90	1.10

(continued)

Table 18. (Continued)

	Vapor Film Projected Diameter - Centimeters											
Frame Station	1 13	2 14	3 15	4 16	5 17	6 18	7 19	8 20	9 21	10	11	12
Frame No. 29	1.05 1.25	1.20 .40	1.20 .90	1.05 1.45	1.00 .75	.95 .45	.45 1.50	.95 1.55	1.55 .75	1.55	.85	1.15
33	1.10 1.20	1.25 .35	1.25 .90	1.15 1.50	1.05 ..80	1.00 .60	.35 1.50	.90 1.55	1.60 .70	1.50	.90	1.30
37	1.20 1.25	1.35 .40	1.25 .85	1.25 1.70	1.25 .60	1.00 .50	.35 1.55	.80 1.50	1.50 .50	1.55	.95	1.30
41	1.30 1.10	1.40 .50	1.35 .90	1.25 1.75	1.50 .45	.85 .50	.35 1.70	.80 1.50	1.65 .40	1.40	1.00	1.45

Framing Rate = 35 frames/9 millisec. = 3,890 frames/sec

Table 19. Film Growth Rate Data for Run Number 20

	Vapor Film Projected Diameter - Centimeters											
Frame Station	1 13	2 14	3 15	4 16	5 17	6 18	7 19	8 20	9	10	11	12
Wire.	.40 .30	.40 .30	.35 .30	.35 .30	.30 .30	.30 .30	.30 .30	.30 .30	.30	.30	.30	.30
Frame No. 1	.45 .40	.40 .40	.45 .40	.50 .45	.50 .45	.50 .40	.50 .40	.45 .45	.45	.40	.40	.45
5	.60 .55	.55 .35	.55 .75	.60 1.00	.75 .55	.75 .45	.75 .75	.80 .95	.65	.65	.55	.55
9	.60 .65	.60 .35	.65 .70	.75 1.05	.75 .50	.85 .35	.55 .75	.65 1.25	.90	.70	.60	.85
13	.70 .80	.70 .45	.75 1.00	.70 1.10	.85 .60	.65 .50	.50 .85	.70 1.55	1.00	.95	.65	1.00
17	.80 .90	.85 .45	.80 1.30	.75 1.25	.85 .45	.40 .50	.50 .95	.95 1.90	1.15	1.10	.50	1.15
21	.90 .70	.90 .45	.95 1.30	.95 1.35	.85 .40	.45 .60	.35 1.00	1.05 1.80	1.20	.90	.60	1.30
25	1.00 .55	1.00 .30	.90 1.45	.90 1.65	.80 .35	.60 .40	.40 1.20	1.20 1.80	1.35	.60	.60	1.35

(continued)

Table 19. (Continued)

	Vapor Film Projected Diameter - Centimeters											
Frame Station	1 13	2 14	3 15	4 16	5 17	6 18	7 19	8 20	9	10	11	12
Frame No. 29	1.20 .50	1.10 .40	.95 1.15	1.00 1.70	.90 .60	.40 .35	.40 1.40	1.20 1.85	1.55	.60	.60	1.60
33	1.10 .60	1.25 .45	1.00 1.15	1.05 1.60	1.00 .50	.40 .35	.50 1.20	1.10 1.65	1.85	.65	.65	1.55
37	1.25 .85	1.25 .45	1.05 1.00	1.15 1.55	1.05 .40	.45 .55	.55 1.20	.75 1.75	1.90	.75	.30	1.60
41	1.10 .90	1.35 .90	1.05 1.05	1.15 1.85	1.20 .60	.35 .70	.65 1.30	.70 1.80	1.90	.65	.40	1.85

Framing Rate = 31 frames/8 millisec. = 3,880 frames/sec

Table 20. Film Growth Rate Data for Run Number 21

	Vapor Film Projected Diameter - Centimeters											
Frame Station	1 13	2 14	3 15	4 16	5 17	6 18	7 19	8 20	9 21	10	11	12
Wire	.35 .35	.35 .35	.40 .35	.40 .35	.40 .35	.35 .35	.40 .35	.35 .35	.35 .35	.35	.35	.35
Frame No. 1	.60 .65	.55 .65	.65 .60	.55 .55	.55 .55	.60 .40	.65 .50	.55 .55	.50 .50	.50	.50	.55
5	.80 1.30	.85 .90	.70 .80	1.00 1.00	.95 .75	.80 .65	.80 .80	.85 1.00	.85 1.40	.80	.95	.35
9	.90 1.75	.80 1.30	.60 .85	.90 1.25	1.10 .85	.85 .80	1.05 .60	.95 1.30	.85 1.75	.95	1.20	.45
13	.90 1.95	.70 1.35	.75 .80	.90 1.25	1.20 .75	.75 .90	1.10 .65	.85 1.15	1.05 2.00	.95	.95	.75
17	.85 2.10	.75 1.55	.75 .75	.85 1.25	.85 1.10	.95 .95	1.00 .80	.95 1.45	1.00 2.15	1.05	.90	.70
21	1.00 1.85	.80 1.60	.75 .65	1.25 .95	1.15 .80	.90 .75	.90 .55	.95 1.00	1.10 2.40	1.05	.85	.60
25	.80 2.00	.85 1.85	.75 .65	1.15 .90	1.20 .80	1.00 .70	.95 .65	.90 .85	.95 2.40	1.00	.60	.65

(continued)

Table 20. (Continued)

	Vapor Film Projected Diameter - Centimeters											
Frame Station	1 13	2 14	3 15	4 16	5 17	6 18	7 19	8 20	9 21	10	11	12
Frame No. 29	1.00 2.00	.80 2.00	.80 .75	1.10 .95	1.30 .95	1.00 .75	1.00 .70	.90 .90	.85 2.60	1.15	.75	.75
33	1.00 2.05	.85 1.95	.75 .75	1.15 .95	1.25 1.00	1.00 .80	1.00 .80	1.00 1.00	1.00 2.60	1.10	.50	.95
37	1.20 2.10	.85 1.85	.70 .70	1.15 1.10	1.25 1.05	.95 .95	1.05 .45	1.00 1.10	1.00 2.40	1.10	.35	.75
41	1.20 2.15	1.00 1.85	.75 .80	1.15 1.20	1.25 1.05	.90 .70	1.05 .50	1.05 1.50	1.00 2.40	1.20	.40	1.00

Framing Rate = 22 frames/6 millisec. = 3,670 frames/sec

Table 21. Film Growth Rate Data for Run Number 22

	Vapor Film Projected Diameter - Centimeters												
Frame Station	1 14	2 15	3 16	4 17	5 18	6 19	7 20	8 21	9 22	10 23	11 24	12 25	13
Wire	.35 .30	.35 .30	.30 .30	.35 .30	.35 .30	.40 .30	.30 .30	.30 .30	.40 .30	.40 .30	.40 .30	.35 .30	.35
Frame No. 1	.80 .75	.75 .80	.80 .70	.70 .70	.60 .70	.60 .75	.50 .75	.50 .70	.60 .70	.70 .60	.80 .55	.80 .50	.80
5	1.20 1.40	1.25 1.40	1.35 1.20	1.15 1.00	.60 .90	.95 1.40	.60 1.25	.70 1.10	.85 .85	1.20 .90	1.40 .80	1.50 .70	1.55
9	1.35 1.70	1.50 1.55	1.55 1.25	1.30 1.15	.90 1.15	.80 1.40	.80 1.50	.70 1.20	.75 .60	1.00 .60	1.75 .70	1.80 .65	1.80
13	1.55 2.00	1.60 1.75	1.55 1.70	1.25 1.30	.85 1.25	.85 1.50	.95 1.65	.70 1.35	.70 .85	.90 .70	1.50 .90	2.20 .60	2.15
17	1.70 2.10	1.90 1.95	1.50 1.70	1.35 1.55	.80 1.50	.85 1.55	.80 1.60	.75 1.40	.75 1.10	.70 .80	1.30 .80	2.50 .75	2.50
21	2.05 2.20	1.95 2.20	1.65 1.75	1.00 1.50	.75 1.65	1.10 1.80	.80 1.85	.75 1.65	.70 .95	.70 .60	1.35 .60	2.30 .70	2.50
25	2.10 2.30	1.95 2.00	1.80 1.70	1.25 1.45	.85 1.70	.75 1.95	.75 1.80	.70 1.40	.70 .40	.60 .50	1.35 .60	2.60 .80	2.25

(continued)

Table 21. (Continued)

	Vapor Film Projected Diameter - Centimeters												
Frame Station	1 14	2 15	3 16	4 17	5 18	6 19	7 20	8 21	9 22	10 23	11 24	12 25	13
Frame	2.10	2.10	1.85	1.35	.75	.85	.80	.60	.40	.70	1.70	2.30	2.35
No. 29	2.30	2.00	1.70	1.60	1.85	2.00	1.75	1.20	.50	.50	.70	.90	
33	1.85	2.35	1.90	1.30	.60	.80	.70	.60	.50	.75	1.65	2.30	2.40
	2.10	1.85	1.70	1.70	1.80	1.80	1.75	1.30	.65	.65	.75	.85	
37	1.90	2.30	2.10	1.50	.75	.70	.70	.70	.50	.40	1.70	2.40	2.55
	2.10	1.75	1.70	1.70	1.75	1.80	1.75	1.20	.50	.70	.80	.80	
41	1.60	2.20	2.05	1.45	.75	.75	.60	.65	.60	.35	1.70	2.50	2.60
	2.30	1.75	1.80	1.75	1.75	1.75	1.80	1.50	.70	.60	.60	.80	

Framing Rate = 30 frames/8 millisec. = 3,750 frames/sec

Table 22. Film Growth Rate Data for Run Number 23

	Vapor Film Projected Diameter - Centimeters												
Frame Station	1 14	2 15	3 16	4 17	5 18	6 19	7 20	8 21	9 22	10 23	11 24	12 25	13
Wire	.30 .30	.30 .30	.30 .30.	.30 30	.30 .30	.30 .30	.30 .30	.30 .30	.30 .30	.30 .30	.30 .30	.30 .30	.30
Frame No. 1	.75 .75	.75 .60	.70 .60	.70 .65	.65 .60	.50 .60	.65 .65	.70 .60	.70 .55	.70 .60	.70 .55	.70 .60	.70
5	1.50 1.10	1.35 1.00	1.30 .95	1.05 1.00	.75 .90	.70 .65	.70 .65	1.00 .75	1.40 .65	1.35 .60	1.30 .50	1.30 .50	1.30
9	1.65 1.20	1.60 1.00	1.25 .95	.90 1.00	.65 1.10	.65 .80	.55 .85	1.05 .85	1.20 .75	1.50 .75	1.65 .75	1.40 .70	1.05
13	1.85 1.60	1.55 1.35	1.20 1.25	.80 1.05	.70 .90	.75 .90	.65 .90	1.20 .95	1.40 .95	1.60 .70	.170 .50	1.50 .50	1.35
17	1.75 1.50	1.55 1.40	.95 1.25	.75 1.05	.60 .95	.75 1.00	.70 1.00	1.30 1.10	1.50 1.20	1.65 .70	1.90 .40	1.65 .40	1.55
21	1.95 1.55	1.75 1.50	1.10 1.35	.70 .95	.60 1.00	.40 1.00	.30 1.10	1.00 1.10	1.65 1.05	1.75 .60	1.70 .65	1.70 .80	1.70
25	1.95 1.60	1.90 1.60	1.30 1.50	.70 1.10	.60 1.00	.55 1.10	.50 1.20	.65 1.30	1.70 1.00	1.85 .60	1.85 .40	1.85 .80	1.75

(continued)

Table 22. (Continued)

	Vapor Film Projected Diameter - Centimeters												
Frame Station	1 14	2 15	3 16	4 17	5 18	6 19	7 20	8 21	9 22	10 23	11 24	12 25	13
Frame	2.20	1.90	1.30	.70	.40	.35	.30	.30	1.55	2.00	2.20	2.00	1.75
No. 29	1.65	1.60	1.50	1.25	1.10	1.10	1.30	1.35	1.10	.70	.70	.70	
33	2.30	2.05	1.20	.40	.65	.80	.60	.50	1.75	2.05	2.05	2.00	1.95
	1.85	1.60	1.50	1.25	1.00	1.05	1.50	1.20	.70	.40	.40	.75	
37	2.15	1.75	.90	.35	.65	.90	.55	.35	1.70	2.05	2.20	2.00	1.90
	1.95	1.60	1.45	1.20	1.10	1.15	1.35	1.20	.55	.45	.60	.75	

Framing Rate = 34 frames/9 millisec. = 3.780 frames/sec

Table 23. Film Growth Rate Data for Run Number 24

	Vapor Film Projected Diameter - Centimeters												
Frame Station	1 14	2 15	3 16	4 17	5 18	6 19	7 20	8 21	9 22	10 23	11 24	12 25	13
Wire	.30	.30	.30	.30	.30	.30	.30	.30	.30	.30	.30	.30	.30
	.30	.30	.30	.30	.30	.30	.30	.30	.30	.30	.30	.30	
Frame	.70	.65	.60	.55	.55	.60	.60	.70	.65	.70	.65	.65	.65
No. 1	.65	.65	.60	.65	.60	.60	.60	.60	.55	.50	.60	.60	
5	1.30	1.30	1.25	.65	.60	.50	.60	.75	1.10	.85	.85	.80	.80
	.90	.85	.85	.85	.85	.70	.70	.60	.75	.70	.75	.70	
9	1.40	1.60	.70	.50	.50	.30	.65	.90	1.00	.95	1.00	1.00	1.00
	1.10	1.10	1.05	1.00	1.10	1.00	.75	.70	.80	.80	.85	.95	
13	1.30	1.35	.70	.40	.40	.35	.50	.80	1.00	1.10	.85	1.10	1.10
	1.30	1.25	1.25	1.20	1.10	.90	.85	.90	1.00	1.00	.85	.90	
17	1.50	1.10	.40	.40	.40	.30	.35	1.00	1.10	1.00	1.00	1.05	1.30
	1.45	1.45	1.40	1.30	1.15	.75	.60	.70	.90	.90	.75	.70	
21	1.60	1.25	.40	.40	.70	.50	.40	.45	1.00	1.00	.95	1.00	1.15
	1.50	1.50	1.50	1.35	1.25	.80	.60	.60	.75	.85	.80	.75	
25	1.65	1.35	.45	.60	.85	.75	.45	.35	.95	1.05	.95	.95	1.30
	1.65	1.70	1.70	1.60	1.75	.95	.70	.70	.75	.75	.95	.80	

(continued)

Table 23. (Continued)

	Vapor Film Projected Diameter - Centimeters												
Frame Station	1 14	2 15	3 16	4 17	5 18	6 19	7 20	8 21	9 22	10 23	11 24	12 25	13
Frame	1.75	1.05	.65	.55	.85	.80	.45	.35	.50	1.00	.90	1.05	1.30
No. 29	1.80	1.90	1.70	1.65	1.40	.65	.55	.65	.95	.95	.95	.90	
33	1.65	.65	.35	.80	1.15	.90	.35	.40	.40	.90	.90	1.05	1.40
	1.75	1.95	1.90	1.60	1.20	.60	.30	.65	1.05	1.00	1.00	1.00	
37	1.70	.55	.35	.80	1.30	1.10	.40	.60	.50	.40	.90	.95	1.45
	1.85	2.10	2.10	1.75	1.35	.50	.45	.60	1.10	1.30	1.10	.90	

Framing Rate = 27 frames/7 millisec. = 3,860 frames/sec

Table 24. Film Growth Rate Data for Run Number 25

	Vapor Film Projected Diameter ~ Centimeters												
Frame Station	1 14	2 15	3 16	4 17	5 18	6 19	7 20	8 21	9 22	10 23	11 24	12 25	13
Wire	.30 .30	.30 .30	.30 .30	.30 .30	.30 .30	.30 .30	.30 .30	.35 .30	.35 .30	.35 .40	.35 .40	.35 .40	.30
Frame No. 1	.65 .65	.60 .65	.50 .55	.40 .50	.35 .55	.40 .60	.55 .55	.55 .55	.60 .50	.65 .55	.70 .55	.60 .55	.65
5	1.25 1.10	.95 .70	.85 .75	.45 1.00	.60 .85	.50 .80	.55 .70	.95 .65	.75 .60	1.10 .75	.65 .75	1.00 .80	1.10
9	1.35 1.00	1.40 1.10	.80 1.00	.60 .95	.80 .85	.50 .80	.60 .65	1.00 .50	1.30 .70	1.30 .70	1.20 .75	1.10 .75	1.20
13	1.45 1.15	.90 1.00	.55 1.05	.65 .95	.75 .90	.50 .75	.45 .60	1.05 .45	1.10 .95	1.30 .85	1.25 .85	1.20 .80	1.30
17	1.30 1.15	.85 1.15	.35 1.10	.70 1.10	.80 1.00	.60 .80	.40 .85	1.10 .85	1.25 .85	1.35 1.00	1.20 .95	1.10 .90	1.00
21	1.45 1.15	.75 1.20	.55 1.20	.85 1.25	.85 .95	.40 .40	.50 .35	.90 .45	1.35 .70	1.20 1.00	1.20 1.00	1.10 1.00	1.05
25	1.10 1.20	.85 1.30	.40 1.30	.90 1.45	1.00 1.00	.60 .40	.40 .50	.70 .40	1.50 .70	1.20 1.00	1.20 1.25	1.15 1.00	1.10

(continued)

Table 24. (Continued)

	Vapor Film Projected Diameter - Centimeters												
Frame Station	1 14	2 15	3 16	4 17	5 18	6 19	7 20	8 21	9 22	10 23	11 24	12 25	13
Frame	1.55	.60	.45	.90	1.15	.55	.35	.35	1.05	1.50	1.25	1.25	1.20
No. 29	1.25	1.35	1.50	1.45	.75	.40	.70	.50	.40	1.05	1.30	1.20	
33	1.70	.80	.45	1.05	1.25	.80	.35	.35	.60	1.45	1.30	1.25	1.35
	1.30	1.50	1.65	1.50	.60	.50	.85	.45	.35	1.15	1.35	1.25	
37	1.65	.55	.60	1.10	.80	.75	.40	.35	.30	1.35	1.40	1.30	1.40
	1.45	1.60	1.80	1.50	.30	.50	.85	.60	.40	.80	1.30	1.35	

Framing Rate = 23 frames/6 millisec. = 3,840 frames/sec

Table 25. Film Growth Rate Data for Run Number 26

	Vapor Film Projected Diameter - Centimeters												
Frame Station	1 14	2 15	3 16	4 17	5 18	6 19	7 20	8 21	9 22	10 23	11 24	12 25	13
Wire	.30 .30	.30 .30	.30 .30	.30 .30	.30 .30	.30 .30	.30 .30	.30 .30	.30 .30	.30 .30	.30 .30	.30 .30	.30
Frame No. 1	.60 .60	.65 .60	.60 .60	.50 .55	.40 .55	.60 .55	.55 .55	.70 .55	.70 .55	.80 .50	.75 .50	.70 .50	.70
5	1.45 .85	1.40 .75	1.30 .80	.85 .75	.80 .75	.80 .75	.70 .70	1.20 .55	1.30 .60	1.25 .70	1.10 .80	.90 .85	1.00
9	1.55 1.10	1.35 1.10	.70 1.00	.60 .95	.60 .90	.60 .85	.90 .80	1.30 .55	1.50 .65	1.40 .90	1.40 .85	.95 .80	1.25
13	1.65 1.10	1.20 1.05	.65 1.05	.55 1.00	.60 1.00	.40 .80	.65 .50	1.45 .60	1.40 .80	1.30 .90	1.15 1.00	1.10 .80	1.05
17	1.40 1.30	.95 1.20	.65 1.20	.70 1.15	.60 .95	.40 .45	.65 .70	1.30 .70	1.40 .80	1.20 .85	1.10 .85	1.00 .80	1.20
21	1.55 1.50	1.15 1.50	.65 1.30	.60 1.30	.70 1.30	.70 .50	.30 .45	1.10 .70	1.50 .90	1.30 .95	1.20 1.00	1.05 1.00	1.30
25	1.75 1.55	1.10 1.55	.50 1.35	.80 1.30	.75 1.15	.60 .60	.40 .55	.85 .45	1.35 .85	1.35 1.00	1.15 1.30	1.05 1.20	1.30

(continued)

Table 25. (Continued)

	Vapor Film Projected Diameter - Centimeters												
Frame Station	1 14	2 15	3 16	4 17	5 18	6 19	7 20	8 21	9 22	10 23	11 24	12 25	13
Frame	1.50	.70	.50	.85	.80	.55	.50	.95	1.50	1.30	1.15	1.10	1.35
No. 29	1.55	1.70	1.50	1.50	.60	.50	.60	.40	.80	1.20	1.30	1.30	
33	1.20	.40	.60	.90	.90	.45	.40	.85	1.35	1.20	1.10	1.15	1.30
	1.60	1.65	1.70	1.35	.40	.60	.65	.40	.80	1.30	1.35	1.35	
37	.90	.60	.85	1.25	.95	.40	.35	.80	1.40	1.30	1.15	1.20	1.45
	1.65	1.75	1.80	1.20	.50	.70	.60	.40	.70	1.35	1.60	1.50	

Framing Rate = 27 frames/7 millisec. = 3,860 frames/sec

APPENDIX H

COMPUTER PROGRAM LISTING

The following computer program listing is for the numerical solution of Equation (2.37). A description of the computer program may be found in Chapter III.

Appendix H

```
C       MAIN TFBHT
C       TRANSIENT FILM BOILING

        COMMON RHOV,   CONDV,DIFFV,RWALL,CONDLM,TVISLM,        THFG,
       1TSAT,TWALL,PRDTLM,TLIQ,       TEND,DR(40),COEFOV,EXPPRN,B,   J2,
       2TWRITE,TSTART,QMUL,N,NWR,J1,TRRITE ,ZWRITE,CC
        DIMENSION Y(1),DY(1),A(1),R(1),DELY(1),PD(1),SD(1),YS(1),DYST(1),
       1YST(1),YSIMP(1)
 1111  READ(5,600,END=1112) RHOV,EXPPRN,CONDV,DIFFV,RWALL,CONDLM,TVISLM
 600   FORMAT(7E10.4)
       READ(5,610)THFG,TEND, TSAT,TWALL,PRDTLM,TLIQ,COEFOV,NWR
 610   FORMAT(7F10.4,I10)
 618   FORMAT(4E10.4,I5)
       READ(5,618)A(1),R(1),RAD,TSTART,RUNNO
       Y(1)=RAD
       WRITE(6,619)
 619   FORMAT(1H ,23X"COMPUTER INPUT VALUES"//)
       WRITE(6,611)RHOV,EXPPRN,CONDV,DIFFV,RWALL,CONDLM,TVISLM,THFG,TSAT,
       1TWALL,PRDTLM,TLIQ,COEFOV,TEND,TSTART,A(1),R(1),Y(1),NWR
 611   FORMAT(1H ,20H                    RHOV=,E10.4,13H        EXPPRN=,E10.4 /
       1            21H                   CONDV=,E10.4,13H         DIFFV=,E10.4 /
       2            21H                   RWALL=,E10.4,13H        CONDLM=,E10.4 /
       3            21H                  TVISLM=,E10.4,13H           THFG=,F10.4 /
       4            21H                    TSAT=,F10.4,13H          TWALL=,F10.4 /
       5            21H                  PRDTLM=,F10.4,13H           TLIQ=,F10.4 /
       6            21H                  COEFOV=,F10.4,13H           TEND=,F10.4 /
       7            21H                  TSTART=,E10.4,13H           A(1)=,E10.4 /
       8            21H                    R(1)=,E10.4,13H           Y(1)=,E10.4 /
       9            21H                     NWR= I10//)
C       INITIALIZATION
        J1=0
        J2=0
        T=0.
        DEL=.00001
        IFVD=0
        IBKP=1
        NTRY=1
        IERR=0
        N=1
        TEND=TEND-TSTART
        TWRITE=TEND/NWR
        ZWRITE=TWRITE/NWR
        QMUL=144.*3600.
        WRITE(6,602) RUNNO
 602    FORMAT(1X,44X,"RUN NUMBER=",I4,////)
        WRITE(6,622)
 622    FORMAT(1X,45X,"BUBBLE GROWTH HISTORY"//)
        WRITE(6,623)
 623    FORMAT(1X,10X,"TIME",11X,"BUBBLE RADIUS",5X,"INTFACE VELOCITY",6X,
       1"CONDUCTION",11X,"CONVECTION",/,69X,"HEAT FLUX AT",8X,"HEAT FLUX A
       2T",/,70X,"INTERFACE",11X,"INTERFACE",/,14X,"(SEC)",16X,"(IN)",12X,
       3"(IN/SEC)", 9X,"(BTU/HR SQ-FT)",4X,"(BTU/HR SQ-FT)"//)
        CALL RKS(              Y,DY,A,R,T,DEL,N,IFVD,IBKP,NTRY,IERR,DELY,
       1PD,SD,YS,YST,DYST,YSIMP)
        WRITE(6,629)
 629    FORMAT(1X,///,21X,"BUBBLE VELOCITY AND ACCELERATION"//)
        WRITE(6,630)
 630    FORMAT(13X,"TIME",11X,  "INTFACE VELOCITY",5X,"INTFACE ACCELERATIO
       1N",/,13X,"(SEC)",13X,"(IN/SEC)",16X,"(IN/SEC-SQ)"//)
        Z=2.*ZWRITE
        D2RDT2=(-3.*DR(1)+4.*DR(2)-DR(3))/Z
        TIME=0.+TSTART
        WRITE(6,632)TIME,DR(1),D2RDT2
```

```
632   FORMAT(2E20.4,E25.4)
      DO 626 K=2,NWR
      D2RDT2=(DR(K+1)-DR(K-1))/Z
      TIME=(K-1)*TWRITE+TSTART
626   WRITE(6,632)TIME,DR(K),D2RDT2
      TIME=NWR*TWRITE+TSTART
      D2RDT2=(3.*DR(NWR+1)+DR(NWR-1)-4.*DR(NWR))/Z
      WRITE(6,632)TIME,DR(NWR+1),D2RDT2
      ZZ=2.*TWRITE
      ND=NWR+2
      NDD=2.0*NWR-1
      DO 627 K=ND,NDD
      D2RDT2=(DR(K+1)-DR(K-1))/ZZ
      TIME=(K-20)*TWRITE+TSTART
627   WRITE(6,632)TIME,DR(K),D2RDT2
      TIME=TEND+TSTART
      D2RDT2=(3.0*DR(NDD+1)+DR(NDD-1)-4.0*DR(NDD))/ZZ
      WRITE(6,632)TIME,DR(40),D2RDT2
      WRITE(6,1009)
1009  FORMAT(1X,////////////////////)
      GO TO 1111
1112  STOP
      END


      SUBROUTINE RKS(              Y,DY,A,R,T,DEL,N,IFVD,IBKP,NTRY,
     1IERR,DELY,PD,SD,YS,YST,DYST,YSIMP)
      DIMENSION Y(N),DY(N),A(N),R(N),DELY(N),
     1PD(N),SD(N),YS(N),DYST(N),YST(N),YSIMP(N)
C     FR10 IS  FIFTH ROOT OF TEN
      FR10=1.5848932
      IERR=0
C       YS  CONTAINS Y VALUES AT LEFT END POINT OF INTEGRATION INTERVAL
C
C       YSIMP CONTAINS Y FOR SIMPSONS RULE CHECK  CHECK NOT MADE FOR
C           FIXED STEP MODE    ISYMP IS CONTROL PARAMETER =1,FIXED,2 VAR
C
C       IF FIXED STEP SIZE GO ONE INTERVAL OF LENGTH DELT AND RETURN TO
C          CNTRL, IF VAR GO TWO INTERVALS BEFORE RETURN TO CONTRL
C
C       IFVD  = 0     VARIABLE INTERVAL
C             = 1     FIXED
C       IBKP  = 0     CUT INTERVAL ONCE BEFORE REPEAT  (UNDER IFVD=0 )
C             = 1     CUT AS REQUIRED
C       NTRY  = 1     CONTINUE INTEGRATING
C               2     RETURN FROM RKS
C               3     STEP REPEATED WITH NEW DELT
C               4     RESTART
C       IERR  = 0     NORMAL
C              -1     DELT=0, RETURN FROM RKS
C               1     A(I)+ R(I)*ABS(Y(I)) = 0. , RETURN FROM RKS
    5 IF(DEL) 20,10,20
   10 IERR=-1
      GO TO 270
   20 CALL DERIV(Y,DY,T)
      NTRY=1
      CALL CNTRL(Y,DY,DEL,T,NTRY,IFVD)
   25 DDT=DEL
      IF(IFVD) 40,30,40
   30 ISYMP=2
      DELT=DEL/2.
```

```
      DO 31 I=1,N
   31 SD(I)=0.0
      IFLAG=1
      S=1.
      GO TO 45
   40 ISYMP=1
      DELT=DEL
   45 DO 46 I=1,N
      YST(I)=Y(I)
   46 DYST(I)=DY(I)
   50 DO 60 I=1,N
      DELY(I)=DELT*DY(I)
      PD(I)=DELY(I)
   60 CONTINUE
      GO TO (80,70),ISYMP
   70 DO 71 I=1,N
   71 SD(I)=SD(I)+S*DY(I)
   80 T=T+DELT/2.
      DO 85 I=1,N
      YS(I)=Y(I)
      Y(I)=YS(I)+DELY(I)/2.
   85 CONTINUE
      CALL DERIV(Y,DY,T)
      DO 90 I=1,N
      DELY(I)=DELT*DY(I)
      PD(I)=PD(I)+2.*DELY(I)
      Y(I)=YS(I)+DELY(I)/2.
   90 CONTINUE
      CALL DERIV(Y,DY,T)
      DO 95 I=1,N
      DELY(I)=DELT*DY(I)
      PD(I)=PD(I)+2.*DELY(I)
      Y(I)=YS(I)+DELY(I)
   95 CONTINUE
      T=T+DELT/2.
      CALL DERIV(Y,DY,T)
      DO 100 I=1,N
      DELY(I)=DELT*DY(I)
      PD(I)=PD(I)+DELY(I)
      Y(I)=YS(I)+PD(I)/6.
  100 CONTINUE
      GO TO (110,120),ISYMP
  110 NTRY=1
      CALL DERIV(Y,DY,T)
      CALL CNTRL(Y,DY,DEL,T,NTRY,IFVD)
      GO TO 300
  120 GO TO (130,140),IFLAG
  130 S=4.
      IFLAG=2
      CALL DERIV(Y,DY,T)
      GO TO 50
  140 CALL DERIV(Y,DY,T)
      AMAX =0.0
      DO 180 I=1,N
      SD(I)=SD(I)+DY(I)
      YSIMP(I)=YST(I)+DELT*SD(I)/3.
      D    =ABS(Y(I)-YSIMP(I))
      C    =A(I)+R(I)*ABS(Y(I))
      IF(C    ) 160,150,160
  150 IERR=1
      GO TO 270
```

```
160 E    =ABS(D    /C    )
    AMAX=AMAX1(AMAX,E)
180 CONTINUE
    IF(AMAX-1.) 215,215,230
215 NTRY= 1
    CALL CNTRL(Y,DY,DEL,T,NTRY,IFVD)
300 IF(NTRY-1) 185,185,310
310 IF(NTRY-2) 270,270,330
330 IF(NTRY-3) 340,340,5
340 T=T-DDT
    IF(DEL) 259,10,259
185 GO TO (40,190),ISYMP
190 IF(AMAX-.75) 200,25,220
200 IF(AMAX-.075) 210,25,25
210 DEL=DEL*FR10
    GO TO 25
220 DEL=DEL/FR10
    GO TO 25
230 I =1+ IBKP
    GO TO (240,250),I
240 T=T-DEL
    DEL=DEL/FR10
    GO TO  259
250 J=1
251 AM=AMAX/10.**J
    IF(1.-AM) 255,257,257
255 J=J+1
    GO TO 251
257 T=T-DEL
    DEL=DEL/(FR10**J)
259 DO 245 I=1,N
    DY(I)=DYST(I)
245 Y(I)=YST(I)
    GO TO 25
270 RETURN
    END


    SUBROUTINE CNTRL(Y,DY,DEL,T,NTRY,IFVD)
    DIMENSION Y(1), DY(1)
    COMMON RHOV,   CONDV,DIFFV,RWALL,CONDLM,TVISLM,        THFG,
   1TSAT,TWALL,PRDTLM,TLIQ,       TEND,DR(40),COEFDV,EXPPRN,B,   J2,
   2TWRITE,TSTART,QMUL,N,NWR,J1,TRRITE ,ZWRITE,CC
    IF(J2.EQ.0) GO TO 1004
    IF(J2.EQ.(NWR+1)) GO TO 1006
641 IF(ABS(T-TRRITE).LT.1.0E-06) GO TO 1004
    IF(T-TRRITE) 1003,1004,1005
1003 NTRY=1
    RETURN
1005 DEL=DEL-T+TRRITE
    NTRY=3
    RETURN
1004 J2=J2+1
    TRRITE=J2*ZWRITE
    R=Y(1)
    DR(J2)=DY(1)
    Q=((B   )/R)*QMUL
    QC=(CC/R)*QMUL*SQRT(ABS(DY(1)))
    Z=T+TSTART
    WRITE(6,1001)Z,R,DR(J2),Q,QC
1001 FORMAT(5E20.4)
```

```
      NTRY=1
      RETURN
 1006 IF(J1.EQ.0) TRRITE=2.*TWRITE
      IF(ABS(T-TRRITE).LT.1.0E-06) GO TO 1007
      IF(T-TRRITE) 1003,1007,1005
 1007 J1=J1+1
      TRRITE=(J1+2)*TWRITE
      R=Y(1)
      DR(J1+NWR+1)=DY(1)
      Q=(R/R)*QMUL
      QC=(CC/R)*QMUL*SQRT(ABS(DY(1)))
      Z=T+TSTART
      WRITE(6,1001) Z,R,DR(J1+NWR+1),Q,QC
      NTRY=1
      IF(J1.EQ.(NWR-1)) NTRY=2
      RETURN
      END


      SUBROUTINE DERIV(Y,DY,T)
      DIMENSION Y(1), DY(1)
      COMMON RHOV,   CONDV,DIFFV,RWALL,CONDLM,TVISLM,        THFG,
     1TSAT,TWALL,PRDTLM,TLIQ,       TEND,DR(40),COEFDV,EXPPRN,B,   J2,
     2TWRITE,TSTART,QMUL,N,NWR,J1,TRRITE ,ZWRITE,CC
      IF(T.LT.1.0E-06) GO TO 161
      AB= (Y(1)**2)/(4.0*DIFFV*T)
      AC=(RWALL**2.)/(4.*DIFFV*T)
      TX=(-E1(AB)+E1(AC))
      B=-2.*CONDV*(TSAT-TWALL)*EXP(-AB)
      IF(TX.NE.0) B =B/TX
      IF(TX.EQ.0) B=0.0
 164  AA=(RHOV*THFG*Y(1))
      C=-(COEFDV/2.*CONDLM*(PRDTLM**EXPPRN)*(TSAT-TLIQ))/(SQRT(TVISLM))
      CC=C*SQRT(2.*Y(1))
      IF(B.EQ.0) GO TO 2013
      DY(1)=((CC+SQRT(CC**2+4.0*AA*B))/(2.0*AA))**2
      RETURN
 2013 DY(1)=(CC/AA)*ABS(CC/AA)
 2012 RETURN
 161  B=0.0
      GO TO 164
      END


      FUNCTION E1(X)
      COMMON RHOV,   CONDV,DIFFV,RWALL,CONDLM,TVISLM,        THFG,
     1TSAT,TWALL,PRDTLM,TLIQ,       TEND,DR(40),COEFDV,EXPPRN,B,   J2,
     2TWRITE,TSTART,QMUL,N,NWR,J1,TRRITE ,ZWRITE,CC
      IF(X.GT.1.0) GO TO 3
      E1 =-ALOG(X)+((((.107857E-02*X-.976004E-02)*X+.5519968E-01)*X-
     1.24991055)*X+.99999193)*X-.57721566
      RETURN
    3 EE=(X*((X**3+9.5733223454*(X**2)+25.6329561486*X+21.0996530827)*X
     1+3.9584969228))
      E1=(EXP(-X)*((X**3+8.5733287401*(X**2)+18.0590169730*X
     1+8.6347608925)*X+.2677737343))/(EE)
      RETURN
      END
```

APPENDIX I

THERMAL PROPERTY DATA

Table 26. Saturation Temperature and Heat of Vaporization Values for Water, Freon 113, and Carbon Tetrachloride.*

	Water	Freon 113	Carbon Tetrachloride
Saturation Temperature (°F)	212	117.63	170
Heat of Vaporization (BTU/lb)	970	63.12	83.7

* Values Given for Pressure of One Atmosphere

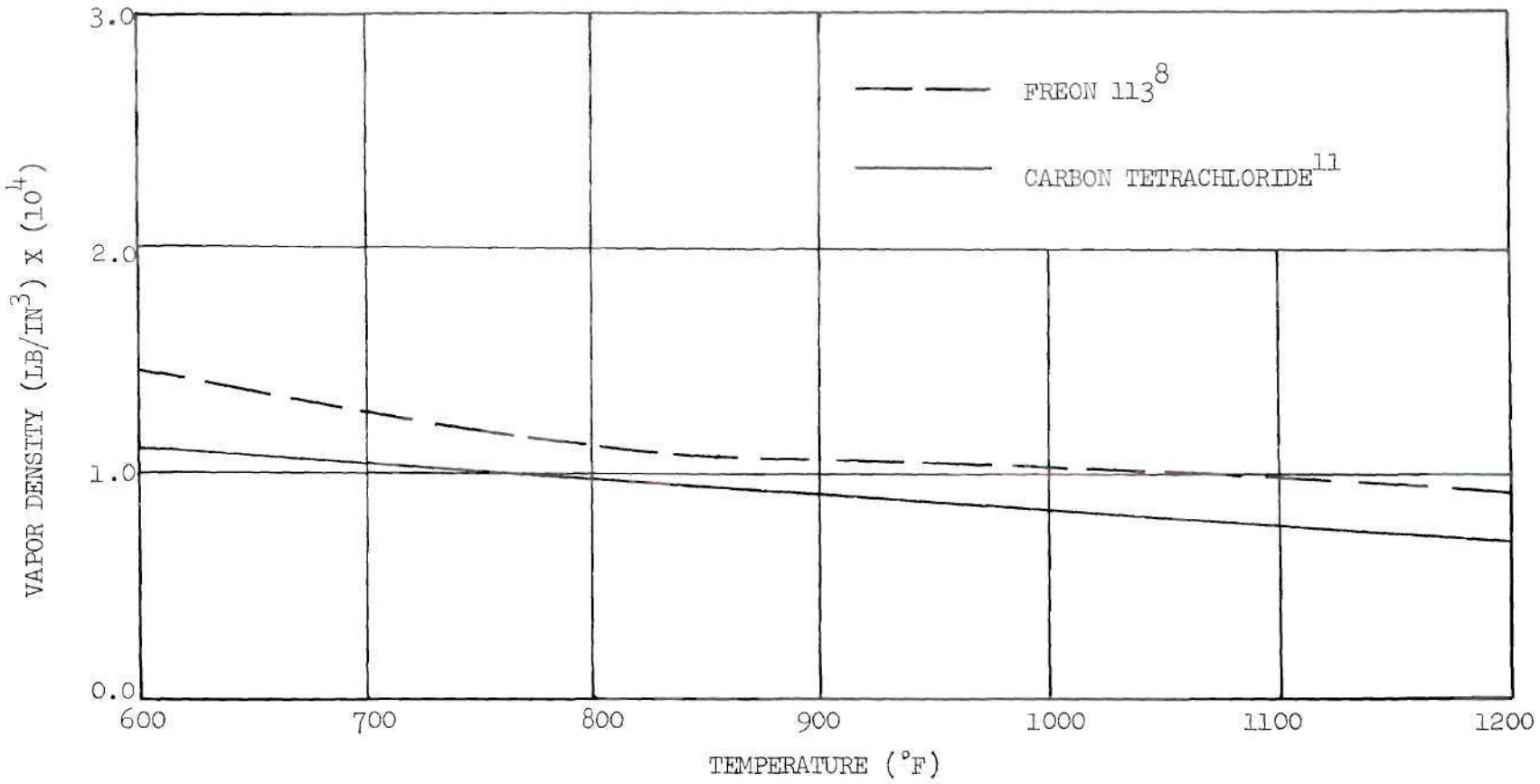

Figure 37. Vapor Density versus Temperature for Carbon Tetrachloride and Freon 113.

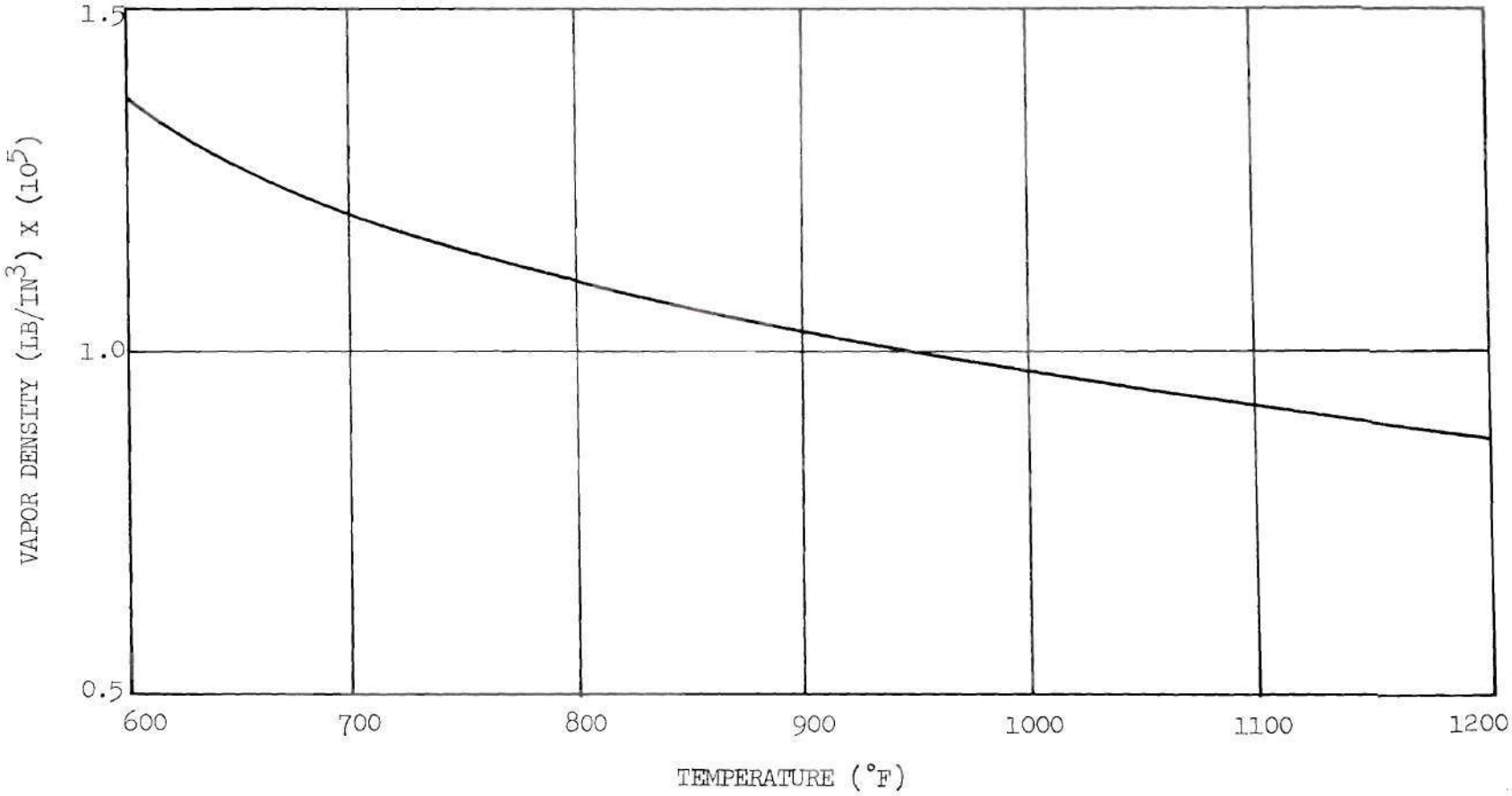

Figure 38. Vapor Density versus Temperature for Water.
Reference 13.

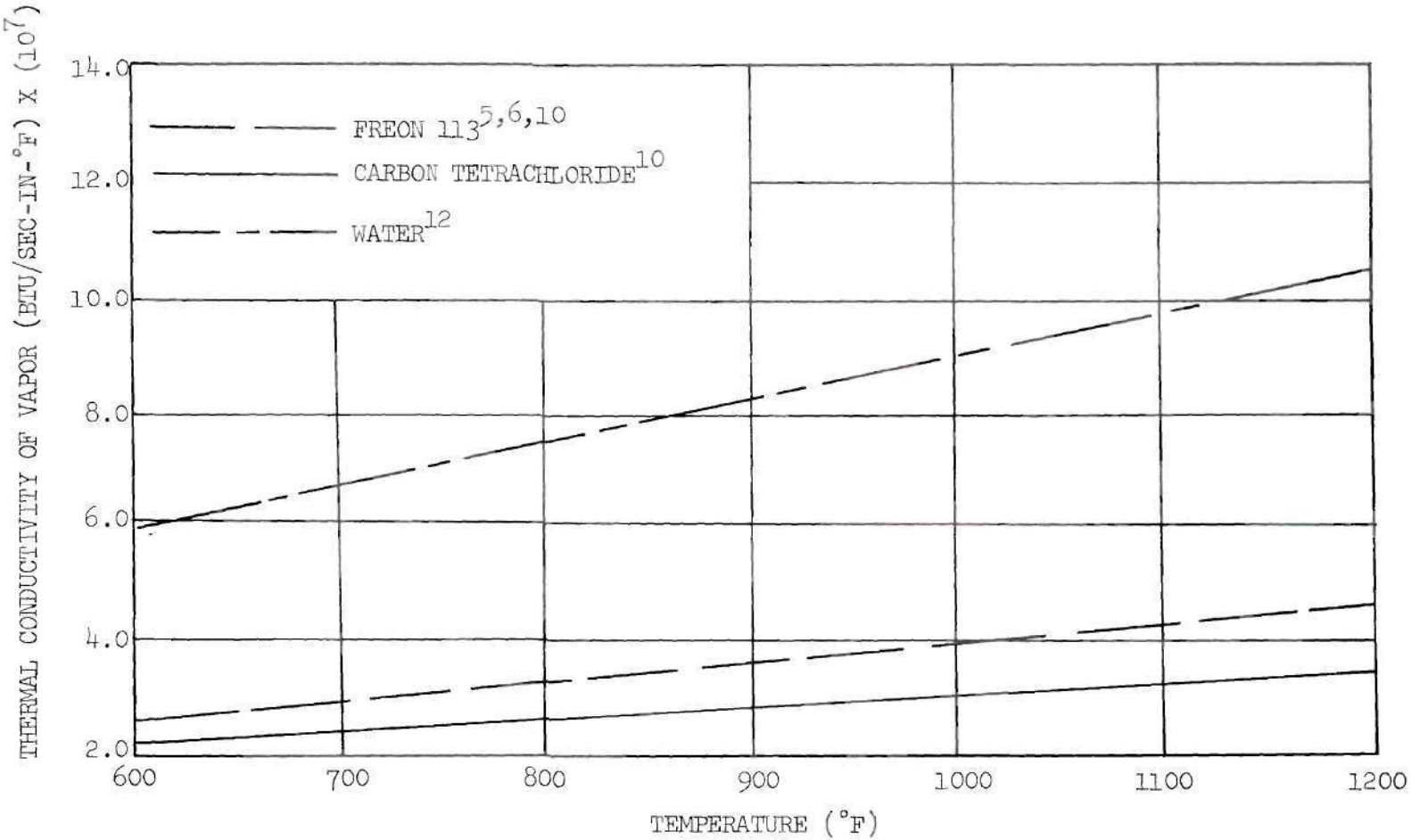

Figure 39. Thermal Conductivity of Vapor versus Temperature for Carbon Tetrachloride, Freon 113, and Water.

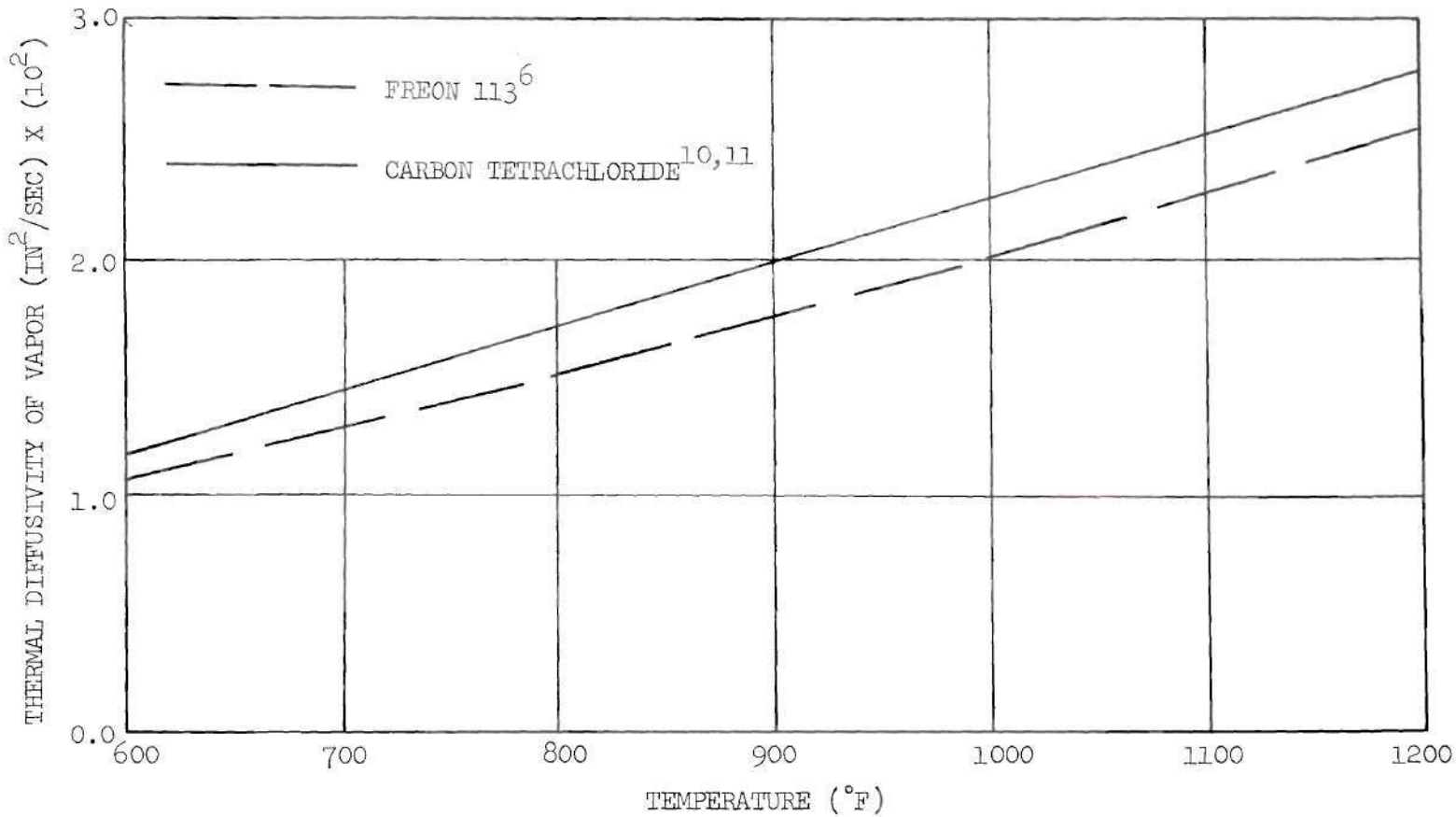

Figure 40. Thermal Diffusivity of Vapor versus Temperature for Carbon Tetrachloride and Freon 113.

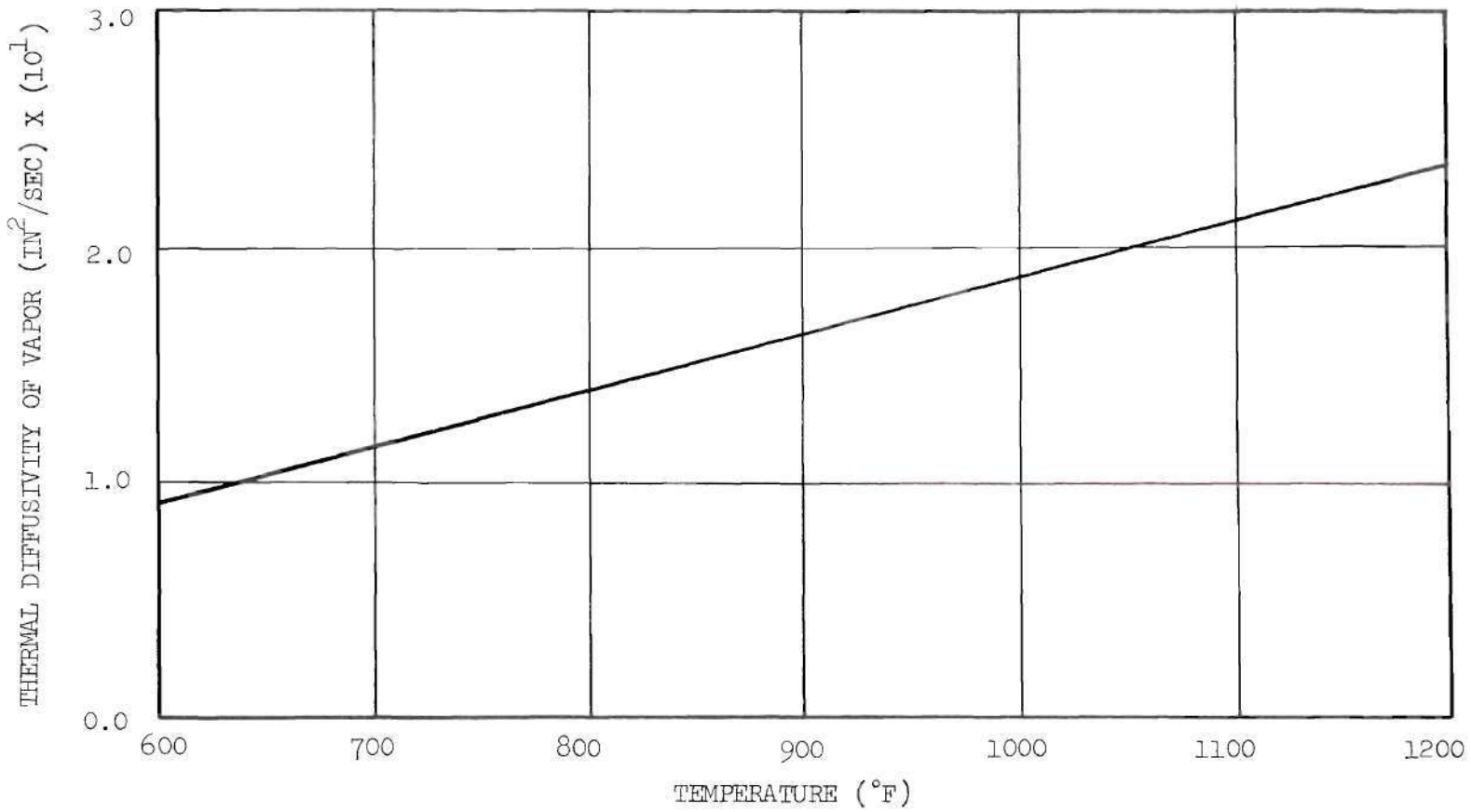

Figure 41. Thermal Diffusivity of Vapor versus Temperature for Water. Reference 12

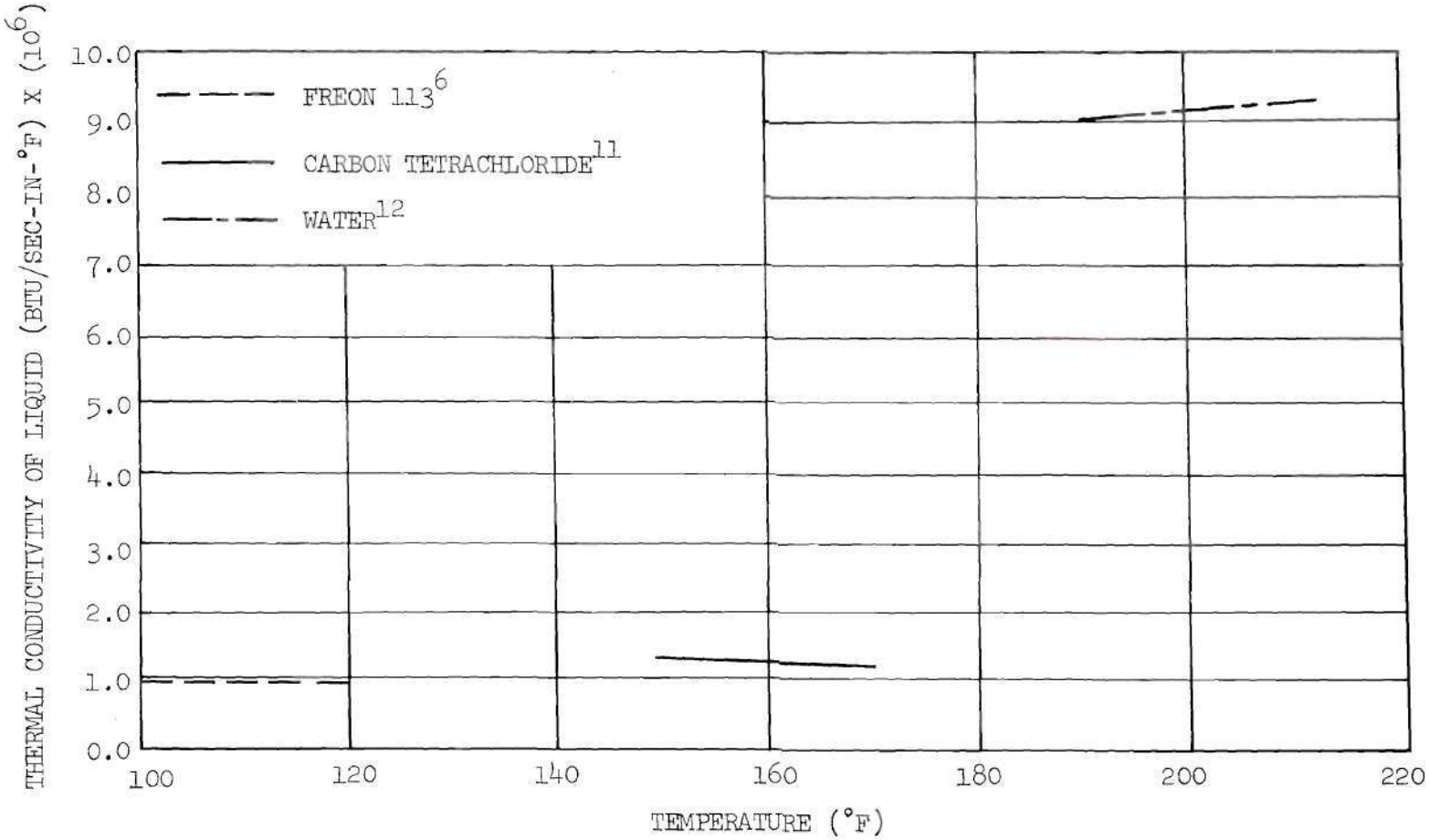

Figure 42. Thermal Conductivity of Liquid versus Temperature for Carbon Tetrachloride, Freon 113, and Water.

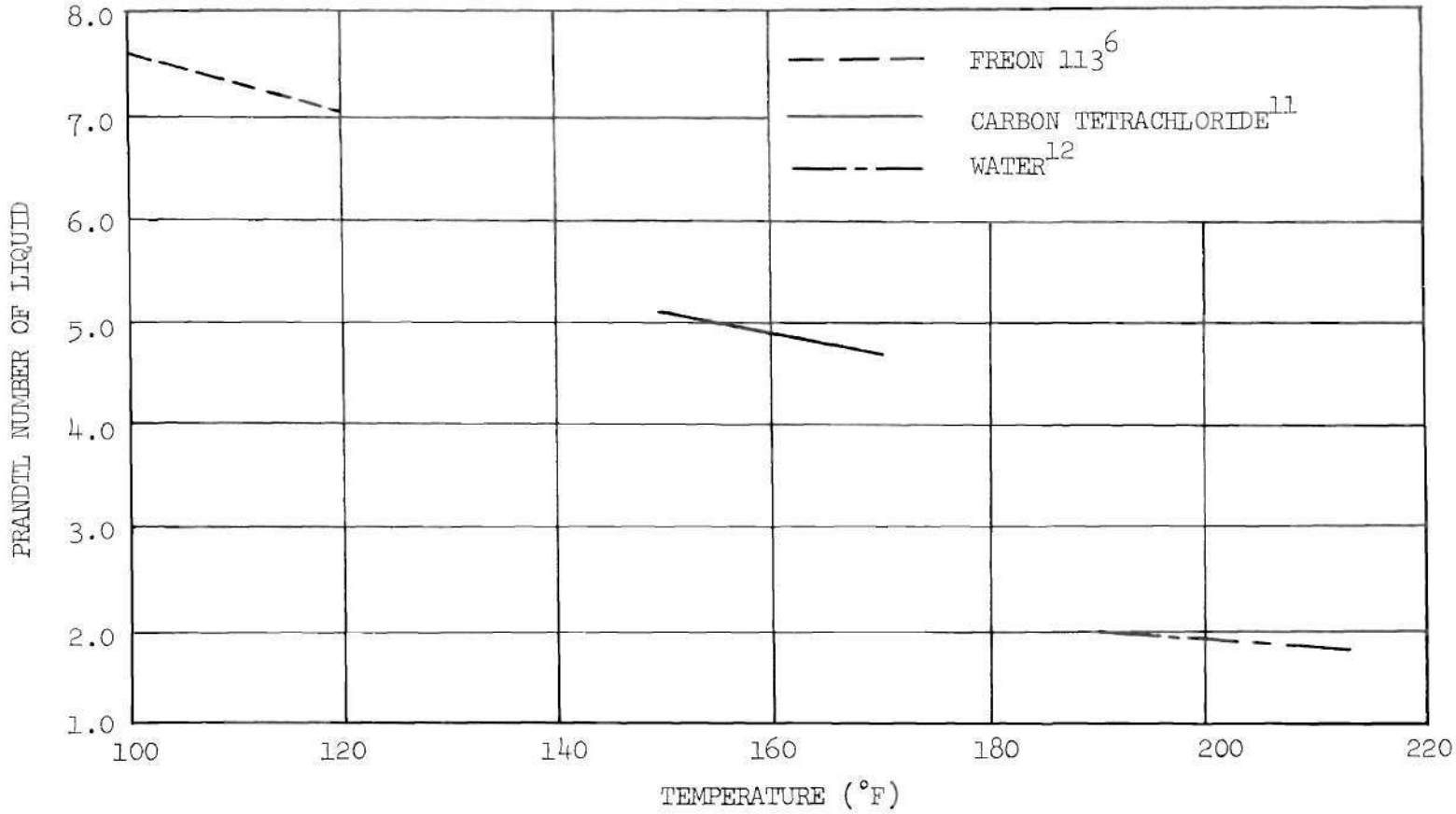

Figure 43. Prandtl Number of Liquid versus Temperature for Carbon Tetrachloride, Freon 113, and Water.

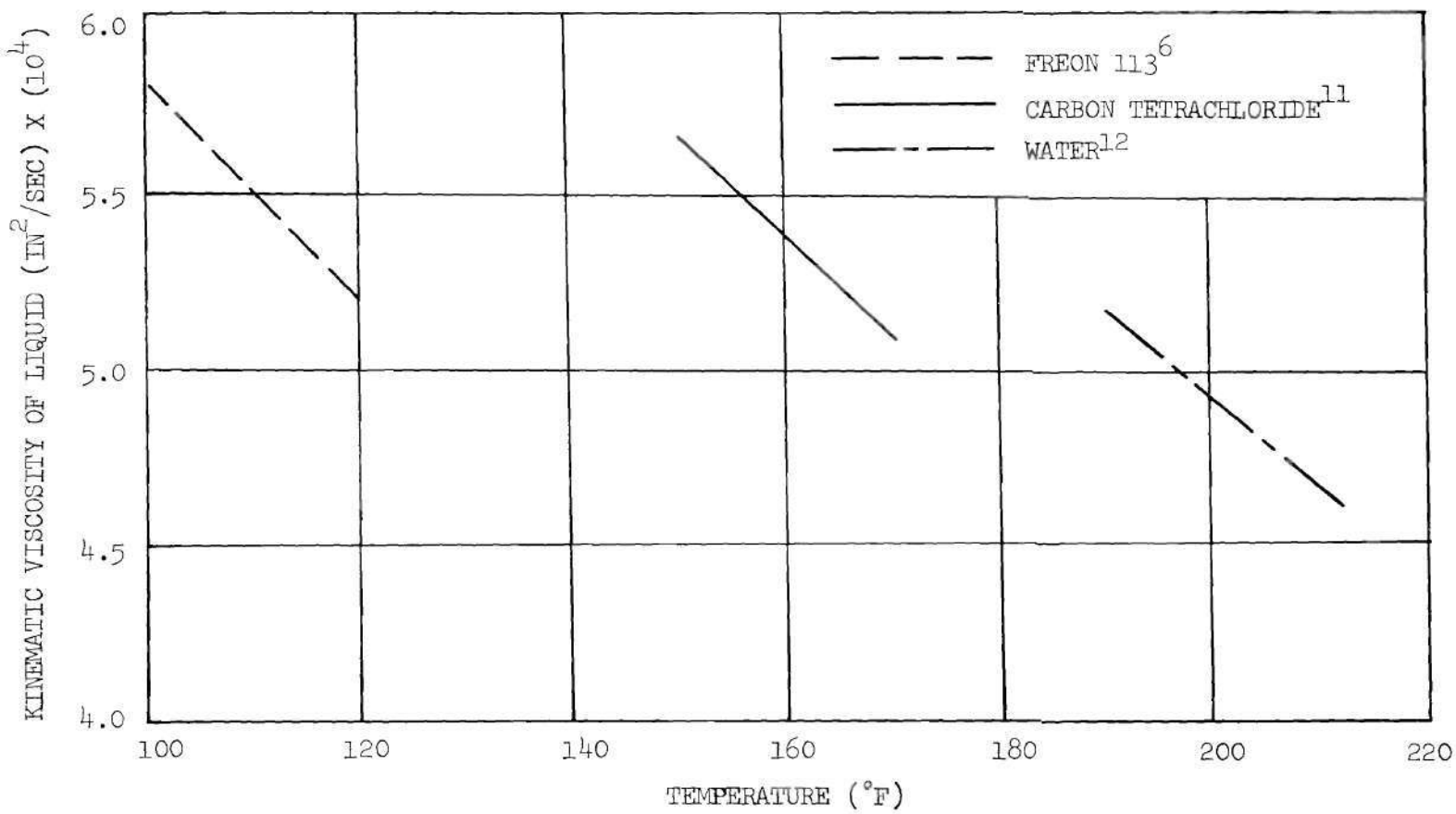

Figure 44. Kinematic Viscosity of Liquid versus Temperature for Carbon Tetrachloride, Freon 113, and Water.

BIBLIOGRAPHY

1. E. L. Richards, "Transient Film Boiling in a Horizontal Annulus Filled with a Saturated Liquid," Ph.D. Thesis, School of Mechanical Engineering, Georgia Institute of Technology, June (1969).

2. D. R. Pitts, "Transient Film Boiling on a Horizontal Cylindrical Surface," Ph.D. Thesis, School of Mechanical Engineering, Georgia Institute of Technology, August (1967).

3. H. H. Yen, "Transient Film Boiling on a Horizontal Cylindrical Surface in a Subcooled Liquid," Ph.D. Thesis, School of Mechanical Engineering, Georgia Institute of Technology, July (1968).

4. M. Jacob, Heat Transfer, Volume I, John Wiley and Sons, Inc., New York, 563 (1949).

5. R. C. Downing, Personal Communication, October 23, 1969.

6. R. C. Downing, "Transport Properties of "Freon" Fluorocarbons," E. I. DuPont de Nemours and Company, FREON Technical Bulletin C-30 (1967).

7. "Properties and Applications of the "FREON" Fluorocarbons," E. I. DuPont de Nemours and Company, FREON Technical Bulletin B-2 (1966).

8. A. F. Benning and R. C. McHarness, "Thermodynamic Properties of "FREON" 113 TRICHLOROTRIFLUOROETHANE CCl_2F-CCl F_2 with Addition of Other Physical Properties," E. I. DuPont de Nemours and Company, Technical Bulletin T-113A (1938).

9. W. H. Markwood, Jr. and A. F. Benning, "Thermal Conductances and Heat Transmission Coefficients of "Freon" Refrigerants," E. I. DuPont de Nemours and Company, Technical Bulletin B-9 (1942).

10. R. A. Svehla, "Estimated Viscosities and Thermal Conductivities of Gases at High Temperatures," NASA TR-132 (1962).

11. CRC Handbook of Chemistry and Physics, 49th Edition 1968-69, The Chemical Rubber Company; R. C. Weast Editor, p. D-107.

12. F. Kreith, Principles of Heat Transfer, International Textbook Company, Scranton, Pennsylvania, 537 (1958).

13. J. H. Keenan and F. G. Keyes, Thermodynamic Properties of Steam, John Wiley and Sons, Incorporated, New York (1936).

14. "Stability at High Temperatures," E. I. DuPont de Nemours and Company, Technical Bulletin X-13.

BIBLIOGRAPHY (Continued)

15. L. A. Bromley, "Heat Transfer in Stable Film Boiling," Chemical Engineering Progress 46, No. 5, 221 (1950).

16. H. C. Hottel and A. F. Sarofim, "Radiative Transfer," McGraw-Hill, 232 (1967).

17. W. W. Coblentz, "Investigations of Infra-Red Spectra," Carnegie Institution of Washington, Part I, 43, 166 (1962).

18. R. C. Downing, Personal Communication, February 22 (1970).

19. American Institute of Physics Handbook, McGraw-Hill, Inc., 2nd ed., 6-90 (1963).

20. Reference 7, p. 9.

21. Reference 20, Part III, Chapter II, p. 17.

22. J. S. Proctor, Personal Communication, Physical and Analytical Division, E. I. DuPont de Nemours and Company, February 23 (1970).

23. Reference 20, Part I, p. 183.

24. W. M. Kays, "Convective Heat and Mass Transfer," McGraw-Hill, Inc., 37 (1966).

25. V. Sernas and F. C. Hooper, "The Initial Vapor Bubble Growth on a Heated Wall During Nucleate Boiling," International Journal of Heat and Mass Transfer 12, No. 9, 1627, Dec. (1969).

26. L. W. Florschuetz and B. T. Chao, "On the Mechanics of Vapor Bubble Collapse," Transactions of the American Society of Mechanical Engineers Series C 87, No. 2, 209 (1965).

27. P. G. Hill and G. R. Peterson, "Mechanics and Thermodynamics of Propulsion," Addison-Wesley Publishing Co., Inc., 11 (1965).

28. H. S. Carslaw and J. C. Jaeger, Conduction of Heat in Solids, Oxford University Press, London (1950).

29. Reference 12, p. 117.

OTHER REFERENCES

Akiyama, M., "Spherical Bubble Collapse in Uniformly Subcooled Liquid," Bulletin, Japan Society Mechanical Engineers, 8, No. 32, 683 (1965).

Bankoff, S. G., "Asymptotic Growth of a Bubble in a Liquid with Uniform Superheat," Applied Scientific Research 12, No. 3, 267 (1963/1964).

Bankoff, S. G., "Bubble Dynamics at the Surface of an Exponentially Heated Plate," Industrial Engineering Chemical Fundamentals 1, No. 4, 257 (1962).

Dergarabdeian, P., "The Rate of Growth of Vapor Bubbles in Superheated Water," Journal of Applied Mechanics, 20, 537 (1953).

Dougherty, D. E. and Rubin, H. H., "The Growth and Collapse of Vapor Bubbles on a Boiling Surface," Proceedings of Heat Transfer and Fluid Mechanics Institute, Pasadena, Stanford University Press, Calif. (1963).

Ellion, M. E., "A Study of the Mechanism of Boiling Heat Transfer," Ph.D. Thesis, Calif. Institute of Technology, (1953).

Engelberg, K., Forster, H. K. and Greif, R., "Heat Transfer to a Boiling Liquid - Mechanism and Correlations," Trans. ASME, Series C, 81 43 (1959).

Forster, H. K. and Zuber, N., "Growth of a Vapor Bubble in a Superheated Liquid," Jour. of Applied Physics, 25, 474 (1954).

Forster, H. K. and Zuber, N., "Dynamics of Vapor Bubbles and Boiling Heat Transfer," American Institute of Chemical Engineers Journal 1, 531-535 (1955).

Hottel, H. C. and Egbert, R. B., "Radiant Heat Transmission From Water Vapor," Transactions, American Institute of Chemical Engineers 38, 531 (1942).

Marcus, B. D., "Experiments on the Mechanism of Saturated Nucleate Pool Boiling Heat Transfer," Ph.D. Thesis, Cornell University (1963).

McAdams, W. H., Addoms, J. N., Rinaldo, P. M. and Day, R. S., "Heat Transfer from Single Horizontal Wires to Boiling Water," Chemical Engineering Progress, 44, 639-646 (1948).

Plesset, M. S. and Zwick, S. A., "A Non-Steady Heat Diffusion Problem with Spherical Symmetry," Jour. of Applied Physics, 23, 95 (1952).

Plesset, M. S. and Zwick, S. A., "The Growth of Vapor Bubbles in Superheated Liquids," Jour. of Applied Physics, 25, 493 (1954).

OTHER REFERENCES (Continued)

Lord Rayleigh, "Pressure Developed in a Liquid During the Collapse of a Spherical Cavity," Philosophical Magazine, 34, 94, (1917).

Rohsenow, W. M., "A Method of Correlating Heat Transfer Data for Surface Boiling of Liquids," Recent Advances in Heat and Mass Transfer, McGraw-Hill, 338-352, (1961).

Savic, P. and Gosnell, J. W., "The Dynamics of the Expanding Vapor Bubble in a Boiling Liquid," Canadian Journal of Chemical Engineering, 40, No. 6, 238, (1962).

Scriven, L. E., "On the Dynamics of Phase Growth," Chemical Engineering Scientific, 17, 55 (1962).

Sparrow, E. M. and Cess, R. D., "The Effect of Subcooled Liquid on Laminar Film Boiling," Trans. ASME, Series C, 84, February (1962).

Viskanta, R. and Grosh, R. J., "Heat Transfer by Simultaneous Conduction and Radiation, Trans. ASME, Series C, 84, 63-72 (1962).

Wittke, D. D., "Collapse of Vapor Bubbles with Translatory Motion," Ph.D. Thesis, University of Illinois (1965).

Zuber, N., "Hydrodynamic Aspects of Boiling Heat Transfer," AECU-4439, June (1959).

Zwick, S. A., "Growth of Vapor Bubbles in a Rapidly Heated Liquid," Phys. Fluids, 3, No. 5, 685 (1960).

VITA

David P. Wehmeyer was born in St. Charles, Missouri on October 31, 1944. He attended St. Charles Borromeo Elementary School in St. Charles, Missouri and graduated from Duchesne High School, St. Charles, Missouri in June, 1962. He entered the University of Missouri at Rolla, Rolla, Missouri in September 1962 and received his Bachelor of Science in Mechanical Engineering from there in June, 1966. During this period he was a co-op with McDonnell Aircraft Corporation in St. Louis, Missouri.

In September, 1966 he entered Georgia Institute of Technology, Atlanta, Georgia with a NDEA Fellowship. He received his Master of Science in Mechanical Engineering in 1968 and since that time has continued to study toward the Doctorate in Mechanical Engineering at the Georgia Institute of Technology.

In 1967 he married the former Miss Barbara Ann Schulte also of St. Charles, Missouri and they now have one little bundle of energy, Stephen Paul.